Ministry of Higher Education
and Scientific Research
University of Babylon
College of Science for Women
Department of Chemistry

Elimination of Methylene Blue Dye From Aqueous Solution Using Fig Leaf Waste

A Thesis

A Thesis Submitted to the Council of the College of Science for Women, University of Babylon as a Partial Fulfillment of the Requirements for the Degree of Master of Science /Chemistry

By

Safaa Talib Kadhim Abed

B.Sc., Chemistry of Science, University of Babylon College of Sciences for Women (2019-2020)

Supervised by

Asst. Prof. Dr. Fouad Fadhil Al-Qaim

2023A.D **1444 A.H**

بسم الله الرحمن الرحيم

﴿وَلَقَدْ آتَيْنَا دَاوُودَ وَسُلَيْمَانَ عِلْمًا وَقَالَا الْحَمْدُ لِلَّهِ الَّذِي فَضَّلَنَا عَلَى كَثِيرٍ مِنْ عِبَادِهِ الْمُؤْمِنِينَ﴾

صدق الله العلي العظيم

النمل: ١٥

Supervisor Certification

I certify thesis entitle

Elimination of Methylene Blue Dye From Aqueous Solution Using Fig Leaf Waste

Was prepared under my supervision at the university of Babylon / College of Science for women as a partial requirement for the degree of master in chemistry/Analytical chemistry.

Signature

Dr. Fouad Fadhil Al-Qaim

Scientific Order: Assistant Prof.

Address: University of Babylon / Collage of

Science for Women

Date: / / 2023

Recommendation of Head of Chemistry Department

According to the available recommendation, I submitting this thesis for Discussion.

Signature of Chemistry Department

Name: Sadiq A. Karim

Scientific Degree: Professor

Address: Head of Chemistry Department

University of Babylon / Collage of Science for Women

Data: / / 2023

Dedication

I dedicate the fruit of my humble effort to whomever I love…

To the Awaited Qaim (may God hasten his relief). To the one who honored me with his father's name, may God have mercy on him.

To the soul that taught me the meaning of losing my martyr brother.

To my beloved mother.

To everyone who taught me crafts and supported my study.

Safaa

ACKNOWLEDGEMENTS

Praise be to **ALLAH**, His Majesty for his uncountable blessings, and to messenger **Mohammed** upon him best prayers and peace, and his pure descendants.

I wish to express my deepest gratitude and appreciation to my supervisor Prof. **Dr. Fouad Fadhil Al-Qaim** for skillful scientific guidance, who always supported my research effort. It is an honor to be one of his students.

I also would like to extend my sincere thanks and appreciation to professor Dr. Ayad Alkaim for his continuous support and encouragement.

I also express my thanks and gratitude to the deanship of the college of science for women department of chemistry, and all my professors who helped me and provided their valuable pieces of advice.

Finally, I would like to express my gratitude to my family for their supporting me in many ways throughout my academic care

Summary

Fig leaf, an environmentally friendly by product of fruit plants, has been used for the first time to treat of methylene blue dye. The fig leaf activated carbon (FLAC) was prepared successfully and used for the adsorption of methylene blue dye (MB). The adsorbent was characterized by Fourier transform infrared spectroscopy (FTIR), X-ray diffraction (XRD), scanning electron microscopy (SEM) and the Brunauer-Emmett-Teller (BET).

In the present study, initial concentrations, contact time, temperatures, pH solution, FLAC dose, volume solution, activation agent and carbonization temperature were investigated. However, the initial concentration of MB was investigated at different concentrations of 20, 40, 80, 120, and 200 mg. L^{-1}. pH solution was examined at these values: pH3, pH7, pH8, and pH11. Moreover, adsorption temperatures of 20, 30, 40, and 50 °C were considered to investigate how the FLAC works on MB dye removal. The adsorption capacity of FLAC was determined to be 24.75 mg. g^{-1} for 0.08 g and 41 mg. g^{-1} for 0.02 g. The adsorption process has followed the Langmuir isotherm model (R^2=0.9841), where the adsorption created a monolayer covering the surface of the adsorbent. Additionally, it was discovered that the maximum adsorption capacity (Qm) was 41.7 mg. g^{-1} and the Langmuir affinity constant (KL) was 0.37 L. mg^{-1}. kinetic study of adsorption experiments showed that the pseudo second order model best describes the kinetic adsorption characteristics. The FLAC, as low-cost adsorbents for methylene blue dye, has shown good cationic dye adsorption performance.

List of contents

List of Tables

List of Figures

List of Abbreviations

Shorten	Full name
AC	Activated carbon
B.D.H	British Drug Houses
BET	Brunauer-Emmett-Teller
C°	Initial Concentration
CAL	Citrus Aurantium leaf
Ce	Equilibrium concentration in solution
Cf	Final concentration
Cs	Equilibrium concentration in solid phase
Ct	Residual concentration of dye at any time
FE-SEM	Field emission scanning electron microscopy
FL	Figs leaf
FT-IR	Fourier Transform Infrared
GL	Grape leaf
Kads1	The pseudo-first-order rate constant
Kads2	The pseudo-second-order rate constant
Kd	Coefficient of distribution
KF	Freundlich constant
KL	Langmuir affinity constant
M	Amount of adsorbent
MB	Methylene blue

PH	Acidic function
Q	Adsorption capacity at various time
Qe	Adsorption capacity at equilibrium
Qm	Maximum monolayer adsorption capacity
Qt	Adsorption capacity at any time
R	Universal gas constant
R%	Removal percentage
R2	Correlation coefficient
T	Temperature
T	Time
UV-Vis	Ultraviolet-Visible Spectroscopy
V	Solution volume in L
W_1	Weight of the original (wet) sample
W_2	Weight of the dried sample
W_3	Weight after heating
W_{ac}	Weight of material after carbonized
W_i	Weight of material before carbonized
XRD	X-ray diffraction spectroscopy
$\Delta G°$	Change in Gibbs free energy
$\Delta H°$	Change in enthalpy
$\Delta S°$	Change in entropy
λ max	Maximum wavelength

Chapter One

Introduction

1. Introduction

1.1 Pollution water

Pollution is the most widespread major problem that has caused a defect in the ecosystem, as well as a dangerous problem that threatens human life. Therefore, it is difficult to obtain pure water in the existence of large amounts of wastewater. It is found that in all industrial countries the ratio of water pollution that affects the human system is increased (Shannon et al. 2008). The most hazardous compounds are heavy metals, oils and dyes. Especially, Organic dyes which are produced in many different local industries for example textile, paper, plastic, leather, food, cosmetic, etc. (Ai and Jiang 2012). Textile dyes have a strong color even in extremely low concentrations. These dyes are non-degradable, bioaccumulation in living organisms and stable toward light, biological and chemical treatments. Additionally, they display high biotoxicity and potential mutagenic and carcinogenic effects (Bao et al. 2011). The dye pollutions in water incline to preclude light penetration and therefore, affect photosynthesis considerably (Banerjee and Chattopadhyaya 2017). Numerous dyes are difficult to remove from contaminated water solutions due to complex structure and synthesis. These dyes are not effectively removed by using traditional techniques (Patidar et al. 2012).

In recent years, efforts have been made to overcome the challenges of wastewater treatment. For wastewater treatment, several techniques have been recognized, including chemical methods such as Fenton oxidation and electrochemical oxidation, physical procedures such as adsorption and membrane filtration, and several biological techniques. (Ruhma Rashid 2021).

These strategies, however, have inherent flaws, prompting researchers to seek out new techniques to fill the void left by previous techniques.

Adsorption was thought to be one of the most promising methods of removing contaminants from contaminated wastewater (Grini and Lichtfouse. 2019). The adsorption process employed a variety of adsorbent materials, including clay minerals, nanomaterials, agricultural wastes, and biological biomasses (Bulgariu et al .2019; Mohammed et al .2020; Labena et al. 2021).

Activated carbon, one of these adsorbents, could be used as a pre-treatment method. Commercial activated carbon, on the other hand, is a type of activated carbon that is used commercially (Dash. 2010). Furthermore, numerous adsorption-related parameters, such as pH, duration, dosage, and pollutant concentration, were identified (Oren and Kaya. 2006).

As a result, this study will cover several types of activated carbon, as well as their preparation techniques and factors influencing the adsorption process, as well as factors influencing the adsorption process and their models and optimization techniques.

1.2 Dyes:

In reality, dyes are organic compounds with three essential groups in their molecules: chromophore, auxochrome, and matrix (Laurent et al. 2010). The chromophore is the dye's active site; it can summarize the spatial localization of atoms absorbing light energy. Chromophore-containing molecules are widely used in surgery, with synthetic dyes increasingly replacing endogenous optical adjuncts (Azzopardi 2017). The chromophore is made up of atom groups, the most common of which are nitro (NO_2), azo (N=N), nitroso (N=O), thiocarbonyl (C=S), carbonyl (C=O), and alkene (C=C). Because electrons in a molecule are excited, the chromophore absorbs electromagnetic waves (Laurent et al 2010). The molecule containing them turns chromogenic (Benaissa 2012). The chromogenic molecule can

only be dyed by adding other groups of atoms known as "auxochrome" (Benaissa 2012). These auxochromic groups allow dyes to be fixed and can change the color of the dye. They can be acidic (COOH, SO3, and OH) or basic (COOH, SO3, and OH) (NH2, NHR and NR2). The remaining atoms of the molecule correspond to the matrix, which is the third component of the dye (Laurent et al 2010). Textile dyes contain functional groups such as carboxylic, amine, and azo groups that are difficult to treat using traditional methods (Temesgen et al 2018).

The most common classes of dyes used in the textile industry are basic dyes, acid dyes, reactive dyes, direct dyes, azo dyes, mordant dyes, vat dyes, disperse dyes, and sulfur dyes (Demirbas 2009), with azo derivatives dyes being the most common class of dyes used today (Forgacs et al. 2004).

1.2.1 Methylene blue

Methylene blue (MB) is a major basic dye that is commonly used in coloring. This dye has the potential to cause permanent eye damage as well as gastrointestinal and skin irritation. MB is a common pollutant in textile wastewater and is widely used in dye houses and the textile industry. Others have investigated the removal of MB from aqueous solutions using low-cost substances (e.g. agricultural wastes) (Eskizeybek et al. 2012; Wang et al. 2015; Asfaram et al. 2016).

This thiazine cationic dye was chosen as a model organic (heterocyclic aromatic) compound because it is known to adsorb more easily onto solids and was used to evaluate the sorbent's behavior for the removal of organic pollutants from its aqueous solutions (Mukheriee et al. 2015). There are numerous dye removal techniques available, such as membrane separation (Katuri et al. 2009; Geckeler and Volchek 1996) degradation by microorganisms and photochemical degradation (Arslan-Alaton et al. 2008) oxidation chemical (Zou et al. 2015) resins for anion exchange

(karcher et al. 2002) coagulation, (Morshedi et al. 2013) Adsorption and flocculation (Markandeya et al. 2015).

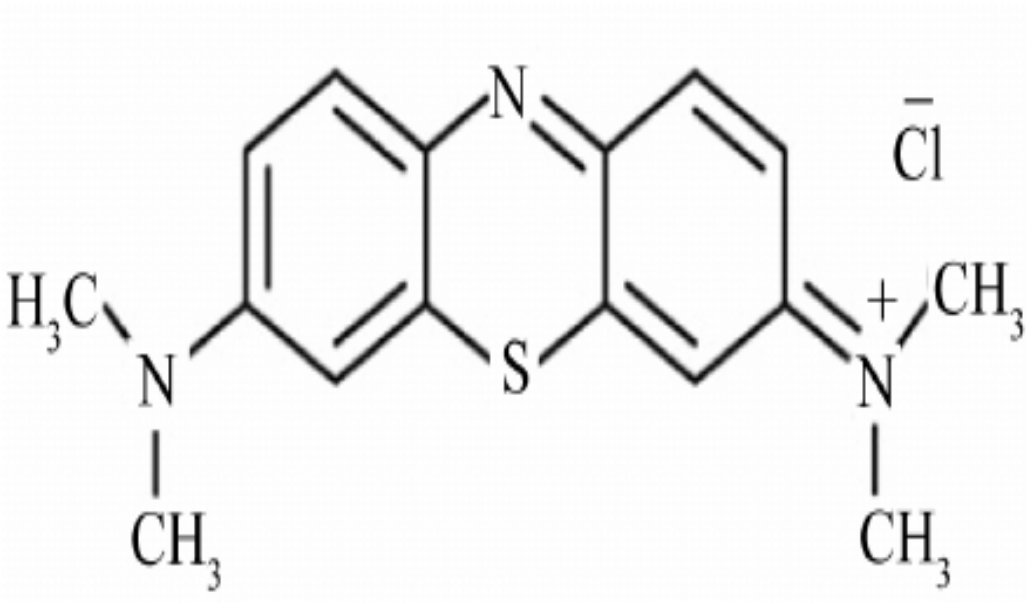

Figure (1-1). Chemical structure of methylene blue

Table (1-1): Physicochemical properties of Methylene blue

Physicochemical properties	Methylene blue
Molecular formula	$C_{16}H_{18}ClN_3S$
Type of dye	Cationic , thiazine type
Molecular Weight	319.85 g/mol
Maximum wavelength (nm)	665nm
Acid dissociation constant (PK_a)	3.8
Solubility in water	43.6 g\L
IUPAC	3,7- bis (Di methyl amino) phenothiazine chloride tetra methylthionine chloride

1.3 Wastewater Treatment Methods for MB's Removal

In general, industrial wastewater treatment technologies are classified into four stages: preliminary, primary, secondary, and tertiary (Sonune and Ghate 2004). The first is a preliminary process used to remove contaminants (such as papers, grits, wood, plastics, cloths, and so on) with minimal effort, as well as the comminution and screening of floating, suspended particles, and oil and grease traps. The primary treatment consists of skimming to remove frothy solids and flotation and sedimentation to remove settleable inorganic and organic impurities. Secondary wastewater treatment entails the microbial breakdown of dissolved organic and colloidal materials, which keeps waste stable (Stasinakis et al 2013). Secondary and advanced treatment strategies that use biological agents (i.e., anoxic, aerobic and anaerobic, facultative, or a combination of these), chemical (Ozonation, fenton reagents, chemical precipitation, ion exchange, photocatalysis, ultrasound, and solar-driven processes), or physical (sedimentation, membrane filtration, coagulation and flocculation, ultrafiltration, nanofiltration, adsorption, and reverse osmosis Treatment strategies for effluents that cannot be removed during secondary treatment (Ye et al 2019; Foo and Hameed 2010; Saratale et al 2021). Similarly, during the treatment of effluent-containing dye, there may be substances left in treated wastewater that require post-treatment, such as the use of bio-waste-derived adsorbent. Previous research reported on the drawbacks of various wastewater treatment technologies, such as lower efficiency, higher capital or operating costs, a large amount of sludge production, and high maintenance costs, which make these technologies unsuitable for economic application (Singh and Arora 2011; Cai et al. 2017). Adsorption technology, on the other hand, provides a wide range of techniques due to its low energy consumption, ease of operation, simple set up, toughness against harmful contaminants, ability to eliminate all dyes, and high efficiency (Tara et al. 2020; Uddin and Baig 2019). Furthermore, no hazardous

materials are produced as a result of using this treatment method. Table (1-2) Advantages and disadvantages various wastewater treatment technologies.

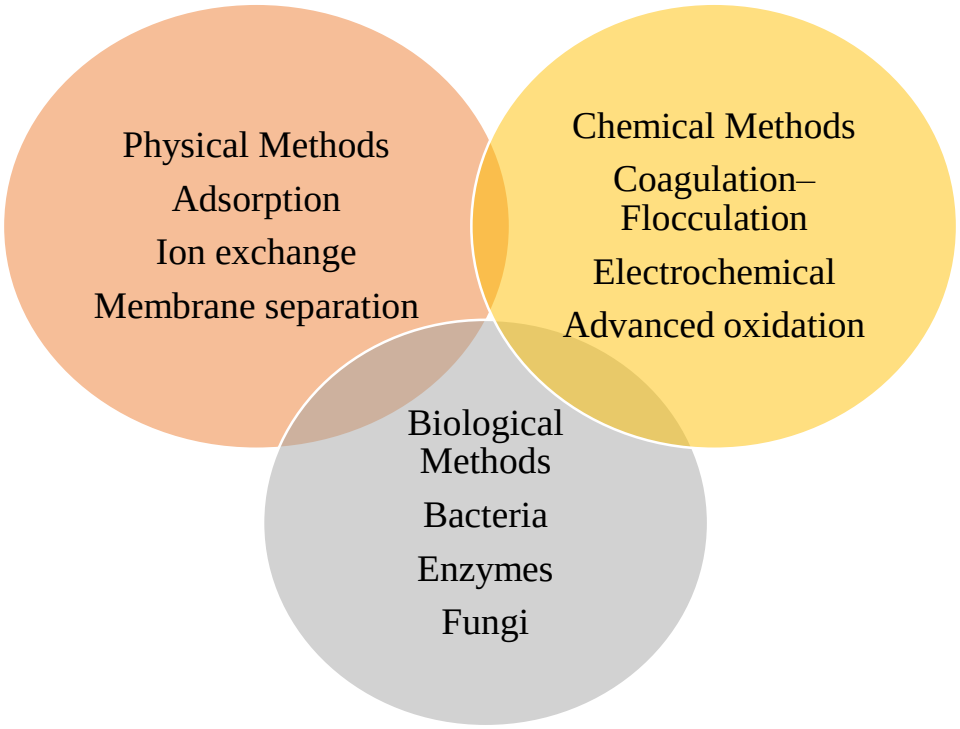

Figure (1-2): Advanced techniques used for wastewater treatment

Table (1-2) advantages and disadvantages various wastewater treatment technologies (Rápó and Tonk 2021).

Technologies	Advantages	Disadvantages
Physical treatments		
Adsorption	▪ Re-generable adsorbent ▪ Efficient for a wide variety of dyes ▪ Simple and flexible	▪ Adsorbents and their regeneration can be expensive
Membrane separation	▪ Effective and useful method	▪ Need periodic replacement ▪ Membrane fouling
Ion exchange	▪ High efficiency and low cost ▪ Able to be regenerated	▪ Not effective to treat all category of dyed
Chemical treatment		
Coagulation–Flocculation	▪ Cost effective ▪ Essential method in textile wastewater treatment	▪ Produces concentrated sludge ▪ pH dependent
Electrochemical	▪ No sludge costs ▪ Does not require addition of chemicals	▪ High electricity costs ▪ Less effective compared to other treatments
Advanced oxidation	▪ Able to remove dye from harsh operating conditions	▪ Expensive ▪ Forms undesired by products ▪ pH dependent

	▪ No sludge generation ▪ Faster reaction kinetics	
Biological treatment		
Bacteria	▪ Easy cultivation ▪ Short lag phase ▪ Eco- friendly and cheap	▪ pH and shock load sensitive
Enzymes	▪ Non- toxic, cost effective and reusable	▪ Amount of enzyme production is limited
Fungi	▪ Applicable for a wide variety of pollutants, environmentally friendly	▪ Long lag phase of growth pH sensitive

1.4 Activated carbon

Activated carbon is a porous carbonaceous substance with numerous applications in desalination, water and wastewater treatment, and air purification due to its unique properties (Yousefi et al. 2019). It is a versatile adsorbent with high porosity and a large surface area that can account for up to 90% of the carbon surface area. (Morin-Crini et al.2019).

The perfect adsorption qualities of activated carbon are due to its outer surface structure, which contains many functional groups such as carbonyl, carboxyl, phenol, quinone, and lactone. These functional groups were reported to be responsible for the contaminants adsorption process into the activated carbon adsorbent material, in addition to the appearance of hydrogen, oxygen, sulphur, and nitrogen. Precision, activation procedures, and thermal purification were used to create these functional groups (AboBakr et al. 2017).

Activated carbon can be made from biomass, olive corn, corn stalks, rice rolls, bagasse, fruit stones, hard shells, fruit pulp, bones, and coffee beans (Abualnaja et al .2021). The raw materials used to make activated carbon should be inexpensive, plentiful, and safe (Jolly et al. 2006).

Furthermore, during initial storage, the mineral concentration and biodegradability of this material should be kept to a minimum (Prauchner et al. 2016). Cellulosic materials are now one of the most commonly used materials in the production of activated carbon.

1.4.1 Commercial activated carbon

Commercial activated carbon, also known as charcoal, is a type of industrial adsorbent due to its ability to remove a variety of contaminants from polluted mediums. Furthermore, activated carbon was distinguished by its thermal stability, large surface area ranging from 500 to 2000 m2/g, good porosity, resistance to bases and acids, low cost, and controllable pore structure. (Mukherjee et al.2015). Granular activated carbon and powdered activated carbon are the two most common forms of activated carbon. The various shapes of commercial activated carbon are depicted in Figure (1-3).

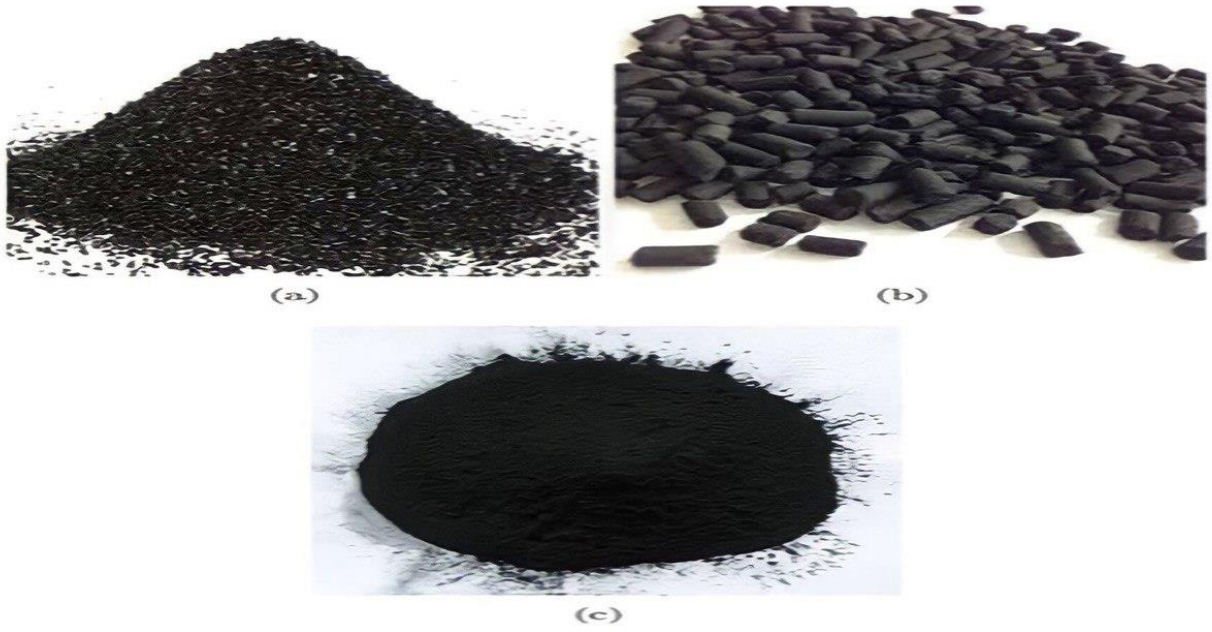

Figure (1- 3): Different types of activated carbon (a) granular, (b) pelletized, and (c) powdered

1.4.2. Biochar

Activated carbon can be made from carbon-rich materials such as lumber, coal, peat, tobacco, nutshells, and lignite (Torretta et al .2017). Agriculture wastes, such as sugarcane bagasse, olive stones, cotton residues, soybean hulls, corn straws, peach stones, pinecones, rice hulls, rice straw, banana peels, apricot stones, corn cobs, bamboo, pulp, and so on, are also carbonaceous sources for the formation of activated carbon (Chan et al .2012; Chen et al .2001; Skodras et al .2007). Previous research, on the other hand, claimed that 40% of activated carbon was extracted from charcoal and that it could remove odor and taste. To produce activated carbon, two continuous stage processes were typically used: carbonization followed by activation; the first stage was performed at high temperatures during the pyrolysis process, and the latter stage was used to improve the pore structure of the activated carbon (Hidayu and Muda .2016; Zubair et al. 2017). According to other research, the stages include a pretreatment process that includes crushing, milling, and sieving to achieve the best size for a successful subsequent process (Alslaibi et al .2013).

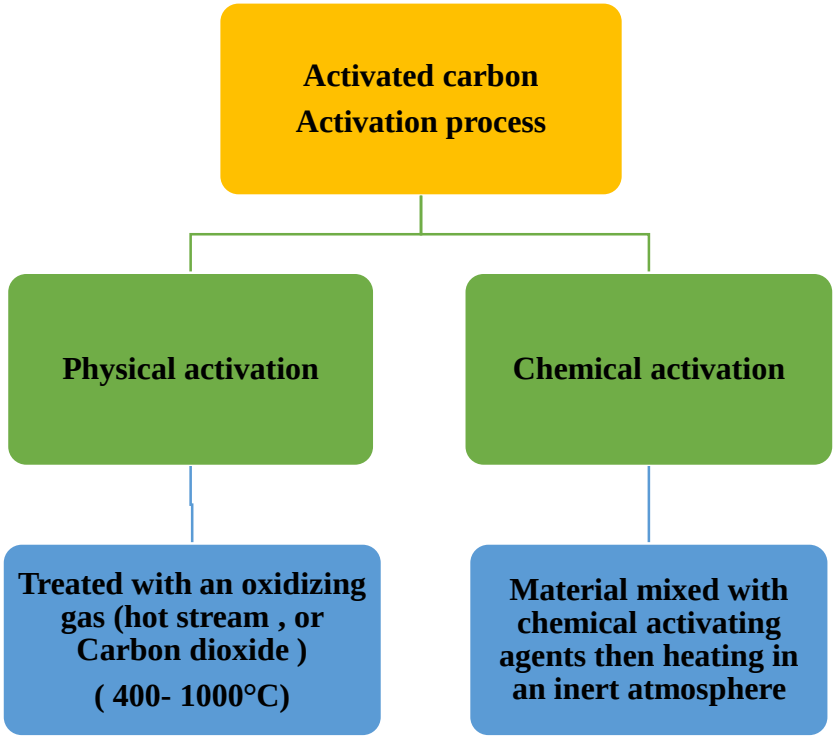

Figure (1-4): Diagram of the process for producing activated carbons via physical or chemical activation.

The chemical and physical activation processes of activated carbons are depicted in Figure (1-4), with chemical activation outperforming physical activation due to its low cost, high surface area of its products, and higher porosity (Allwar. 2012). Chemical activation, on the other hand, requires additional costs for chemical activation agents as well as additional stages of chemical agent washing processes (Shehzad et al. 2015). Microwave-assisted chemical activation increases pollutant adsorption surface area and efficiency. Impregnating activated carbon with chemicals such as metal oxides and hydroxides is another method for increasing removal efficiency. Various characterization techniques, such as scanning electron microscopy (SEM), X-ray diffraction, and surface area, can be used to study the surface and physical properties of prepared materials.

1.5 Activated carbon application

In terms of application, AC has been widely used in water purification, energy storage, and as a catalyst for rapid social and economic development (Elmouwahidi et al. 2017; Karadirek and Okkay 2018; Kumar and Jena 2016; Li et al. 2017; Xu et al. 2018; Zhang et al 2019) because of the importance of AC in so many fields.

Activated carbons were used to remove metals from polluted wastewater due to their large surface area and high pore number. Dyes, phenols, pesticides, humanistic substances, polychlorinated biphenyls (PCBs), detergents, and organic pollutants are all effectively removed from polluted streams by activated carbon (Al- Degs et al. 2006; Carrott et al. 2005; Mourao, et al .2006; Malhas, et al .2002).

Furthermore, the ability of activated carbon to remove color and other pollutants from textile and dye wastes was stated and commercially available in the application. Acidic, dispersed, and basic dyes, for example, were efficiently removed from textile polluted wastewater using filtrasorb circledR activated carbon, whereas direct dyes were not (Mckay et al. 1999). Several studies have reported the ability of activated carbon to remove cationic and anionic dyes such as methylene blue and reactive black (Hameed et al. 2007). The interaction of numerous chemicals with activated carbon, such as sodium dodecyl sulfate, sodium dodecylbenzene sulfonate, or dioctyl sulfosuccinate sodium, helps to increase its adsorption capacity for heavy metals (Ahn, et al .2009; Moerz et al. 2014).

1.6 Preparation of Activated Carbon

Activated carbon is prepared in two main ways:

Activation and carbonization (Ayinla et al. 2019; Kleszyk et al. 2015). Carbonization is used to reduce the volatile content of raw materials by pyrolyzing carbon precursors at temperatures ranging from 300 to 900 °C and producing char with primary porosity and a high fixed carbon content. The goal of activation is to increase AC's specific surface area or pore volume by opening new pores and developing existing ones. Aside from that, activation can change or adjust the surface chemical nature of AC, giving it unique properties. In terms of AC properties, activation is thought to be more important than carbonization. As a result, more emphasis has been placed on its activation.

Physical activation, chemical activation, and physiochemical activation are currently used to produce AC (Arslanoğlu 2019; Fu et al. 2019; Lu et al. 2016; Oginni et al. 2019; Singh et al. 2019). Physical activation is a two-stage process that begins with carbonization in the presence of an inert gas (N_2 or Ar) and ends with activation in the presence of an oxidizing gas (O_2, CO_2, H_2O steam) at temperatures ranging from 800-1200 °C (Balahmar et al. 2017; Danish and Ahmad 2018; Yin et al. 2014). The primary benefits of physical activation over chemical activation are its clean, green production and the absence of secondary waste disposal.

However, the disadvantages of physical activation are related to its high activation temperature, lengthy processing time, low carbon yield, and low specific surface area. The type of carbon precursors, particle size, gas flow, heating rate, carbonization time, and carbonization temperature are the main factors influencing physical activation. Chemical activation, also known as "wet oxidation," is a single-

stage process in which carbonization and activation occur concurrently at temperatures ranging from 450 to 850 °C (González-García 2018).

Chemical activation has a number of advantages, including a low heating temperature, a quick processing time, a high carbon yield, well-controlled porosity, and a high specific surface area (Nayak et al. 2017; Wang et al. 2014; Zhang and Shen 2019). Chemical activation has several drawbacks, including its extreme corrosivity and the unavoidable washing process (Chen et al. 2012; Dai et al. 2018). The main factors influencing chemical activation are the type of activating agent, mixing method, mass ratio of activating agent to carbon precursor, and heating method (Sevilla and Mokaya 2014).

Physio-chemical activation is a combination of physical and chemical processes that begins with the chemical impregnation of carbon precursors with activating agents and ends with physical activation in an oxidizing gas atmosphere. The benefits of physio-chemical activation include controllable textural properties and surface modification. The inherent disadvantages of physio-chemical activation are its complexity and high energy consumption, which limit its widespread application in industry. Chemical activation is regarded as the most promising method for producing AC with excellent performance among these techniques. Furthermore, during activation, the activating agents play critical roles in the formation of pores or surface chemical groups.

1.7 Activation mechanisms of chemical activating agents

During the chemical activation process, many chemical regents have been used as activating agents. Activating agents are classified into four types based on the acidic basic theory and activation mechanism: alkaline, acidic, neutral, and self-activating agents. Different types of activating agents react with cellulose,

hemicellulose, lignin, or polysaccharide in carbon precursor, resulting in a variety of activation mechanisms that should be investigated further for future applications. (Gao et al 2020). Figure (1-5).

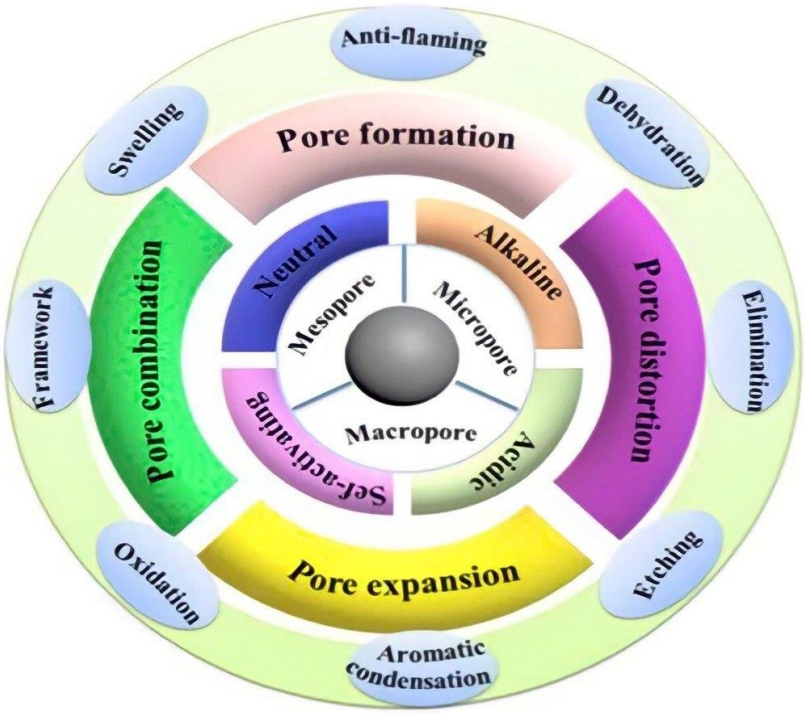

Figure (1-5): Schematic diagram of activation mechanism by alkaline and acidic activating agent. (Gao et al 2020)

1.8 Methods for activation of activated carbon

When obtaining activated carbon, some chemical substances were used as activation agents. The precursor undergoes a variety of reactions depending on the activating agent, which alters the adsorption behavior. Alkaline or acidic and neutral chemical groups are the most often used compounds as possible activator agent

1.8.1 Activation by phosphoric acid (H_3PO_4)

Phosphoric acid, with the chemical formula H_3PO_4, was widely used in the activation of various lignocellulosic materials (Batzias and Sidiras 2007). It is the most widely used chemical in the activated carbon activation process, capable of producing high-porous activated carbon from raw materials. Furthermore, H_3PO_4 is less toxicologically and environmentally hazardous than potassium, zinc chloride, and hydroxide. Furthermore, H_3PO_4 has a low activation temperature, is not volatile, and can form a large number of alkaline or acid-soluble phosphates with elements such as nickel, iron, boron, and others that can be integrated into carbon precursors (Chen et al. 2019). H_3PO_4 was an effective activator agent, with carbon electron micrograph and scanning electron microscope images revealing tunnel-shaped pores formed on the activated carbon surface area.

Furthermore, it had a honeycomb structure that was fully developed as the corners of the cavities were visible (De Rossi et al. 2018).

1.8.2 Activation by zinc chloride ($ZnCl_2$)

Among other activating reagents, zinc chloride was widely used to produce activated carbon, particularly cellulosic and lignocellulosic precursors (Yousefi et al. 2019). During activation, zinc chloride acts as a dampening agent for samples impregnated with this material. The movement of volatile substances through the saturated pores of zinc chloride is not disrupted, and the volatile substances are then released from the activated carbon surface during the activation process. As the mass ratio of zinc chloride increases, the release of volatile substances becomes more accessible, and nitrogen absorption on activated carbon increases. (Arami-Niya et al. 2018). The activation of zinc chloride causes an electrolytic action known as swelling in the molecular structure of cellulose. Furthermore, inflation causes

cellulose molecules to break down and expand different intraand inter-coated cavities, resulting in a larger surface area in activated carbon to Ref (Reddy et al. 2012). Lignocellulosic materials are converted into carbon, hydrogen atoms, oxygen, carbon monoxide, carbon dioxide, methane, and aldehydes during the activation process, and diatomaceous distillates are produced (Anisuzzaman et al. 2016).

1.8.3 Activation by potassium carbonate (K_2CO_3)

Potassium carbonate has the chemical formula K_2CO_3, and it is a well-known activator in the production of activated carbon (Abbas and Ahmed 2016). Using potassium carbonate as an activation agent for dietary supplements is not hazardous, as opposed to potassium and sodium hydroxide, which have negative effects (Budinova et al. 2008). Furthermore, potassium carbonate was found to be a better activating agent than potassium hydroxide, producing more activated carbon yield, surface area, and pore volume. Furthermore, activated carbon produced by potassium carbonate has a higher capacity for adsorption of large molecules such as methylene blue; it also contains less ash and sulfur (Karagoz et al. 2008).

1.8.4 Activation by Sodium Hydroxide (NaOH)

Chemical activation with alkaline materials such as potassium hydroxide and sodium hydroxide results in a large number of microspores on the surface of activated carbon (Martins et al. 2015). Sodium hydroxide has been widely demonstrated to be an efficient activating agent for the production of activated carbon. As a result of possible reactions between the active substances and the organic precursor surface, micropores form on the activated carbon surface. This is due to alkali metal intercalation into the carbon structure, which results in the release of CO, CO_2, and H_2 gases produced by the high-temperature decomposition of

Na_2CO_3 and hydroxyl reduction, respectively. (Martins et al. 2015). After the preparation process is complete, the sodium hydroxide and other substances evaporate, leaving behind activated carbon with a rough surface and various pore sizes. This procedure deals with the formation of the porous structure of activated carbon. These canals serve as appropriate passageways for adsorbent substances to permeate the surface of activated carbon. NaOH initially separates and destroys the graphite layers through oxidation-reduction and then follows them, expanding the pores.

1.8.5 Activation by potassium hydroxide (KOH)

Recently, various potassium compounds such as K_2CO_3 and KOH have been widely used in the production of activated carbon (Hui and Zaini 2015). Among all types of activators, potassium hydroxide was widely used because of its high surface area and ability to produce activated carbon. Also, under the same circumstances, the fine pore size distribution, low environmental contamination, less corrosiveness, and lower cost (Zuo et al. 2016). Chemical activation using phosphoric acid and zinc chloride was used on lignocellulosic materials that had not previously been carbonized. Metal compounds, on the other hand, such as potassium hydroxide, were used to activate coal precursor materials (Yakout and El-Deen 2016). Several studies have demonstrated the effectiveness of KOH-activated carbon in the adsorption of various organic chemicals such as phenols, heavy metals, dyes, and pesticides (Tounsadi et al. 2016). Cavities observed on the surface of activated carbon after the activation process were caused by the evaporation of potassium hydroxide from sites previously occupied by this activator (Uddin et al. 2017). However, KOH-activated carbon has a larger pore volume and surface area; however, it has a lower yield (10-40%) when compared to other activators such as $ZnCl_2$ and H_3PO_4 (Ahmed and Theydan 2014).

1.8.6 Activation by Sulfuric acid (H_2SO_4)

Sulphuric acid is a chemical activator capable of dissolving a wide range of minerals and impurities from activated carbon precursor (Al-Qodah and Shawabkah 2009; Cheng et al. 2016; Olivares-Marn et al. 2012). Chemical purification of dry carbonisation with concentrated sulphuric acid is an alternative method. According to Eq. (Olivares-Marn et al. 2012), sulphuric acid is a highly reactive material that can be combined with organic compounds (such as carbohydrates and other organic materials) to remove water and break down organic precursors into carbon elements.

$$CnH_2nOn + H_2SO_4 \rightarrow nC + H_2SO_4 \cdot nH_2O$$

Sulphuric acid also reacts with the mineral compounds in lignocellulosic material. In fact, because sulphuric acid is used as a cleaning and deashing agent from activated carbon precursors, using H_2SO_4 for carbonisation has some advantages in addition to being low cost (Olivares-Marn et al. 2012). Sulphuric acid activation has been used for a variety of porous structures, in which the sulphuric acid activation process enters the material and results in large and medium porosity on the surface of the activated carbon (Al-Qodah and Shawabkah 2009; Cheng et al 2016; Olivares-Marin et al 2012).

1.9 General Aspects of Adsorption Process

Heinrich Kayse, a German scientist, first used the term "adsorption" in 1881(Choudhary 2017). Environmental adsorption studies on the adsorptive removal of contaminants from the aqueous phase have significantly increased over the past ten years. Because of its simplicity in terms of design, operation, cost, and energy efficiency, it is preferred to alternative approaches. (Tan and Hameed 2017)

Adsorption: Adsorption is a surface phenomenon that involves the adsorption of adsorbate molecules onto adsorbent. The variable surface energy is the fundamental principle underlying the adsorption process. The desire to stabilize surface energy leads to interactions between adsorbent surface and adsorbate molecules. Adsorption of pollutants onto adsorbent is affected by a variety of factors including temperature, solution pH, adsorbate concentration, contact time, coexisting ions, temperature, and adsorbent surface properties such as maximum available surface area, pore size, and pore distribution.

The term absorption is frequently used interchangeably with adsorption. The difference between absorption and adsorption is that molecules in absorption penetrate a three-dimensional matrix, whereas molecules in adsorption attach to a two-dimensional matrix (Qi et al.2017; Sims et al 2019; Al-Ghouti and Da'ana 2020). Because the process is usually reversible (the opposite process is called desorption), sorption is responsible not only for substance extraction but also for substance release. Adsorption can occur as a result of physical forces or chemical bonds, but it is most commonly caused by surface energy. Surface particles that are partially exposed tend to attract other particles into position. There are several classifications for adsorption, and Table (1-3) shows the nature of the bond (physical or chemical bonds) formed between the adsorbent and the pollutant, which describes its characteristics. (Rápó and Tonk 2021).

Table (1-3): The difference between Chemical (primary) bond and physical (secondary) bond (Rápó and Tonk 2021).

Primary bonds	Secondary bonds
Specific, chemical adsorption, chemisorption	Physical adsorption, Physisorption, van der waals Interactions are long-range but weak
Electron transfer, covalent bonding	No chemical bonding or Coulomb interaction
Single layer, slow	Multilayered , fast
Can act at short distances	Occurring on almost any solid surface
Changes the structure of the molecule	The bond energy generated depends on the polarizability
Irreversible	Reversible process

1.9.1 Mechanism of Adsorption onto Activated Carbon

The mechanism of adsorption of various pollutants onto AC must be thoroughly investigated. There are four main processes at work: (a) bulk transfer, (b) film diffusion, (c) pore diffusion, and (d) intraparticle diffusion. Bulk transfer is the instantaneous transport of adsorbate molecules in the solution phase. The adsorbate molecules are transferred to the external surface of the adsorbent molecule by a hydrodynamic boundary in the film diffusion form. Pore diffusion is the transfer of adsorbate molecules into adsorbent pores, lowering the overall adsorption rate. Finally, intraparticle diffusion is the movement of adsorbate molecules from the adsorbent's surface into the pores and along the pore-wall surfaces (Weber and Smith.1987)

The likely adsorption method is shown in Figure (1-6). Their adsorption depends on a number of interactions, including electrostatic, $\pi - \pi$-and n-π interactions, bonding, and electrostatic interactions (Coughlin and Ezra 1968). There are π - π interactions, also called - electron donor-acceptor interactions, between adsorbate molecules and the -electrons of AC. There is a noticeable decrease in the electron density along the margins and surface of the AC where there are electron withdrawing groups. C-cation interactions between the -electron cloud of AC and metal cations are often favorable for the removal of metal cations by AC. For example, (Tran et al. 2015) used pyrolysis to create biochar with properties similar to AC from orange peels. Cadmium ion adsorption onto the surface of biochar followed C-cation interactions, with a maximum adsorption capacity of 114.69 mg/g. Bui and Choi (Bui and Choi. 2010) discovered that the adsorption of metal cations is strongly dependent on the pH of the solution. Hydrogen bonding, in addition to the interactions mentioned above, is important in the adsorption of organic aromatic compounds onto AC. These interactions exist between the

functional groups of the adsorbent, such as N-H in atrazine and O-H in paracetamol, and AC. The O-H groups on the surface of AC form hydrogen bonds with the functional groups in the organic adsorbates, according to one mechanism. The net intensity of the interactions governs the magnitude of adsorption. Some complexes between solvent molecules and surface oxides are formed in this mechanism, which may prevent solute molecules from migrating from the outside to the micropore structure of AC (Jeirani et al 2017). These interactions are highly temperature dependent, as they disappear as the temperature rises due to an increase in the kinetic energy of the adsorbed molecules.

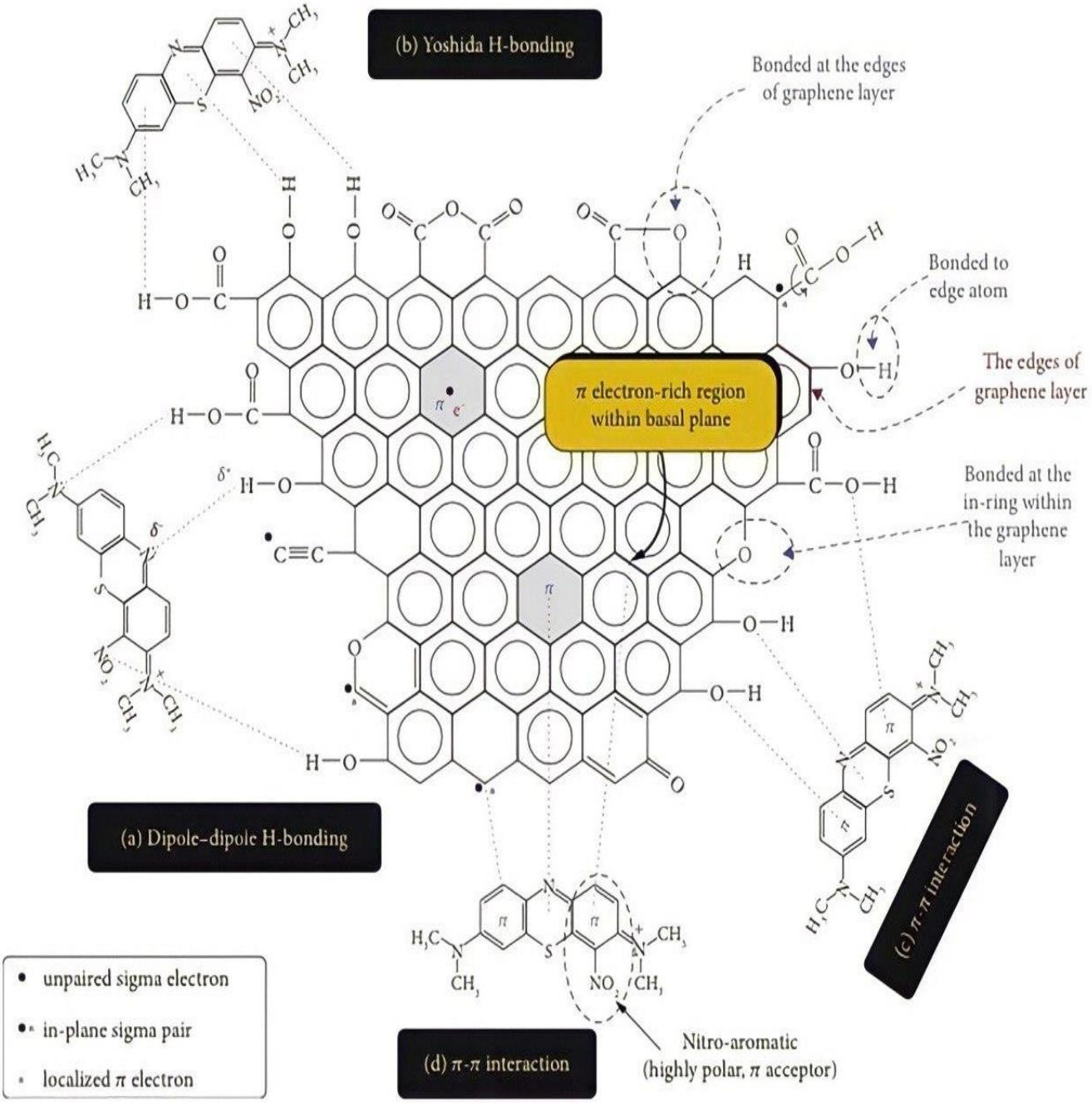

Figure (1-6): Possible interactions between various pollutants and activated carbon (Sharma et al 2022).

1.10 Thermodynamic studied

The adsorption processes are well known to be strongly dependent on the working temperature, which is controlled by thermodynamic parameters such as the standard enthalpy change (ΔH°, J/mol), the standard entropy change (ΔS°, J/mol), and the standard free Gibbs energy change (ΔG°, J/mol). (Tran et al. 2020).

These parameters are computed from the Gibbs–Helmholtz equation:

$$\Delta \boldsymbol{G}^{\circ} = \Delta \boldsymbol{H}^{\circ} - \boldsymbol{T}\Delta \boldsymbol{S}^{\circ} \quad (1\text{-}1)$$

Because Gibbs free energy, enthalpy, and entropy are state functions, G, H, and S are affected by the adsorption system's final and initial states. Because Gibbs free energy, enthalpy, and entropy have broad properties, it is important to consider the amount of substance that these thermodynamic parameters correspond to (Chen et al.2021) The values of entropy (S) and enthalpy (H) can be increased or decreased during dye adsorption as the temperature rises.

1.11 Adsorption Isotherm

Adsorption isotherms aid in the identification of the mechanism of adsorbate molecule adsorption onto the adsorbent. Models can also help determine an adsorbent's maximum adsorption capacity. The type of interactions between adsorbate and adsorbent, which can be easily determined using the Langmuir and Freundlich isotherm models, determines whether adsorption is mono-layered or multilayered. In addition to these two, the Temkin, Redlich-Peterson, and Dubinin-Radushkevich isotherm models are frequently used. (Sharma et al.2022)

1.11.1 Langmuir Isotherm Model.

The Langmuir model is an empirical model that assumes monolayer adsorption, which occurs at similar sites, as illustrated in Figure (1-7). Even at adjacent sites, the adsorbed molecules have no side interactions. In that model, adsorption is homogeneous (Al-Ghouti and Da'ana 2020). Because the Langmuir model describes chemisorption, the adsorbate molecules react with the adsorbent surface. This model's equations have both linear and nonlinear forms, which are shown below.

$$qe = \frac{qm\,Ka\,Ce}{1+Ka\,Ce} \quad [\text{Non – linear form}] \quad (1\text{-}2)$$

$$\frac{Ce}{qe} = \frac{Ce}{qm} + \frac{1}{Kaqm} \quad [\text{linear form}] \quad (1\text{-}3)$$

where qe is the adsorption capacity of adsorbent at equilibrium in mg/g; qm represents the maximum adsorption capacity in mg/g; Ka is the Langmuir constant in L/mg; and Ce is the equilibrium concentration of adsorbate in mg/L

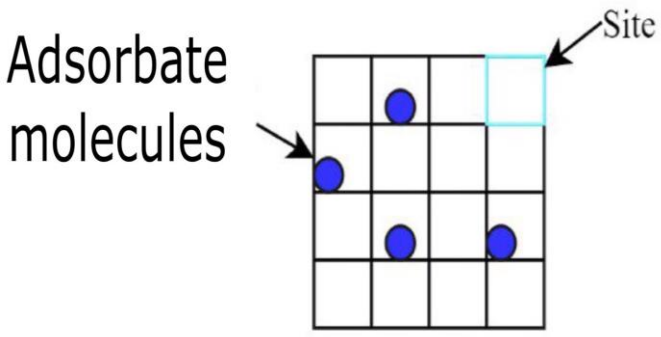

Figure (1-7): The adsorbent surface (Husien et al. 2022)

1.11.2. Freundlich Isotherm Model.

The Freundlich isotherm model, as opposed to the Langmuir isotherm, assumes adsorption of adsorbate molecules onto energetically heterogeneous sites. This model explains adsorbate's multilayered adsorption. (Sharma et al 2022).

The nonlinear equation a can be used to represent this model.

$qe = K\text{f Ce}^{1/n}$ (1-4)

The Freundlich isotherm model's linearized form is

$\ln qe = \ln Kf + \frac{1}{n} \ln Ce$ (1-5)

where qe is the amount of metal ion adsorbed at equilibrium time (mg/g), Ce is the equilibrium concentration of dye in solution (mg/L), Kf is the capacity of the adsorbent, and n is the intensity of adsorption constant for Freundlich. The plot of ln qe versus ln Ce is employed to determine the Kf and n from intercept and slope, respectively.

1.12 Adsorption Kinetics.

The adsorption kinetic models are generalized by a number of governing mechanisms such as mass transfer coefficient, chemical reaction, or diffusion control. Kinetic studies aid in determining the best reaction conditions for a full-scale batch process adsorption experiment. Adsorption kinetics shows the rate of solute uptake and the mechanism by which this rate governs the residence time of adsorbate at the solution interface. A variety of models, including pseudo-first-order, pseudo-second-order, intraparticle diffusion model, and Elovich model, can be used to analyze kinetic data. (Sharma et al 2022).

1.12.1 Pseudo-First-Order Kinetics.

The adsorption at the solid-liquid interface is explained by a pseudo-first-order kinetic model. The linearized form of the pseudo-first-order kinetic model is (de Luna et al. 2013):

$$\text{Log (qe – qt)} = \log qe - \frac{k1}{2.303}t \quad (1\text{-}6)$$

where qe and qt represents the adsorption capacity of adsorbent at equilibrium and time t in mg/g, respectively, k1 is the pseudo first-order rate constant, and t is the contact time (minute). Linear plot of log (qe-qt) versus t gives the value of k1 and qe which can be calculated from its slope and intercept, respectively

1.12.2. Pseudo-Second-Order Kinetics

The pseudo-second-order kinetic model assumes that chemical interactions between adsorbate and adsorbent molecules control the rate-limiting step in adsorption. The following equation can explain this model's differential form (Ho and Mckay 1999; Sharma et al. 2017)

$$\frac{dqt}{dt} = k_2 (qe - qt)^2 \quad (1\text{-}7)$$

where k2 represents the pseudo-second-order rate constant (g (mg min)-1). The linearized form of this model is (Sharma et al 2022):

$$\frac{t}{qt} = \frac{1}{K2qe2} + \frac{1}{qe}t \quad (1\text{-}8)$$

Linear plot of t/qt versus t gives the value of qe and k2 which can be calculated from its slope and intercept, respectively.

1.13 Literature review

According to the previous studies, utilization of fig leaves in terms of adsorption dyes has not reported yet. However, the present study has compared with some other publications on different plant leaves for adsorption of methylene blue as reported in Table :(1- 4)

Commonly used as a reference dye in adsorption investigations is methylene blue. It has been claimed that using too much methylene blue can directly oxidize hemoglobin, leading to methemoglobinemia. Additionally, it can lead to hemolysis-related issues, particularly in newborns. Continual exposure may cause noticeable anemia (Kadhom et al. 2020). After being dried, the residual pineapple leaves were put in a 1:1 ratio to a 500 mL beaker with 136.28 g/mol of $ZnCl_2$ as an activator agent. This mixture was then permitted to soak for 24 hours at room temperature. Throughout this time, a glass rod was occasionally used for stirring. After that, it was carbonized for an hour at 500 °C and dried for 24 hours at 110 °C. The ability of the activated carbon to efficiently remove dye was evaluated using methylene blue (MB). The maximum adsorption capacity was 288.34 mg. g^{-1}.

In other study, the grape leaf has been used to create the activated carbon. The grape leaves are thoroughly cleansed with distilled water before being dried in an oven for three hours at 150° C. It was then thermally activated for two hours at 500 °C in a nitrogen-filled electric furnace (Mousavi et al. 2022). With a starting concentration of 100 mg. L^{-1}, an adsorbent concentration of 12.5 g. L^{-1}, a pH solution of 11, and a time period of 90 minutes, the maximum adsorption capacity was 0.2 mg/L and the removal efficiency was 97.4%.

The Ensete ventricosum midrib leaf (EVML) was used as the optimal adsorbent in a study to remove methylene blue from synthetic water (Mekuria et al. 2022). The

adsorbents were crushed with a mortar and pestle and then sieved to a 300 m mesh size. Then, 50 g of the adsorbent was added to a 250 mL flask containing 0.1 M HCl and stirred for 6 hours to remove the colored components. Over a broad pH range, it was discovered that EVML adsorbents have noticeably high MB adsorption capacity of 35.5 mg. g^{-1}. Instead of using activated carbon, the necessary adsorbent was generated as ash from banana leaves (Alam et al. 2022). Under the following conditions, methylene blue dye was subjected to adsorption: 23.9 mg. 100 mL^{-1} of adsorbent dose, 3 hours of shaking time, and 356 rpm shaking speed. To get the greatest reduction of MB (93.75%), all these variables were statistically analyzed (Alam et al. 2022). The same study found that when banana leaf ash was compared to other carbon sources, it had the maximum adsorption capacity, up to 128.5 mg. g^{-1}, while the range for other materials was between 73.8 and 93.6 mg. g^{-1} (Alam et al. 2022).

According to the findings of the other study, banana leaves were chemically activated to create activated carbon, in which they were then impregnated with H_3PO_4 and burned at three different temperatures of 450, 550, and 600 °C (Martín-González et al. 2013). The end product, activated carbon, was utilized to batch-process methylene blue absorption. The dynamic experimental data were modeled using pseudo-second-order kinetic models utilizing non-linear regression, while the equilibrium experimental data were fitted to be correlated to the Langmuir model (Martín-González et al. 2013). The highest adsorption capacity was found to be between 19.08 and 48.01 mg. g^{-1}, while the removal percentage ranged between 40 and 90% in less than 20 minutes (Martín-González et al. 2013).

Agave salmiana leaves have been reacted with phosphoric acid to produce microwave-activated carbon (Canales-Flores and Prieto-García 2020). The samples were cleaned in distilled water, allowed to dry in the sun for 72 hours, then crushed and sieved to create particles of 0.3 to 1 mm diameters. Prior to activation, the

precursors were pyrolyzed with nitrogen gas at 500 °C in a muffle furnace. The materials that resulted were then H_3PO_4 impregnated (Canales-Flores and Prieto-García 2020). Activated carbon showed significant MB removal efficiency of 72% and an adsorption capacity of 89.3 mg. g^{-1} as a result of the activation agent and microwaves (Canales-Flores and Prieto-García 2020).

A low-cost biosorbent known as saccharum arundinaceum leaf powder (PSAL), which is derived from agricultural waste, can be used to remove MB from wastewater in the textile, printing, and industrial industries. The dried powder is first soaked in acetic acid and hydrogen peroxide before being washed with water to create activated carbon. The samples were then dried at room temperature after that (Halysh et al. 2020). Methylene blue's equilibrium adsorption and kinetics were examined using batch studies (MB). The largest amount of MB dye that could be adsorbed was 25.4 mg. g^{-1} in alkaline media (pH 10), where it was more easily absorbed.

Peels from the cucumber plant, Cucumis sativus, were utilized as an adsorbent for the MB (Shakoor and Nasar 2017). By increasing the adsorbent dosage, the removal efficiency rose until it optimally reached 85% at 6 g. L^{-1}. Subsequent dosage increases only slightly improved the efficiency. However, as the dosage of adsorbent was increased, the adsorption capacity dropped. After one hour of contact, the adsorption capacity achieved its equilibrium value of 21.45 mg. g^{-1}.

Table (1-4): Experimental conditions and maximum adsorption capacity for numerous leaves waste materials as a low cost adsorbents compared with FLAC.

Leaves-source	Reagent used	MB Conc. (mg. L^{-1})	AC/solution (g/mL)	Treatment time (min)	(Q_{max}) mg/g	References
Fig leaf	H_3PO_4	80 mg. L^{-1}	0.8/25	60 min	41.67mg/g	The present study
Pineapple leaf	$ZnCl_2$ 500 °C	50 mg. L^{-1}	0.5/50	15 min	288.34 mg/g	(Mahamad et al. 2015)
Grape leaf	No reagents (500 °C for 2 hours)	100 mg.L^{-1}	1.25/100	90 min	[a]0.2 mg/L	(Mousavi et al. 2022)
Enset leaf	HCl (no carbonization)	10 mg. L^{-1}	2.5/1000	60 min	35.5 mg/g	(Mekuria et al. 2022)
Banana leaves	H_3PO_4 (450, 550 and 600 °C)	2.5 mg. L^{-1}	0.0035/25	60 min	19-48 mg/g	(Martín-González et al. 2013)
Agave salmiana leaves	H_3PO_4 (500 °C for 4 hours)	50 mg. L^{-1}	0.2/50	180 min	95.5 mg/g	(Canales-Flores and Prieto-

						García 2020)
Sugarcane leaves	CH3COOH/H_2O_2 70:30	300 $mg.L^{-1}$	0.4/50	300 min	36.5 mg/g	(Halysh et al. 2020)
Cucumis sativus peels	No reagent	100 $mg.L^{-1}$	0.4/100mL	60 min	21.45 mg/g	(Shakoor and Nasar 2017)

[a] It was written as it.

1.14 Aim of the study:

1- To preparation activated carbon from fig leaf using H_3PO_4 activation agents.

2- To investigate the effect of the activation agents, pH, carbonization temperature, solution volume, initial concentration, contact time and FLAC amounts.

3- Compare FLAC with others plants leaves (Grape leaf and citrus Aurantium leaf) activated carbon.

4- To study the surface properties in terms of adsorption model and heat transfer.

Chapter Two

Experimental Part

Experimental Part

2-1 Chemicals and Materials

The Chemicals used in this work are shown in Table (2-1)

Table (2-1): Chemicals and Materials used in the study, purity, and their manufacturers

NO.	Chemicals and Materials	Formula Compound	Purity%	Manufacturer
1.	FIG Leaves (powder)	----------	----------	Collected from a farm in Babylon
2.	Citrus aurantium leaves (powder)	----------	---------	Collected from a farm in Babylon
3.	Grape leaves (powder)	----------	---------	Collected from a farm in Babylon
4.	Phosphoric acid	H_3PO_4	85	Sigma-Aldrich
5.	Sulfuric acid	H_2SO_4	99	(B.D.H)
6.	Hydrochloric acid	HCl	AnalaR	(B.D.H)
7.	Sodium hydroxide	NaOH	99.9	(B.D.H)
8.	Methylene blue	$C_{16}H_{18}ClN_3S$	99.9	Sigma- Aldrich

2.2 Instruments and Equipment

There are several techniques used in the current study, most of them are listed in table (2-2).

No.	Instrument	Model	Company supplied	Location
1	UV-Visible spectrophotometer, Single beam	UV mini-1240	Shimadzu, Japan	College of science for Women – Babylon University
2	UV-Visible spectrophotometer, Double beam	UH4150	Hitachi, Japan	College of science for Women – Babylon University
3	FTIR spectrophotometer	8400S	Shimadzu, Japan	College of science for Women – Babylon University
4	Field-Emission Scanning electron microscope (SEM)	MIRA3	TESCAN, Czechia Republic	University of Tehran
5	X-Ray diffraction (XRD)	D2 Phaser	Bruker AXS Gmbh, Germany	University of Tehran
6	BET surface area analyzer	NanoSORD	Haskarsazan Iran	University of Tehran

7	Shaker water bath	CL002	K&K Scientific, Korea	College of science for Women – Babylon University
8	Muffle furnace	42127	Aurora, IL USA	College of science for Women – Babylon University
9	Oven	LDO- 060e	Labtech , Korea	College of science for Women – Babylon University
10	PH- meter	Lovibond@ water testing	Hanna, Romania	College of science for Women – Babylon University
11	Centrifuge	CL008	JANETZI-T5, Belgium	College of science for Women – Babylon University

2.3 Materials and methods

2.3.1 Materials collection and pretreatment

The fig leaves used in the current project came from waste at an Iraqi fig farm in Babylon, Iraq. After being cleaned with distilled water, fig leaves were allowed to air dry. The crushed, undersize particles from the sieving of the dried fig leaves through a 75 mesh screen were employed for the subsequent stages. H_3PO_4, H_2SO_4 and NaOH were provide from Merck as activation agents. Methylene blue ($C_{16}H_{18}ClN_3S$), a basic (cationic) dye, is the adsorbate model utilized in adsorption studies; it was purchased from Dyestuffs and Chemicals Co. (China). Analytical grade chemicals were utilized exclusively; no further action was required.

2.3.2 Activated carbon preparation

The fig leaves (FL) were collected as crispy (i.e. dry), washed with water strongly (3-5 times) to remove the dust and other solid matters then dried. Afterwards, the fig leaves were crushed using electric grinder and sieved for 75 mesh. A 7.5 mL deionized water was added in beaker contained 3 g fig leaves powder. And then, 2.5 mL of concentrated H_3PO_4, H_2SO_4 and NaOH was added, separately and stirred continuously until all powder immersed well. It was left for 2 hours then washed with water for several time ">10 times" until pH close to 6.6 as tested using pH meter "Lovibond@ water testing ". After that sample was dried in normal conditions for 1-2 nights. Dried powder was then carbonized in furnace at 350°C for two hours. Full experimental methodology has been presented in Figure. (2-1)

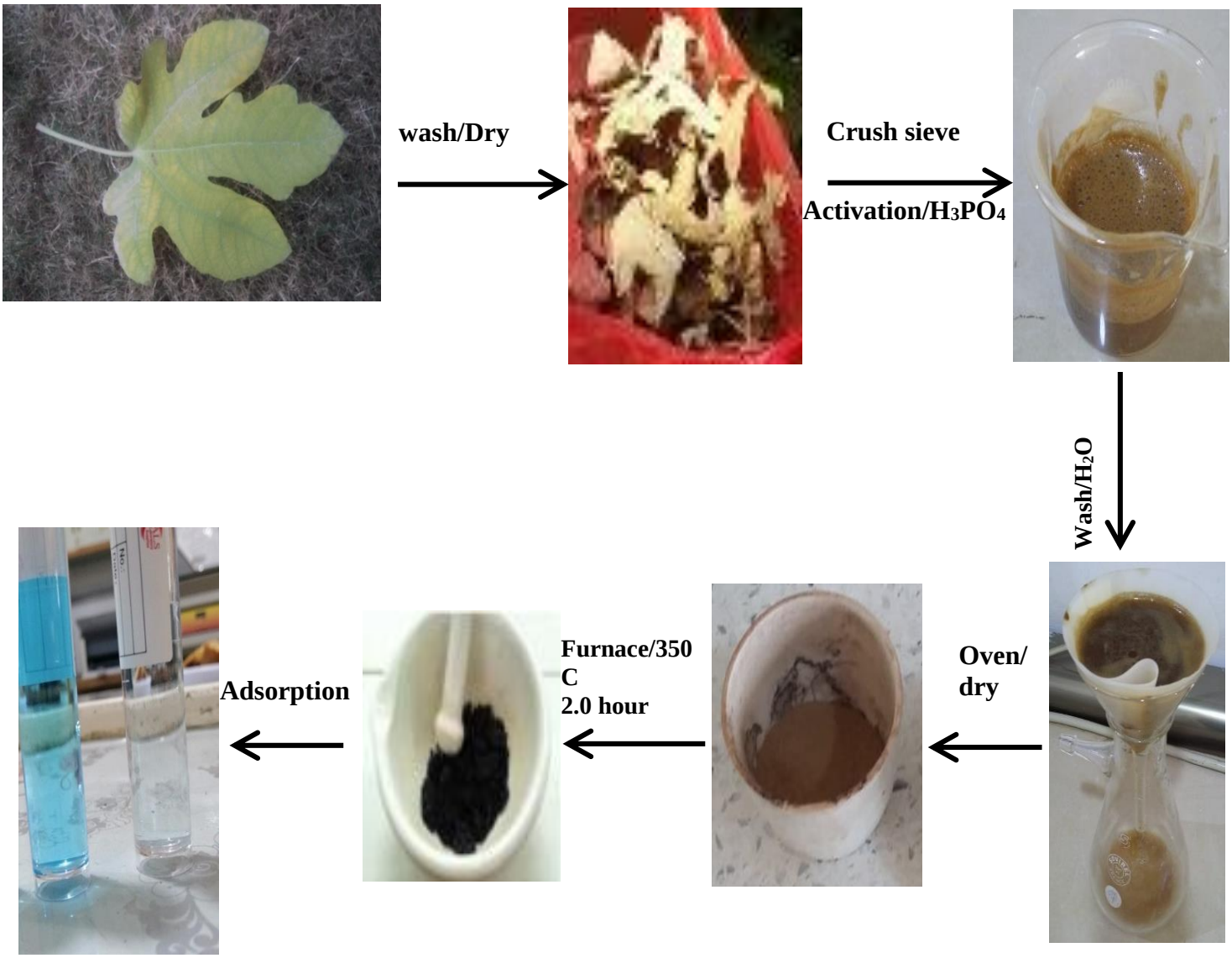

Figure (2-1): Full experimental methodology for adsorption of methylene blue dye.

2.4 Characterization and Measurements of the FLAC

Fourier transform infrared (FTIR) spectroscopy was used to determine the presence of functional groups and chemical interaction for the treated fig leaf activated carbon using a Perkin Elmer Spectrum One spectrometer with universal attenuated total reflectance sampling for the range of 400-4000 cm^{-1}. Cu K radiation with a wavelength of 1.54184, X-ray powder diffraction (XRD) in a Bruker D2 Phaser 2nd Gen apparatus, and a Lynxeye detector (ID mode). The adsorbent was characterized also by scanning electron microscope (SEM) and the specific surface area by the Brunauer-Emmett-Teller (BET).

2.4.1 Ultraviolet–visible (UV-Vis) spectroscopy

To ensure that Fig leaves Activated carbon has worked successfully and to study the optical properties, the UV-Visible spectrometry was used. The spectrum of the dye solution was measured using a Double – beam Uv-vis spectrophotometer. The wavelength range extended from 200-800 nm, which enabled the UV and visible regions to be monitored simultaneously. The wavelength was set at 665nm. All absorbance measurements were recorded using a single – beam and Double – beam UV-VIS spectrophotometer.

2.4.2 Fourier Transform Infrared (FT-IR) Analysis:

Fourier-transform infrared spectroscopy is a type of vibrational spectroscopy that is widely used and one of the oldest approaches for analyzing various molecules. One of the most important components of an FTIR spectrometer is the interferometer, which generates an interferogram that is then Fourier-transformed into a typical spectrum (Baker et al 2014; Subramanian and Rodriguez-Saona 2009). In FTIR, IR radiation is absorbed by functional groups in the analyte, causing atoms

bonded with covalent bonds to vibrate. Rising peaks in the IR spectrum are produced by vibrational excitations that result in a change in the bond dipole. Bond vibrational modes occur in molecules containing two or more atoms and can involve changes in bond length (symmetrical, asymmetrical) or bond angle (bending, e.g., deformation, rocking, wagging, and twisting. (Rohman, 2019; Severcan et al 2012; Rohman and Salamah 2018). FTIR spectra were recorded using the FTIR instrument (Shimadzu. 8400S) in the 4000-400 cm^{-1} frequency range. Dried FLAC and KBr powder them was mixed (1 mg) of sample with (10mg) KBr powder in an agate mortar. The mixture was pressed into a pellet under 1 ton, and the spectrum was recorded immediately.

2.4.3 X-Ray diffraction (XRD)

X-ray diffraction is a powerful nondestructive, quick qualitative and quantitative analysis of pure and multi-component mixtures that requires minimal sample preparation. XRD identifies the long-range order (ie, the structure) of crystalline materials and the short-range order of non-crystalline materials. (Khan et al .2019). Cu K radiation with a wavelength of 1.54184, X-ray powder diffraction (XRD) in a Bruker D2 Phaser 2nd Gen apparatus, and a Lynxeye detector (ID mode)

2.4.4 Field Emission Scanning Electron Microscopy (FE-SEM):

The field emission scanning electron microscope (FE-SEM) is a powerful tool for characterizing sample morphology such as grain size, particle size, particle distribution, crystal defects, and surface structure. Because it uses electrons as the

probe, FE-SEM has a large depth of field, higher resolution, and more control over the degree of amplification. (Koop et al 2007).

2.4.5 Nitrogen adsorption-desorption isotherms (BET)

Brunauer-Emmett-Teller (BET) nitrogen adsorption/desorption technique is applied for activated carbon characterization. BET is a technique that is generally used to determine porosity and surface area of microporous and mesoporous materials. Porosity and surface area are the key parameters in FLAC studies as they indicate the structural properties of FLAC.

2.5 Preparation of the Methylene blue dye (MB) solution and determine of Maximum Wavelength (λmax).

2.5.1 preparation of Methylene blue dye

A standard solution of Methylene blue at 1000 mg. L^{-1} was prepared by dissolving a specific weight of (0.1gm) solid dark green powder dye in a 100 mL of distilled water with stirring to complete the dissolving and complete the volume.

2.5.2 Determination of optimum wavelengths (λmax)

To determine the maximum wavelength of the MB dye solution was taken in the range (200-800) nm. The maximum wavelength of the dye solution was determined from its highest absorption in the UV-Visible spectrum, which was found at the wavelength (λmax=665nm)

2.6 Effect of different parameters on the adsorption process:

2.6.1 Effect of Initial Dye Concentration:

A 25 mL of different concentrations of methylene blue dye solution (20, 40, 80, 120 and 200 mg. L^{-1}) were mixed with 0.08 g of adsorbents and subjected to the shaker for 60 min at room temperature. The samples were centrifuged at 3000 rpm after adsorption, and the filtrates were examined. Using a UV-vis spectrophotometer and the calibration curves, the dye concentrations in the water were initially and residually measured at their highest absorbance wavelengths (665 nm). The following equations (1,2) were used to calculate the removal% and adsorption capacity of MB dye:

$$R\% = \frac{C_0 - C_t}{C_f} \times 100\ \% \qquad (2-1)$$

$$Q = \frac{(C_0 - C_t)}{m} \times V \qquad (2-2)$$

where the starting dye concentration (C_0) (measured in mg. L^{-1} for MB), the residual concentration (C_t) was measured for the MB dye in mg. L^{-1} and the final dye concentration (C_f) (measured in mg. L^{-1} for MB) are given.

R% is the percentage of MB dye solution removed after adsorption; Q is the adsorption capacity (mg. g^{-1}) at various times; and m is the amount of FLAC (g). In order to create the necessary dye solutions, stock MB solution (1000 mg. L^{-1}) was dissolved in deionized water. Adsorbent was added in 25 mL of wide spectrum of concentrations (20, 40, 80, 120 and 200 mg. L^{-1}) MB solution together with 0.08 g to test the effect of initial concentration of dye on adsorption removal and adsorption capacity

2.6.2 Effect of contact time

A 25 mL of different concentrations of methylene blue dye solution (20, 40, 80, 120 and 200 mg. L^{-1}) with different times (10,20,40,60,80,100 and 120 min.) were mixed with 0.08 g of adsorbents and subjected to the shaker at room temperature. The samples were centrifuged at 3000 rpm after adsorption, and the filtrates were examined. Using a UV-vis spectrophotometer and the calibration curves, the dye concentrations in the water were initially and residually measured at their highest absorbance wavelengths (665 nm).

2.6.3 Effect of FLAC amount

Different amounts of FLAC (0.02, 0.04, 0.06, 0.08 and 0.1 g) have been investigated on 80 mg. L^{-1} of MB dye and subjected to the shaker for 60 min at room temperature. The samples were centrifuged at 3000 rpm after adsorption, and the filtrates were examined. Using a UV-vis spectrophotometer and the calibration curves, the dye concentrations in the water were initially and residually measured at their highest absorbance wavelengths (665 nm).

2.6.4 Effect of pH

At a pH of (3, 7, 8, 11), with an 80 mg. L^{-1} concentration of MB dye, the impact of the pH was shown. Using solutions of 1 M HCl and 1 M NaOH, the pH of the solution was changed. A 0.08 g of adsorbent was added to 25 mL of a 80 mg. L^{-1} solution of MB dye at 60 min. The samples were centrifuged after adsorption then examined

2.6.5 Effect of Temperature

Temperature has been investigated on adsorption of methylene blue dye in four different temperature values which are 20, 30, 40 and 50°C. The concentration of

MB dye was 80 mg. L^{-1} and the adsorbent was 0.08 g and subjected to the shaker for 60 min at room temperature. The samples were centrifuged at 3000 rpm after adsorption, and the filtrates were examined. Using a UV-vis spectrophotometer and the calibration curves, the dye concentrations in the water were initially and residually measured at their highest absorbance wavelengths (665 nm).

2.6.6 Effect of volume solution

The effect of volume solution has been investigated at different values of 25, 50 and 100 mL at fixed conditions 80 mg. L^{-1} MB and 0.08 g FLAC. The samples were centrifuged at 3000 rpm after adsorption, and the filtrates were examined. Using a UV-vis spectrophotometer and the calibration curves, the dye concentrations in the water were initially and residually measured at their highest absorbance wavelengths (665 nm).

2.6.7 Effect of Activation agent:

The effect of the activation process was presented in five aspects: AC1: only burn; AC2: pristine powder; AC3: impregnated in H_3PO_4; AC4: impregnated in NaOH; AC5: impregnated in H_2SO_4 have been applied to select the best agent for 80mg. L^{-1} and 0.08 g of adsorbent and subjected to the shaker for 60 min at room temperature. The samples were centrifuged at 3000 rpm after adsorption, and the filtrates were examined. Using a UV-vis spectrophotometer and the calibration curves, the dye concentrations in the water were initially and residually measured at their highest absorbance wavelengths (665 nm).

2.6.8 Effect of carbonization temperature:

The effect of the carbonization temperature was studied in four different furnace temperature (150 °C, 250 °C, 350°C, 500 °C) have been applied to select the best agent for 80 mg. L^{-1} and 0.08 g of adsorbent and subjected to the shaker for 60 min at room temperature. The samples were centrifuged at 3000 rpm after adsorption, and the filtrates were examined. Using a UV-vis spectrophotometer and the calibration curves, the dye concentrations in the water were initially and residually measured at their highest absorbance wavelengths (665 nm).

2.7 Carbon source (Investigation the removal% and adsorption capacity using different plant leaves):

A 25 mL of methylene blue dye solution (80mg. L^{-1}) and 0.08 g of adsorbents from prepared (Fig leaf AC (FLAC), Grape leaf AC (GLAC), citrus Aurantium leaf AC (CAL) and subjected to the shaker for 60 min at room temperature. The samples were centrifuged at 3000 rpm after adsorption, and the filtrates were examined. Using a UV-vis spectrophotometer and the calibration curves, the dye concentrations in the water were initially and residually measured at their highest absorbance wavelengths (665 nm).

2.8 Determine of point of zero charges:

The point of zero charges (pH_{pzc}) is determined by 50 mL of water and put it in series of conical flasks and the initial pH (pH_i) of the solutions was roughly adjusted between (3-11) by adding either 0.1M HCl or NaOH. Then added of 0.1g of FLAC and put the solutions in shaker for 120 min at room temperature then record the pH_f values after separated by centrifuge.

2.9 Determine the yield, moisture content and volatile production of Activated carbon:

In this experiment, the weight of the FG Leaves impregnated with phosphoric acid (H_3PO_4) was taken, after that the sample was placed in a burning furnace at a temperature of 350 °C for two hours, then the production yield of the activated carbon was found through the following equation.

$$\text{Yield (wt\%)} = \frac{Wac}{wi} \times 100\% \quad (2\text{-}3)$$

Where W_i the weight of material before carbonized and the W_{ac} the weight of material after carbonized.

The activated carbon was placed into a pre-weighed ceramic crucible and dried at 150 °C for 3 h. The sample was weighed after cooling down and the moisture content was calculated by equation:

$$\text{Moisture (wt\%)} = \frac{W1-W2}{W1} \times 100\% \quad (2\text{-}4)$$

where W_1 is the weight of the original (wet) sample and W_2 is the weight of the dried sample. The dried sample was heated at 950 °C for 30 min in a muffle furnace and the volatile matter was calculated by equation

$$\text{Volatile matter (wt\%)} = \frac{W2-W3}{W2} \times 100\% \quad (2\text{-}5)$$

where W3 is the weight after heating

Chapter Three

Results and Discussion

3. Results and Discussion

3.1 Physicochemical Characterization of the prepared fig leaf activated carbon of adsorbents surfaces.

3.1.1 Fourier transform infrared spectroscopy (FTIR)

Fourier transform infrared spectroscopy (FTIR) is the method that can be used to qualitatively assess the presence of the principal functional groups on the exterior of the bio-sorbent. Leaves are thought to be a biomass-rich lignocellulosic source display a lot of oxygen functional groups on its surface (Tran et al. 2017). However, from the searching on analysis and characterization the functional groups on the surface of waste leaf plants, it was observed the most common functional groups presents in leaf activated carbon are O-H group, C=O group, C-O group, C-H group and C=C group as shown in the previous studies (Guo et al. 2020; Jawad et al. 2017; Kushwaha et al. 2014). The FTIR characterization of fig leaf activated carbon (FLAC) is further performed in Figure (3-1) to study the surface functional groups of these materials. It is possible to attribute the signal at 3065 cm^{-1} to vibrations of hydroxyl functional groups (Abdulhameed et al. 2021). The bands at 1622 cm^{-1} represent the vibrational stretching of carbonyl group C=O (Abdulhameed et al. 2021; Jawad et al. 2020). A significant band at 1317 cm^{-1} that was C-O band had a drop in intensity. Out of plane vibration of C-H band had observed at 781 cm^{-1}. After MB adsorption, the findings of the FTIR study showed that the O-H peak shifted toward a lower wavenumber (3464 cm^{-1}), indicating the presence of both hydrogen bonding and dipole-dipole interactions. After MB adsorption, the C=O group peaks significantly diminished in intensity and somewhat shifted from 1626 to 1616 cm^{-1} in wavenumber. This result suggests the existence of n–π interactions. Moreover, FTIR research revealed that following MB adsorption, the peak corresponding to the C-O bond reduced in intensity and downshifted (from 1317 to 1311cm^{-1}). This

downshift shows that adsorbents and MB have interactions that are negative (Tran, You, and Chao 2017)

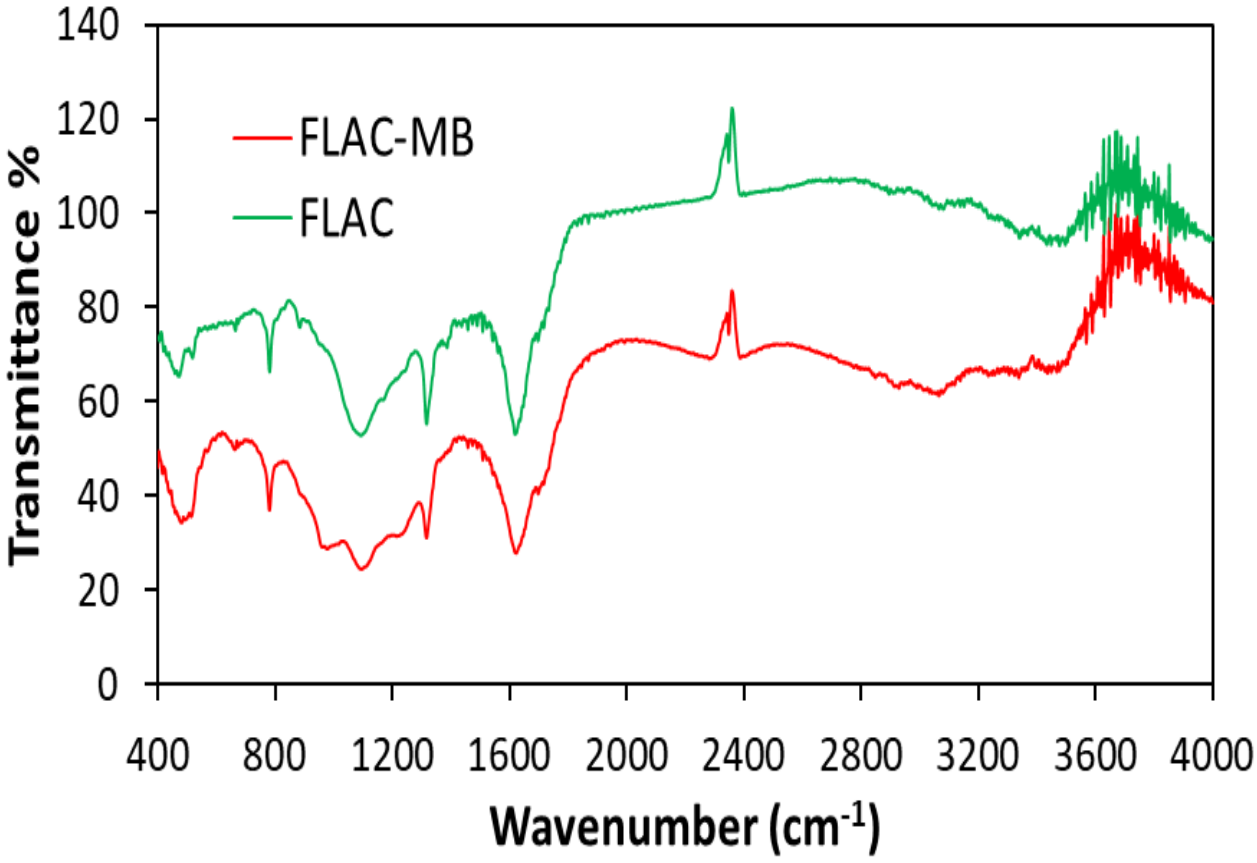

Figure (3-1): Surface morphology characterization for FLAC Intensities of most common identified functional groups for FLAC using FTIR

3.1.2 X-ray diffraction (XRD)

The XRD spectrum of a FLAC sample activated in H_3PO_4 media is shown in Figure (3-2). A largely amorphous structure is revealed by the appearance of a broad diffraction background and the lack of a sharp peak (Nizam et al. 2021). The outcome demonstrates that the FLAC sample has an amorphous structure, indicating

that the organic components of fig leaf waste were mostly affected by the H_3PO_4 alteration.

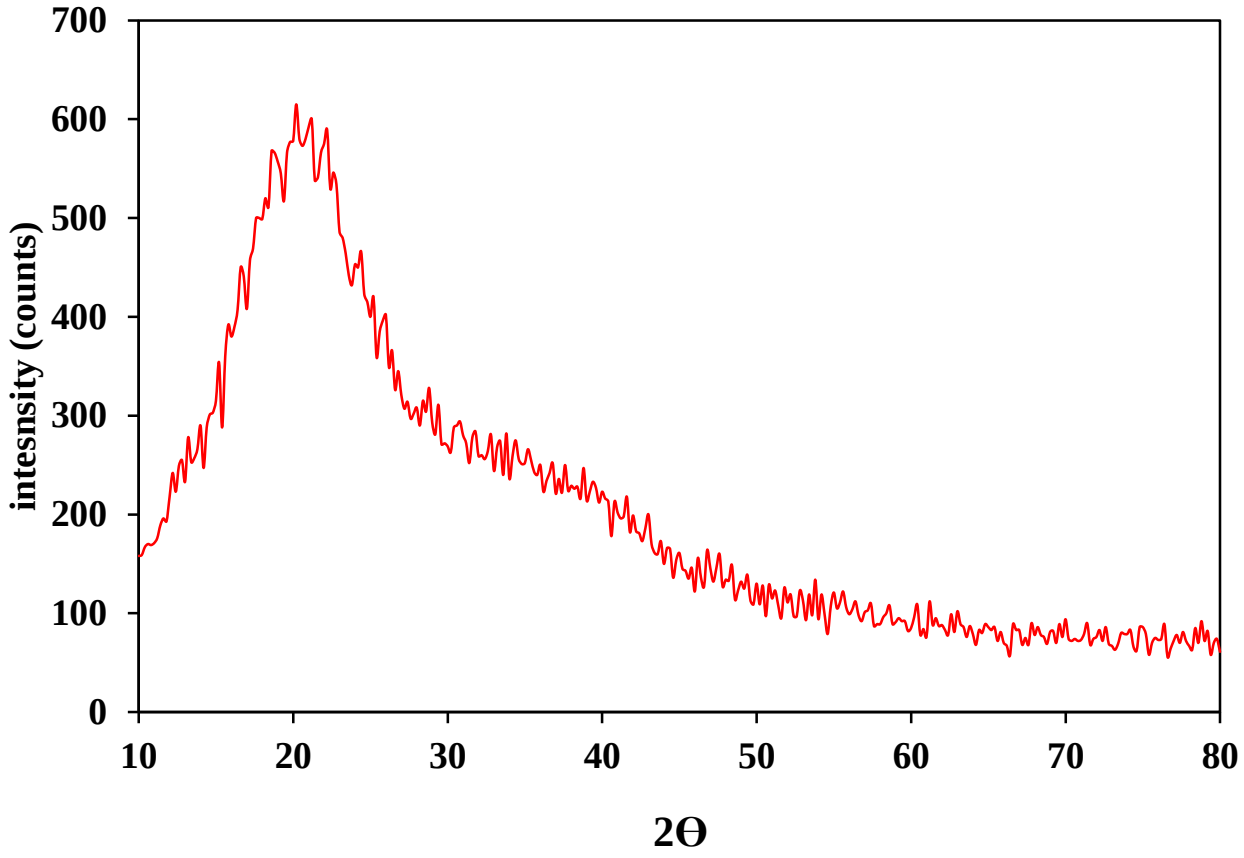

Figure (3-2): Surface morphology characterization for FLAC XRD spectrums of FLAC sample

3.1.3 Scanning Electron Microscopy (SEM)

Fig leaf was activated with H_3PO_4 for scanning electron microscopy (SEM) evaluation, and it was found that this produced a more uniform surface and high porosity, which led to a high adsorption capacity Figure (3-3). The exterior surfaces of the activated carbons feature various-sized voids. The presence of these holes may facilitate the facile diffusion and trapping of large numbers of MB molecules in the pore structure of activated carbon. As a result, the use of chemical treatment helps to thoroughly clean and remove the natural colors that are present in fig leaves,

freeing up the pores that they occupy and improving the fig leaves' capacity to absorb things. The pores on the surfaces of activated carbon that are created after chemical treatment are caused by the evaporation of the activating agent during carbonization, which leaves behind the ruptured surface of activated carbon with pores formerly occupied by the activating agent (Bencheikh et al. 2020).

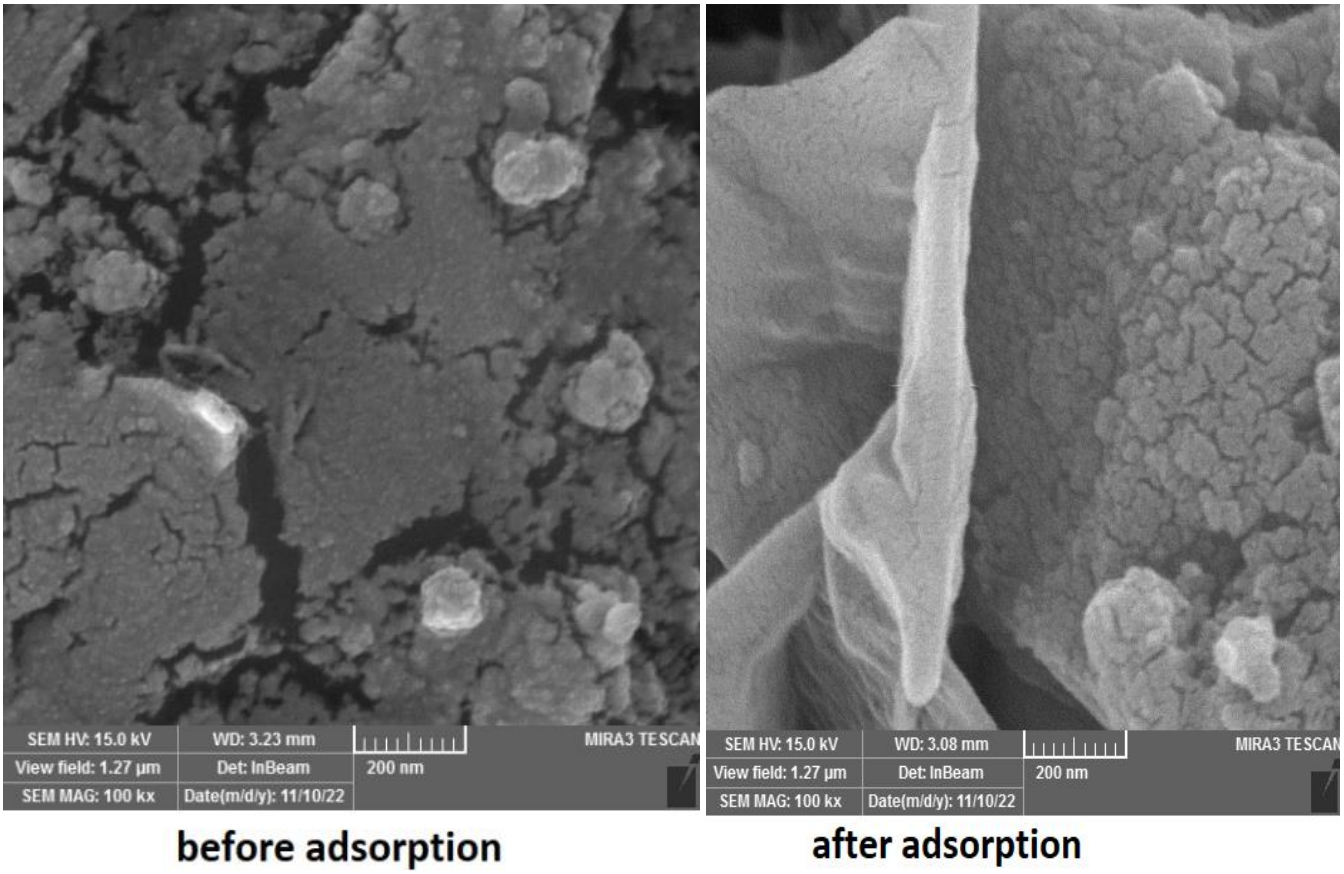

Figure (3-3): Surface morphology characterization for FLAC micrographs of FLAC before and after adsorption.

3.1.4 Nitrogen adsorption-desorption isotherms

Nitrogen adsorption-desorption tests were carried out to describe the porous FLAC architectures Figure (3-4). The FLAC was estimated to have a Brunauer-Emmett-Teller (BET) specific surface area of 18.3 m^2/g. Table (3-1) included a list of other porosity parameters. The high level of surface activity and vast surface area of porous carbons frequently lead to effective dye adsorption (Khangwichian et al. 2022). It was discovered that larger particles (327.9 nm) helped to boost adsorption capacity. Since heteroatoms can produce a redistribution of the surface charge of carbon materials, it has been demonstrated that the inclusion of heteroatoms in carbon materials greatly improves their performance

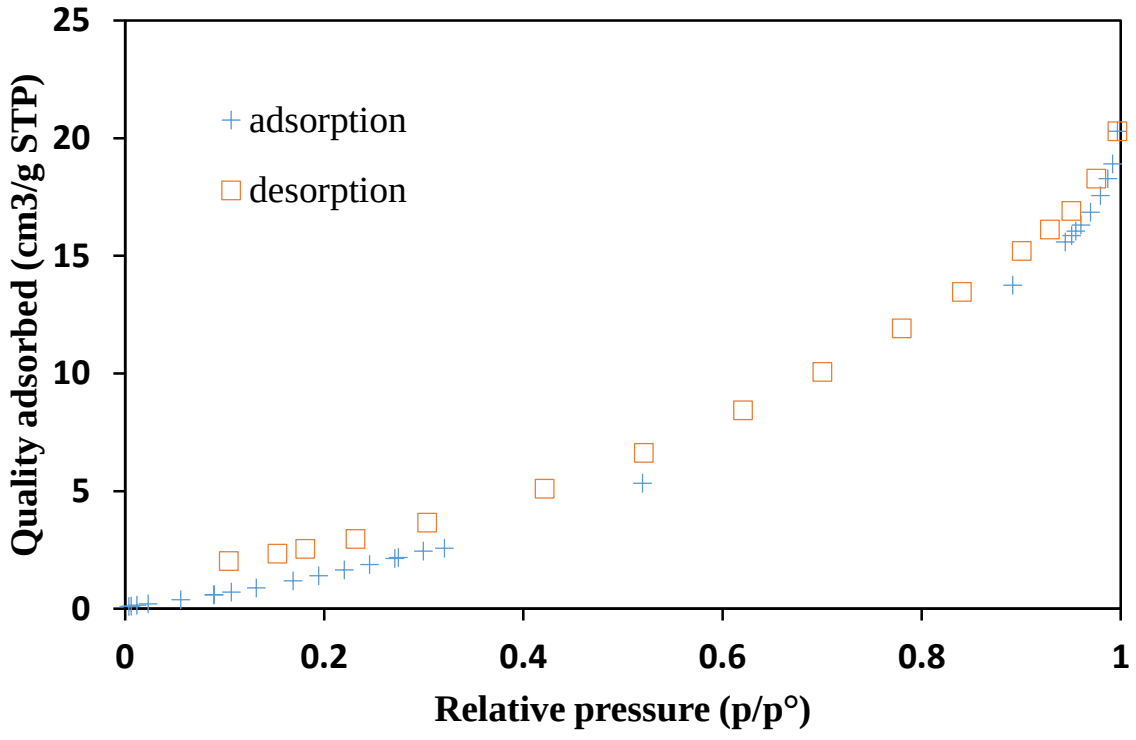

Figures (3-4). Surface morphology characterization for FLAC Nitrogen adsorption-desorption isotherms.

Table: (3-1)

Characteristics of FLAC adsorbent**.**

BET surface area (m^2/g)	Langmuir surface area (m^2/g)	Total pore volume (cm^3/g)	Average particle size (nm)	Micropore surface area (m^2/g)	Median pore width (nm)
18.2976	60.7756	0.0245	327.9	2.3137	1.2643

3.2 Calibration Curve of Methylene Blue Dye Solution

To construct the calibration curve of different concentrations of Methylene blue dye, a series of solutions was prepared by successive dilution of the dye standard solution and with series of concentrations (0.5, 1, 2,4,8,12 mg. L^{-1}). the absorption of this solution was recorded at (λmax= 665nm). The calibration curve was determined by drawing the relationship between absorbance and concentration as shown in Figure (3-5)

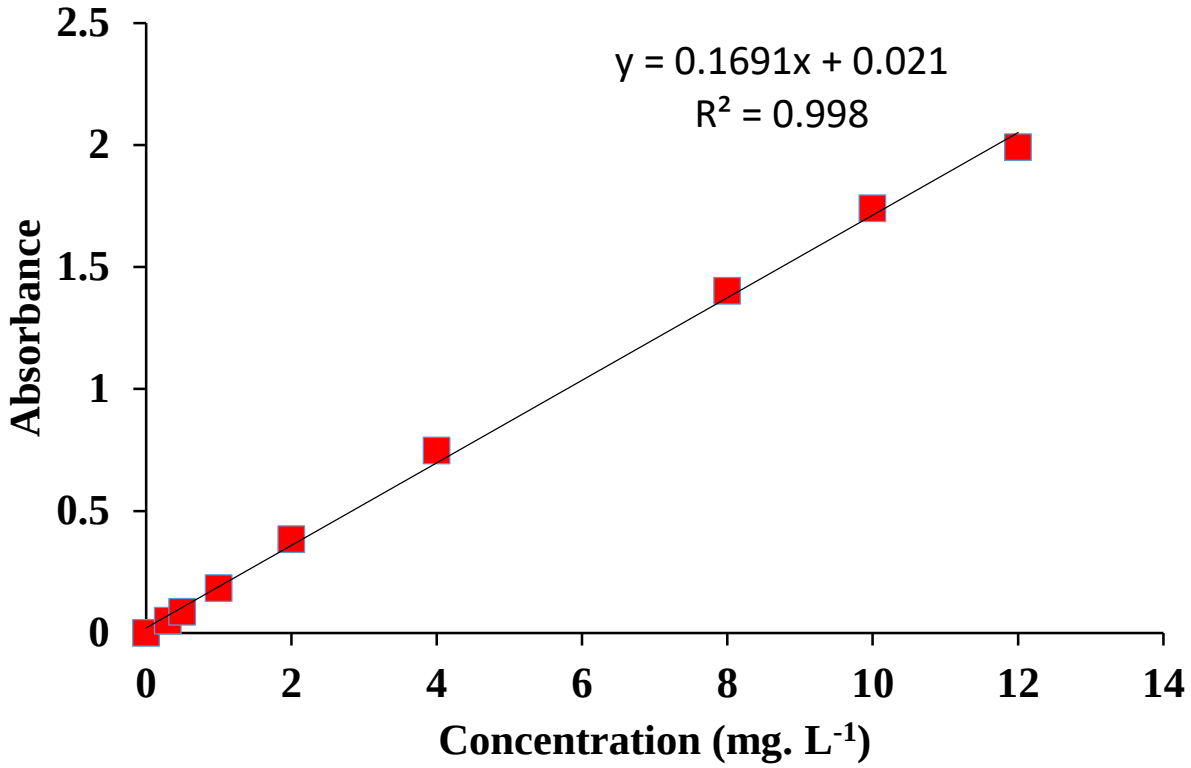

Figure (3- 5): Calibration curve of Methylene blue dye solution

Table (3-2): Statistics data of calibration for different concentrations of Methylene blue dye.

Parameters	Proposed Method Methylene blue dye
λ_{max} (nm)	665
Dynamic concentration range	0.5-12
Regression equation	y = 0.1691x + 0.021 Y= m X + C
Slope (m)	0.1691
Intercept (C)	0.021
Correlation coefficient (R^2)	0.9985
Color	Blue

Limit of Detection LOD (mg.L^{-1})	0.15
Limit of Quantitation LOQ (mg.L^{-1})	0.5
Molar absorptivity (L/mol. Cm)	60952.382

3.3 Effect of Parameters on adsorption process:

3.3.1 Effect of initial MB concentration

The initial dye concentration is one of the most important factors influencing the adsorption process because it indirectly affects dye removal efficiency by reducing or increasing the availability of binding sites on the adsorbent surface. The efficiency of dye removal (E) and the maximum amount of dye bound in equilibrium (q) in such water treatment systems are proportional to the initial dye concentration (Yagub et al 2014; Terangpi and Chakraborty 2017).

$$E(\%) = \frac{C^\circ - Cf}{C^\circ}.100\ \% \qquad (3\text{-}1)$$

$$q = \frac{(C^\circ - Cf).V}{m} \qquad (3\text{-}2)$$

UV-vis measurement is used to assess the removal% and adsorption capabilities of prepared fig leaf activated carbon. In order to study the removal efficiencies and adsorption capacities of the MB dye, the initial MB concentrations were tested at these concentration 20, 40, 80, 120 and 200 mg. L^{-1} at room temperature, as shown in Figure (3-6) and Table (3-3).

Research on how different adsorbents respond to the initial concentration of adsorbate has shown consistent results. In their investigation on the adsorption of methylene blue using oil palm trunk nanocrystalline cellulose, it was observed that an increase in the initial concentration of methylene blue is related to an increase in

the removal effectiveness of methylene blue (Mustikaningrum et al.2022.). In order to overcome the solid-liquid mass transfer resistance, a greater starting concentration was necessary. A vacant active site on the surface of the adsorbent that is not occupied by the adsorbate molecule will exist at very low concentrations.

It can be regarded as a reduction in the system's adsorption capacity. Additionally, the active site on the surface of the adsorbent will decrease to slow down the adsorption process if an increase in initial concentration surpasses the optimal point. Figure (3-6) shows the graph of the fluctuation in methylene blue concentration on adsorption capacity (mg. g^{-1}). In general, it may be said that the adsorption capacity increases with increasing starting concentration. The mass transfer resistance between the liquid (methylene blue) and the solid adsorbent is significantly overcome by the higher starting concentration (Al-Ghouti and Al-Absi 2020). The number of site FLAC might not be enough to adsorb enough methylene blue molecules at high concentrations, which would lower the amount of color removed by the adsorption process. Methylene blue molecules enter the boundary layer and then diffuse to the surface of the adsorbent to start the adsorption process. The molecules continue to diffuse inside the adsorbent.

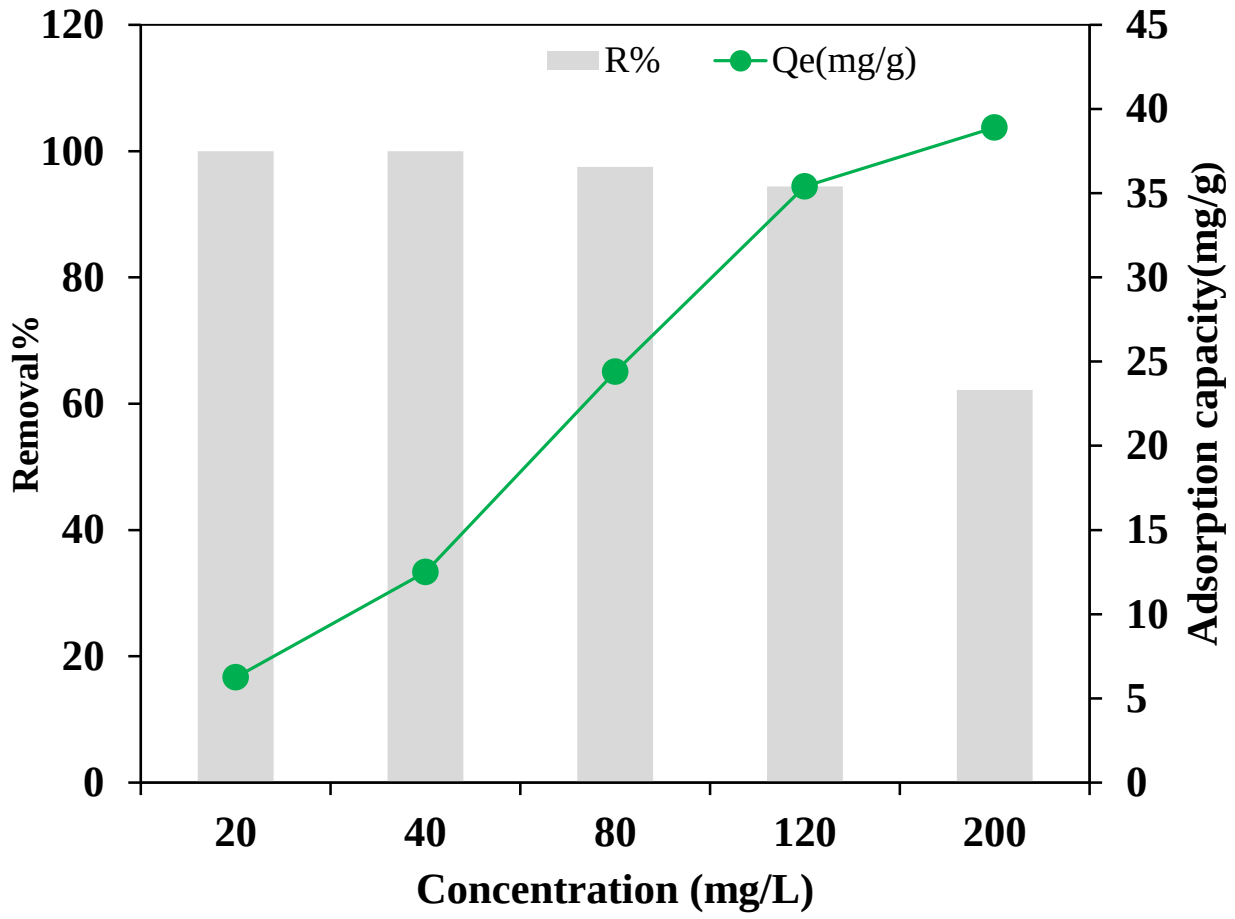

Figure (3-6). The effect of initial concentration (pH 7, 0.08 g adsorbent, 60 min) on the removal efficiency and adsorption capacity of MB using FLAC.

3.3.2 Effect of contact time

The contact time between the dye and the prepared adsorbent has been investigated to determine the equilibrium time for maximum adsorption and recognition of the kinetics of the adsorption process (Kuang et al 2020).

The investigation of contact time has an effect on two factors: the availability of adsorbent active sites and the concentration difference driving force between the solution bulk and the adsorbent surface. At the start of adsorption, the concentration driving force and active sites of adsorbents are at their peak. Dye molecules occupy active sites over time, and adsorption becomes more slowly due to a decrease in both concentration driving force and adsorbent active sites (Magdy et al. 2017).

From Figure (3-7) a and Table (3-3), the adsorption of MB by FLAC is >77% when the concentration was 40, 80 and 120 mg. L^{-1}, respectively at contact time of 10 minute. The removal efficiency rises to >94% when the concentration was 20, 40, 80 and 120 mg. L^{-1}, respectively at contact time of 60 minute which is the equilibrium time.

Adsorption capability was also taken into account and assessed, as seen in Figure. (3-7) b. It is clear that removal percentage and adsorption capacity have the opposite relationships. However, the lowest adsorption capacity was 6.25 mg/g at equilibrium time with MB dye concentration of 20 mg. L^{-1}. While the maximum adsorption capacity was 38.9 mg/g and the MB concentration was 200 mg. L^{-1}. This pattern aligns with previously published findings. According to (Izan et al. 2020.), the percentage of MB removed decreased significantly as the initial concentration of methylene blue dye was raised on magnetic char. The MB intake, however, went from 42.6 to 63.7 mg. g^{-1}. Blaga et al. (Blaga et al. 2022) used leftover biomass from the brewing sector to examine how the initial concentration of methylene blue affected adsorption capability. He discovered that raising the MB dye concentration

from 5 to 70 mg. L^{-1} caused the adsorption capacity to rise from 50 to 230 mg. g^{-1}. This suggests that at greater initial MB concentrations, MB cation-adsorbent surface collisions take place more frequently, increasing MB adsorption capacity (Jiang et al. 2021).

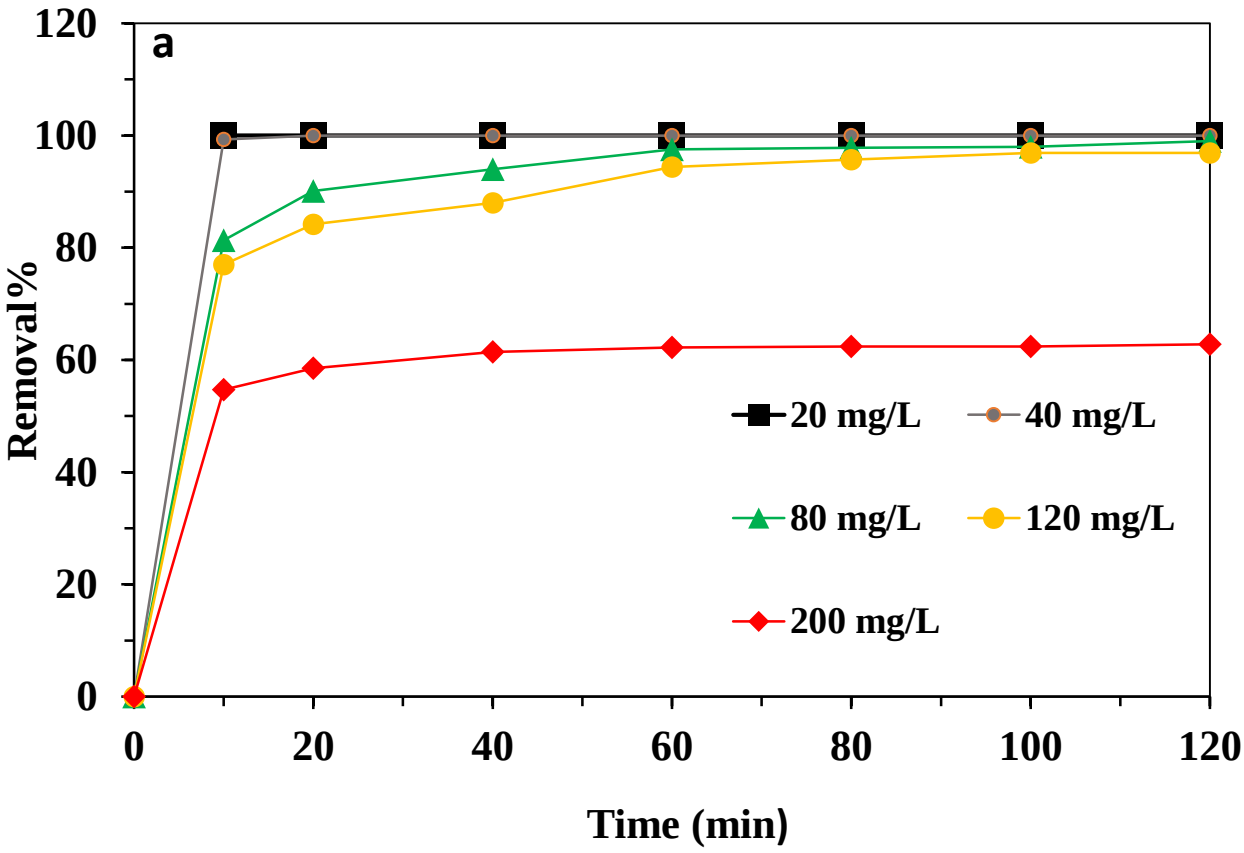

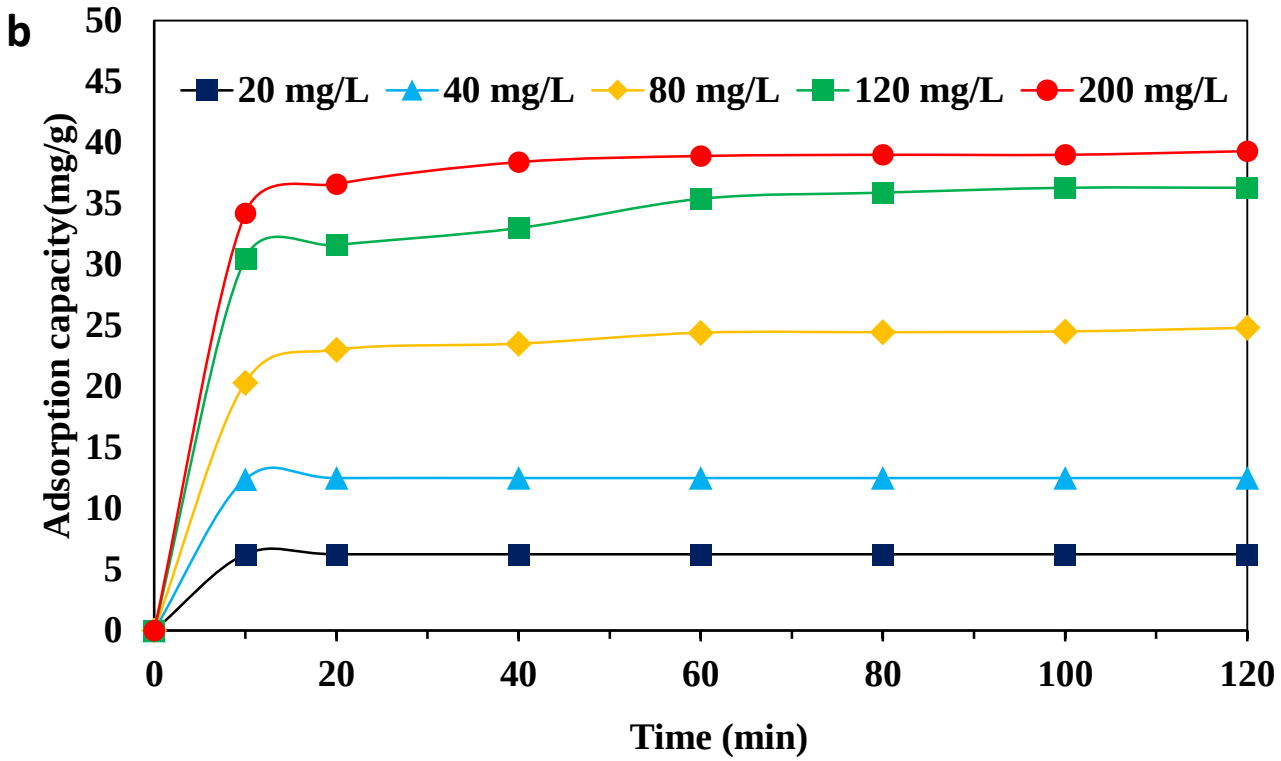

Figure (3-7). The effect of contact time (pH 7, 0.08 g adsorbent, 60 min) on (a) the removal efficiency and (b) adsorption capacity of MB using FLAC.

3.3.3 Effect of temperature

Temperature is another important physicochemical factor because it influences the treatment process by changing the nature of the reaction from endothermic to exothermic, or vice versa (Yeow et al. 2020). Moreover, it has a significant impact on adsorption since it has the ability to alter the amount of adsorption (Badawy et al. 2020).

Figure (3-8) and Table (3-3) shows the change in MB adsorption removal and capacity by fig leaf activated carbon at various temperatures. The elimination efficiency of FLAC is 77.3% at room temperature, or 30°C. At 50°C, the removal efficiency increases to up to 86.4%. The mobility of the dye molecules was dynamic

as the temperature rose, and there were more active sites for adsorption as well (Bharathi and Ramesh 2013). The adsorption capacity was increased steadily with increasing temperature from 20°C to 50°C. For MB dye adsorption, the adsorption capacity reach to 28.8 mg. g^{-1} at 50°C while it was the lowest value of 22.6 mg. g^{-1} at 20°C. Based on the data presented, the temperature increase causes an increase in the adsorption capacity due to the swelling of the internal structure of the adsorbent, which allows methylene blue to penetrate further (Hu et al. 2018).

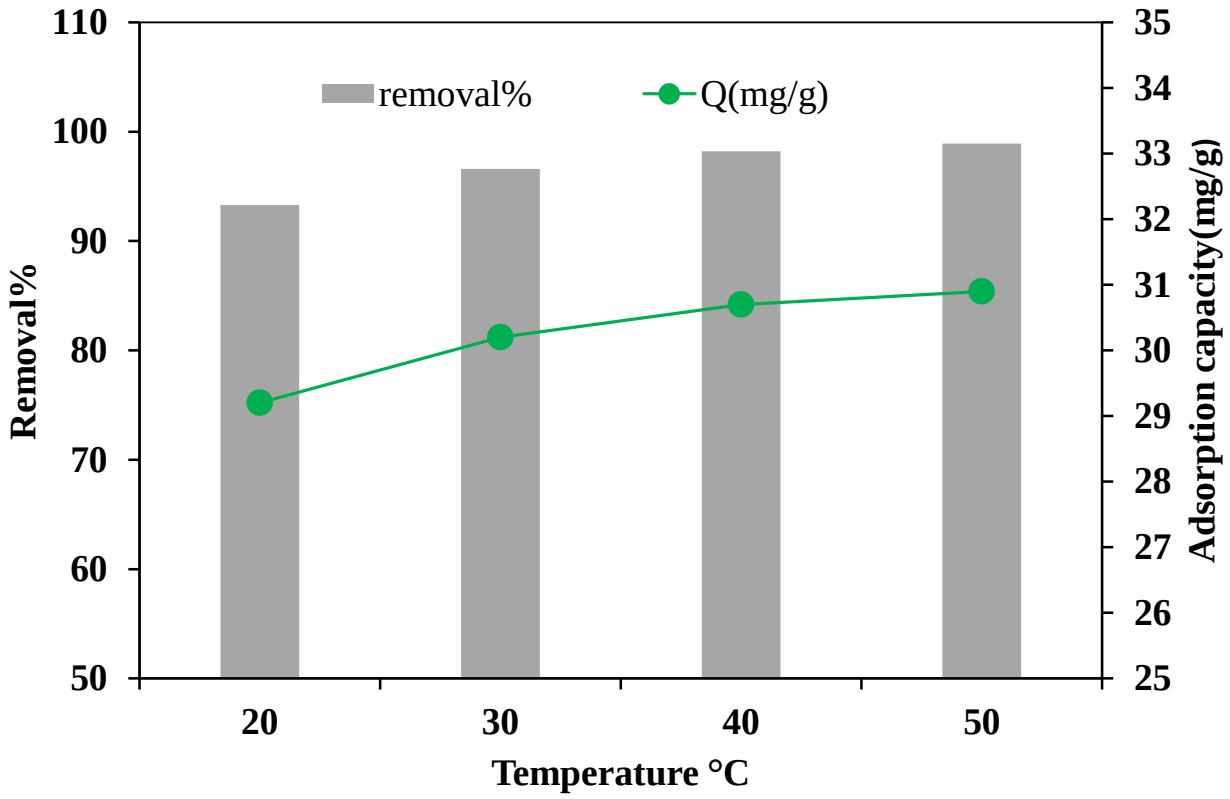

Figure (3-8). The effect of temperature (80 mg. L^{-1} MB, pH 7, 0.08 g adsorbent, 60 min) on the removal efficiency and adsorption capacity of MB using FLAC.

3.3.4 Effect of initial pH solution

This factor influences the adsorbent's capacity as well as the process's efficiency. The pH of the solution influences the chemistry of contaminants, the activity of functional groups in the adsorbent, competition with coexisting ions in the solution, and the adsorbent's surface charge. The aqueous medium's pH can also affect the adsorbent's properties, the adsorption mechanism, and the dissociation of dye molecules. The pH of the solution can affect not only the adsorbent but also the chemical structure of the dye. The pH of the adsorbed ion changes its surface charge and degree of ionization (Rápó et al. 2018; Rápó and Tonk.2021).

Figure (3-9) and Table (3-3) shows how the fig leaf activated carbon performs in terms of MB adsorption at various initial solution pH ranges (pH3, pH7, pH8 and pH11). With acidic conditions, the MB absorption by FLAC is comparatively low, whereas the high adsorption property is realized under basic concentration. The cationic MB dye molecules experienced electrostatic mutual repulsion with greater H^+ ions on the FLAC surface at lower pH levels. As we know, the OH group's active site was beneficial for adsorption of adsorbate on activated carbon surface (Islam et al. 2017). Therefore, at pH 3, the elimination effectiveness is just 88.5%. When the pH is increased from 3 to 7, the adsorption removal rises to 99.3%. The elimination effectiveness of FLAC is 95% when pH reaches 8 and 11. This finding was in agreement with other previous studies. According to a publication, decreased MB adsorption at pH3 may be caused by the adsorbent's predominantly protonated amino and carboxylic acid functional groups, which increase the cationic MB dye's electrostatic repulsion. When the initial pH rises till an alkaline medium, the high MB adsorption onto the adsorbents was observed (Shelke et al. 2022).

Additionally, it was found that the proton generation competes with the MB cation for adsorption on the active FLAC sites under acidic conditions, resulting in a

reduction in adsorption capacity (Nordin et al. 2021). The high cation exchange capacity of FLAC is probably to blame for the high MB adsorption that becomes apparent as the pH of the solution rises to a high 11. The alkaline state of the solution suggests that the adsorbent surface has more negative charges than positive ones (Murthy et al. 2020). The high adsorption capacity of FLAC roughly 24.5 mg. g^{-1} is caused by electrostatic attraction to cationic MB due to the negative charge on its surface. Thus, it is evident that FLAC requires a neutral or basic environment in order to achieve high adsorption efficiency.

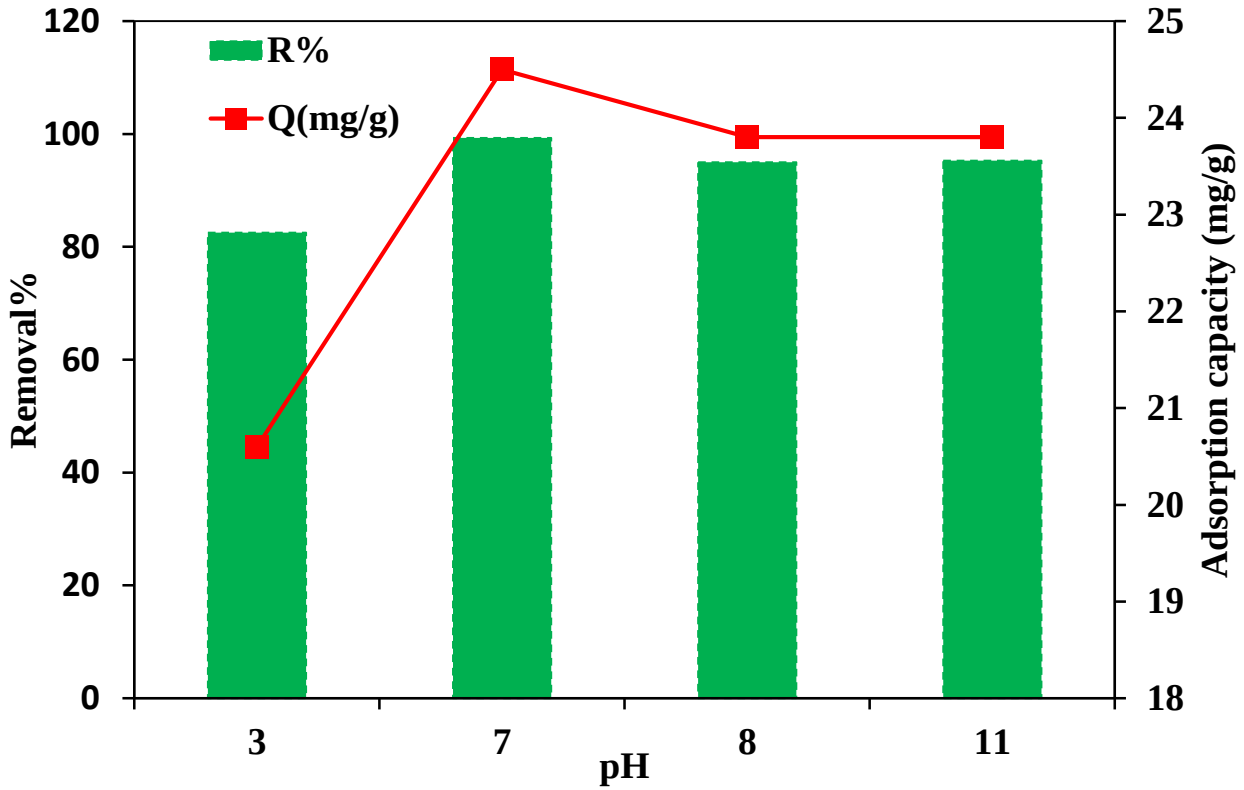

Figure (3-9): The effect of pH solution (80 mg. L^{-1} MB, 0.08 g adsorbent, 60 min) on the removal efficiency and adsorption capacity of MB using FLAC.

3.3.5 Effect of FLAC amount

The amount of the adsorbent is an important parameter because it determines the adsorbent capacity for a given initial concentration (Sentürk and Alzein 2020). Kroeker's rule states that the specific adsorbed volume decreases with increasing adsorbent mass for a constant initial concentration (Pernyeszi et al. 2019). Thus, increasing the adsorbent dose has a positive correlation with dye removal efficiency and performance. At constant contaminant concentrations, increasing adsorbent dosage provides more active surface area for adsorption and more active adsorption sites (Ma et al.2020)

Figure (3-10) and Table (3-3) displays the results of the evaluation of the dosage of fig leaf activated carbon for the adsorption of 80 mg. L^{-1} of MB dye solution at pH 7. As can be seen, the plot demonstrates that at FLAC dosages of 0.02 and 0.1 g, respectively, the adsorption efficiency of MB rose from 67.5% to 100%. This is brought on by the rise in the number of available empty adsorption sites and the adsorbent's surface area for adsorption (Abuzerr et al. 2018). High removal efficiency may result from high adsorbent dose. But as the dosage is increased, the adsorption ability decreases. It might not be enough to give negative charges for MB adsorption if the adsorbent dosage is increased further since it could change the nature of the solution (Izan et al. 2020). As can be seen, the adsorption capacity was decreased from 41 to 20 mg. g^{-1} when the FLAC increased from 0.02 to 0.1 g.

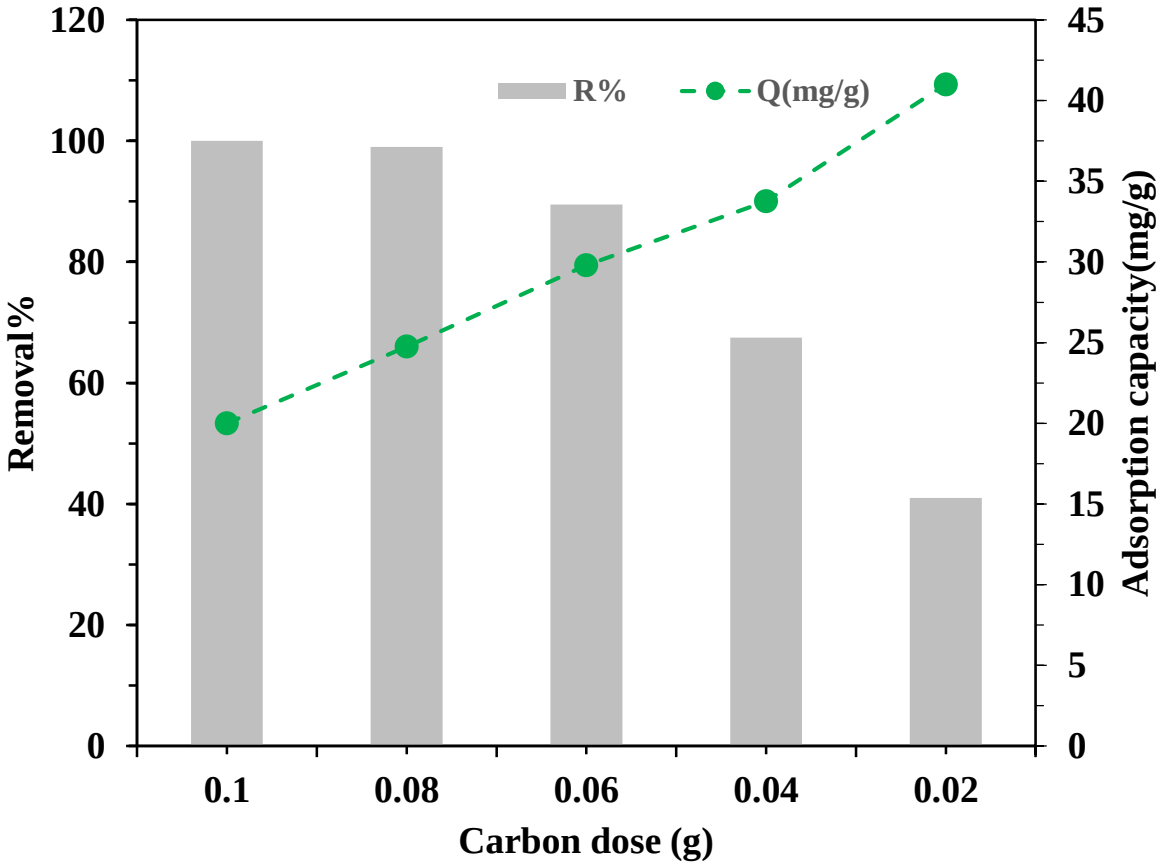

Figure (3-10). The effect of FLAC dosage (pH 7, 80 mg. L^{-1} MB, 60 min) on the removal efficiency and adsorption capacity of MB using FLAC.

3.3.6 Effect of solution volume

With the exception of 100 mL, FLAC exhibits great removal efficiency in the adsorption of the methylene blue dye at different volumes of solution (25, 50, and 100 mL). The highest removal rate was 99.5% with a 25 mL dosage. As the volume of the MB dye solution increases, the removal efficiency declines. At 50 mL of dye solution, the greatest adsorption capacity of 44.5 mg. g^{-1} is obtained. These findings are depicted in Figure (3-11) and Table (3-3).

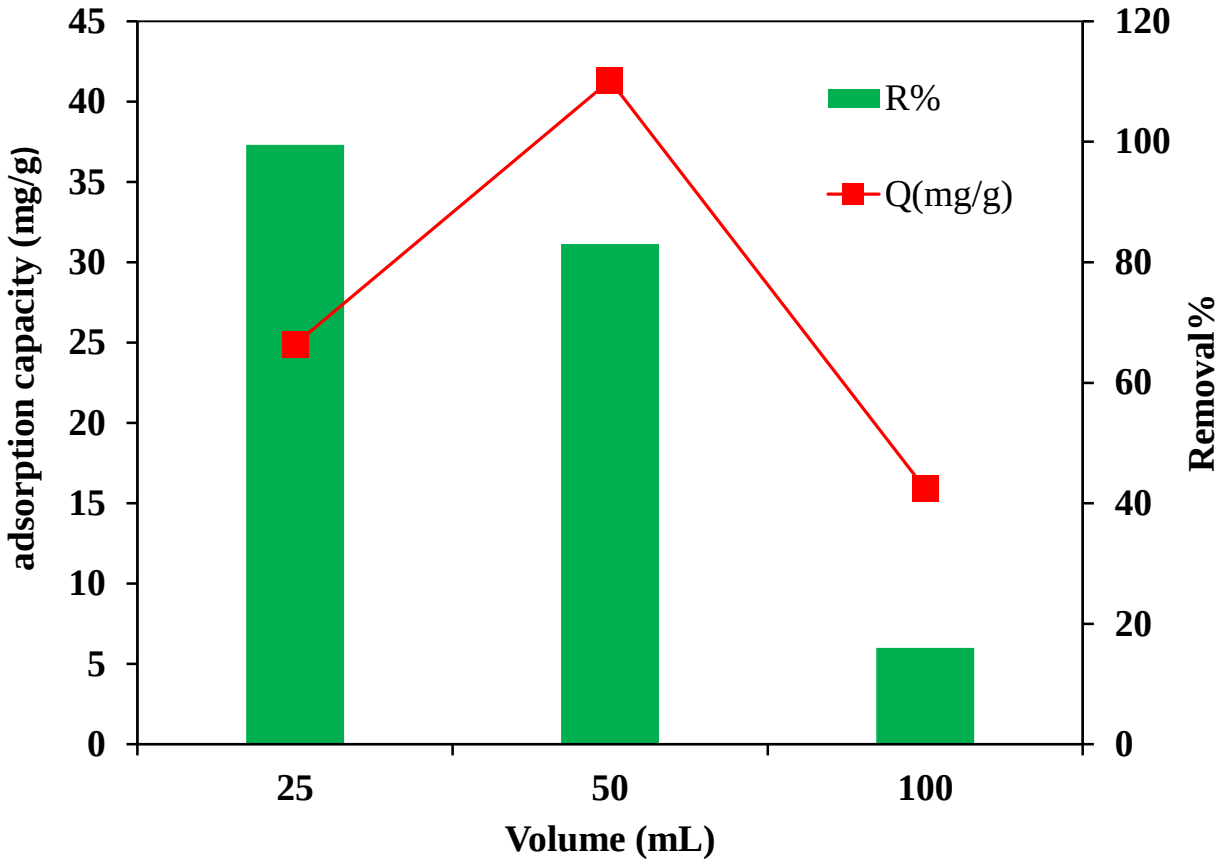

Figure (3-11). The effect of MB solution volume (pH 7, 80 mg. L^{-1} MB, 0.08 g, 60 min) on the removal efficiency and adsorption capacity of MB using FLAC.

3.3.7 Effect of activation agent

The activation process can undoubtedly influence the removal% and mass of adsorbed dye on the adsorbent. The effect of the activation process was presented in five aspects: AC1: only burn; AC2: pristine powder; AC3: impregnated in H_3PO_4; AC4: impregnated in NaOH; AC5: impregnated in H_2SO_4 on the removal% and adsorption capacity as presented in Figure (3-12) and Table (3-3)**.** 0.08 g of adsorbent was added to 25 mL of an 80 mg. L^{-1} MB solution in conical flasks and shaken for 60 min at room temperature. The elimination percent of MB by AC3 is

99.6%, and the adsorption capacity is 24.9 mg. g^{-1}. By testing the others, the lowest removal efficiency is 75% when pristine powder is used without any further chemical treatment. The impregnation of fig leaf powder in NaOH solution has not improved the efficiency of adsorption as much as acid did

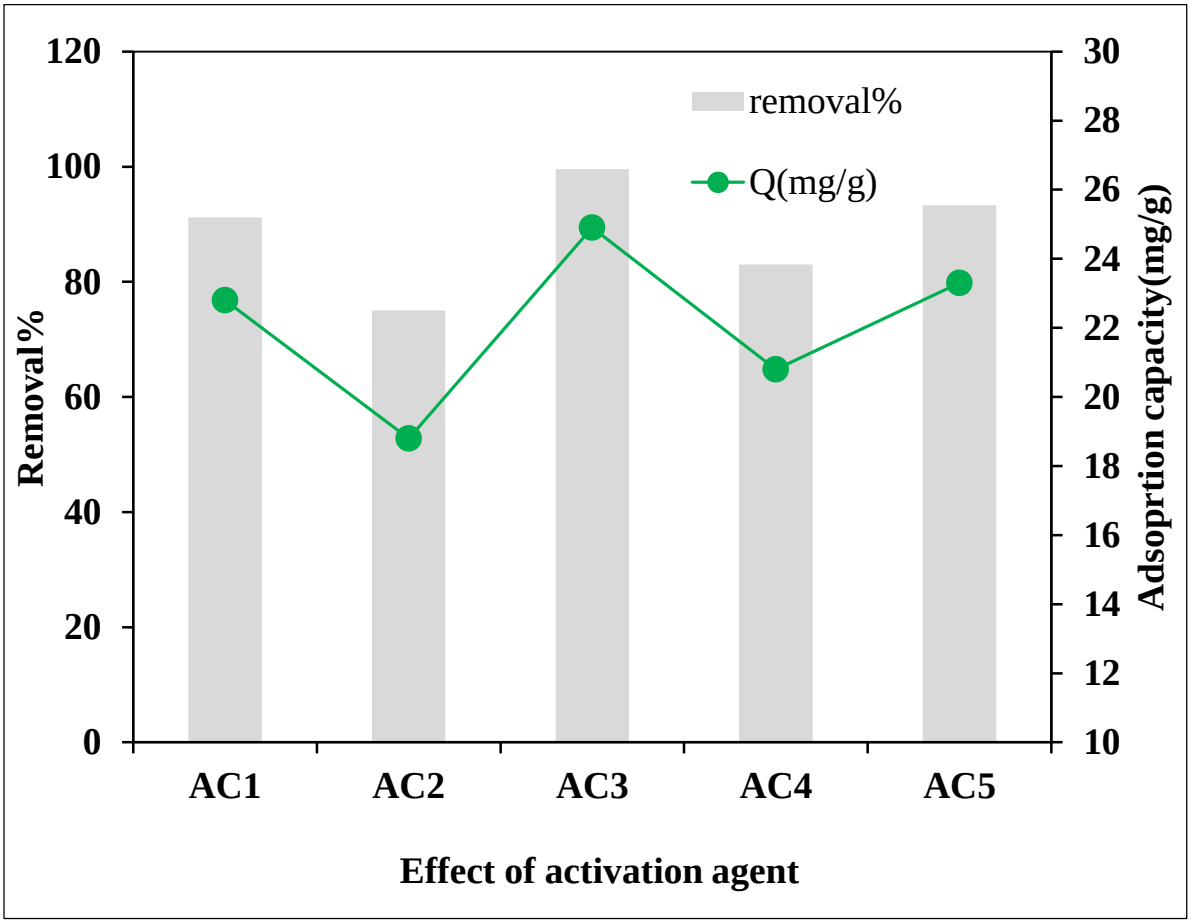

Figure (3-12). The effect of activation agent (pH 7, 80 mg. L^{-1} MB, 0.08 g adsorbent, 60 min) on the removal efficiency and adsorption capacity of MB using (AC1: only burn; AC2: pristine powder; AC3: impregnated in H_3PO_4; AC4: impregnated in NaOH; AC5: impregnated in H_2SO_4).

3.3.8 Effect of carbonization temperature

The carbonization temperature can affect the removal % and mass of adsorbed dye on the adsorbent material due to the effect of the carbonation temperature on the presence of functional groups on the surface, as Figure (3-13) and Table (3-3) shows the effect of carbonization at four different temperatures (150 °C, 250 °C, 350 °C, 500 °C).

0.08g of adsorbent was added to 25 mL of an 80 mg. L^{-1} MB solution in conical flasks and shaken for 60 min at room temperature. The elimination percent of MB by 350 °C is 98% and the adsorption capacity is 24.5 mg. g^{-1}. By testing the others, the lowest removal efficiency is 44.8% when the carbonization temperature is 500 °C

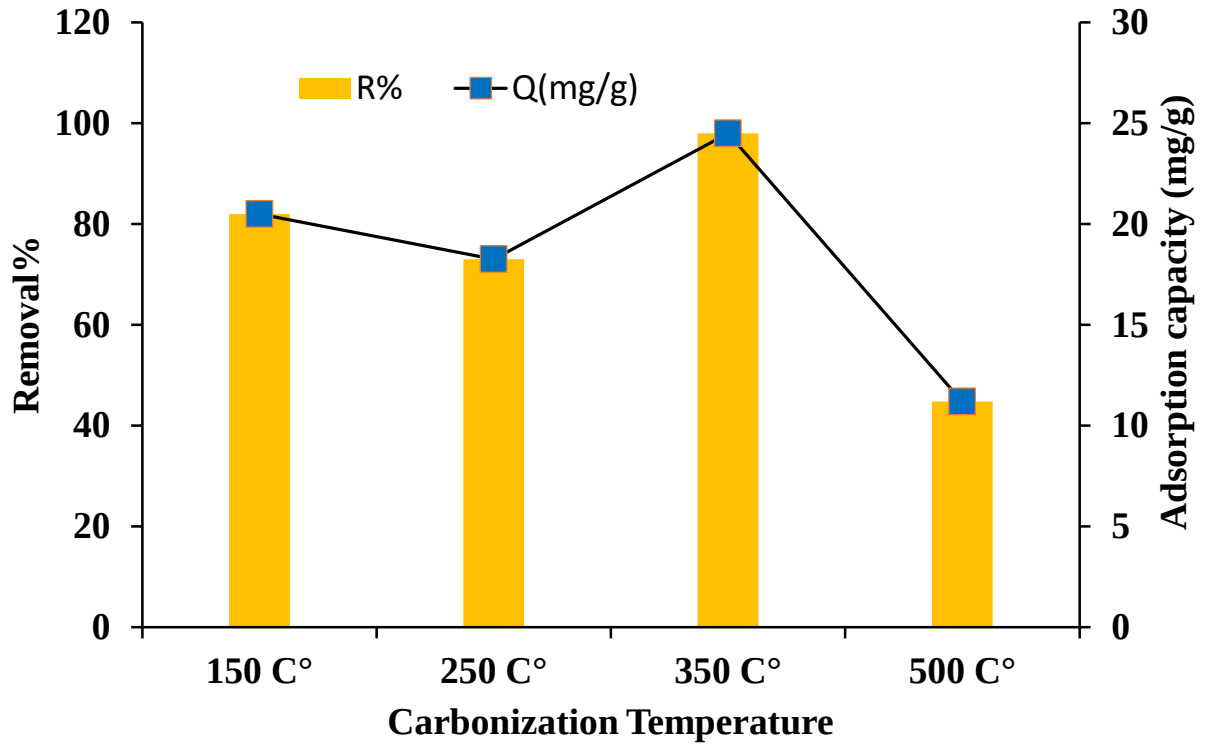

Figure (3-13): The effect of carbonization temperature (pH 7, 80 mg. L^{-1} MB, 0.08 g adsorbent, 60 min) on the removal efficiency and adsorption capacity of MB using FLAC

3.4 Carbon source (Investigation the removal% and adsorption capacity using different plant leaves):

A study comparing carbon source with leaves of other plants (Fig leaf AC (FLAC), Grape leaf AC (GLAC), citrus Aurantium leaf AC (CAL) as adsorbents. 0.08 g of adsorbent was added to 25 mL of an 80 mg. L^{-1} MB solution in conical flasks and shaken for 60 min at room temperature. Figure (3-14) shows that the best removal efficiency was 99.6% and adsorption capacity 24.9 mg. g^{-1} of FLAC compared with (GL, CAL). While, the lowest removal efficiency is 80% when GLAC is used.

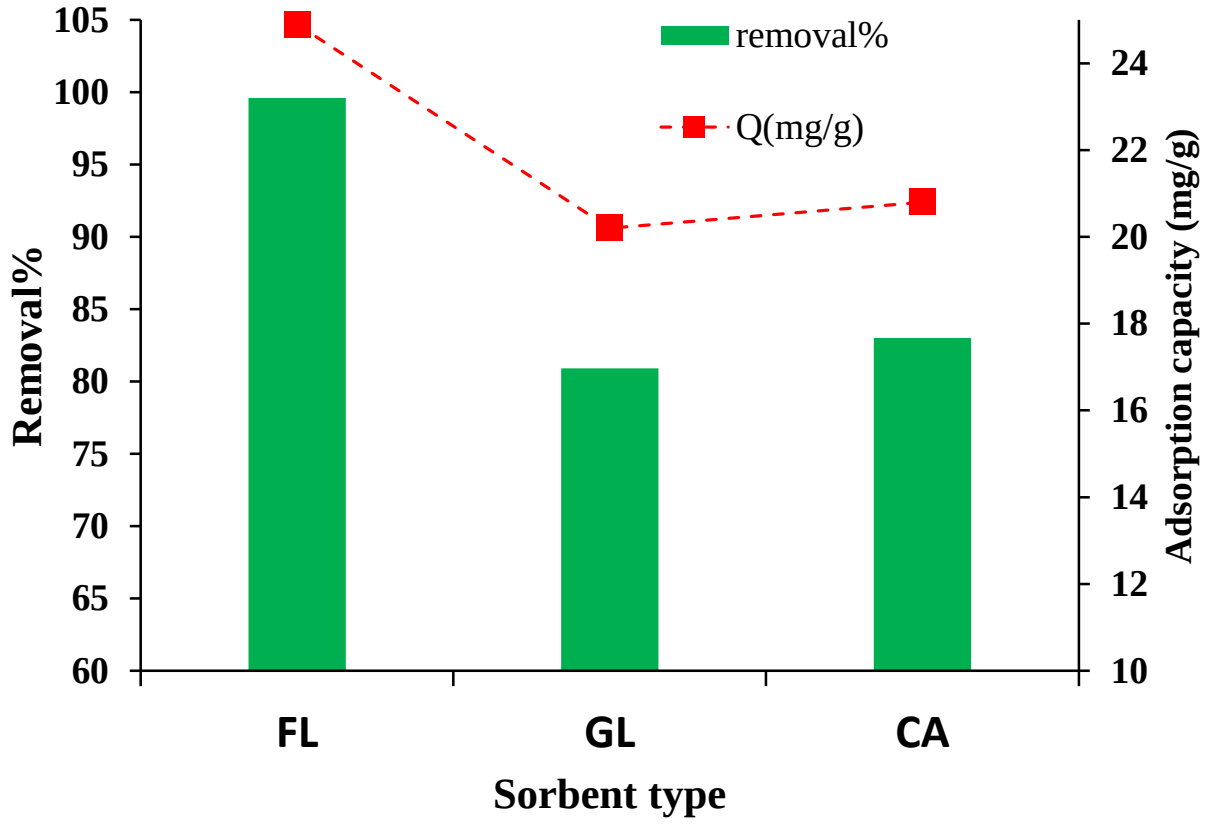

Figure (3-14): Effect of carbon source (pH 7, 80 mg. L^{-1} MB, 0.08 g adsorbent, 60 min) on the removal efficiency and adsorption capacity of MB using FLAC, GLAC, CAL

Table (3-3): Removal% and adsorption capacity (Q) under effect of all selected parameters.

	Effect of initial concentration (mg. L^{-1})						
	20	**40**	**80**	**120**	**200**		
R%	100	100	97.5	94.4	62.2		
Q (mg/g)	6.25	12.5	24.4	35.4	38.9		
	Effect of contact time (min)*						
	10	**20**	**40**	**60**	**80**	**100**	**120**
R%	81.3	90.1	94	97.5	97.8	98	99
Q (mg/g)	20.31	23	23.5	24.4	24.44	24.5	24.88
	Effect of temperature C°						
	20	**30**	**40**	**50**			
R%	93.3	96.6	98.2	98.9			
Q (mg/g)	29.2	30.2	30.7	30.9			
	Effect of initial pH solution						
	3	7	8	11			
R%	82.5	99.3	95	95.3			
Q (mg/g)	20.6	24.5	23.8	23.8			

	Effect of FLAC amount (g)				
	0.1	0.08	0.06	0.04	0.02
R%	100	99	89.5	67.5	41
Q (mg/g)	20	24.75	29.8	33.75	41
	Effect of volume (mL)				
	25	50	100		
R%	97.5	83	16		
Q (mg/g)	24.9	41.3	15.9		
	Effect of activation agent				
	AC1	AC2	AC3	AC4	AC5
R%	91.2	75	99.6	83	93.3
Q (mg/g)	22.8	18.8	24.9	20.8	23.3
Effect of Carbonization Temperature					
	150°C	250°C	350°C	500°C	
R%	82	73	98	44.8	
Q (mg/g)	20.5	18.25	24.5	11.2	

*80 mg. L^{-1} MB has been selected

3.5 Determine of point of zero charges

Based on the precursor origin and the preparation mode, AC can possess acidic, basic or neutral nature (amphoteric). The point-of-zero charge (pH $_{PZC}$) test estimates the pH at which the net charge of the surface is zero (Jawad et al 2018). 50 mL of water in series of conical flasks the pHi values was adjusted by adding an HCl or NaOH in the range (3-11) then adding 0.1g of FLAC and shaken for 2 hours at room temperature, and the pHf of the liquid was measured and the results were shown in the figure (3-15). The difference between the initial pH (pHi) and final pH (pHf) values (ΔpH = pHi–pHf) were plotted against pHi, the point of intersection of the resulting curve with abscissa, at which ΔpH =0, gave the pH pzc.

This result of the experiment performed with the FLAC, where the pH ranged from 3 to 11. The PH $_{PZC}$ of the FLAC was 7, which indicates the neutral nature character of the FLAC surface.

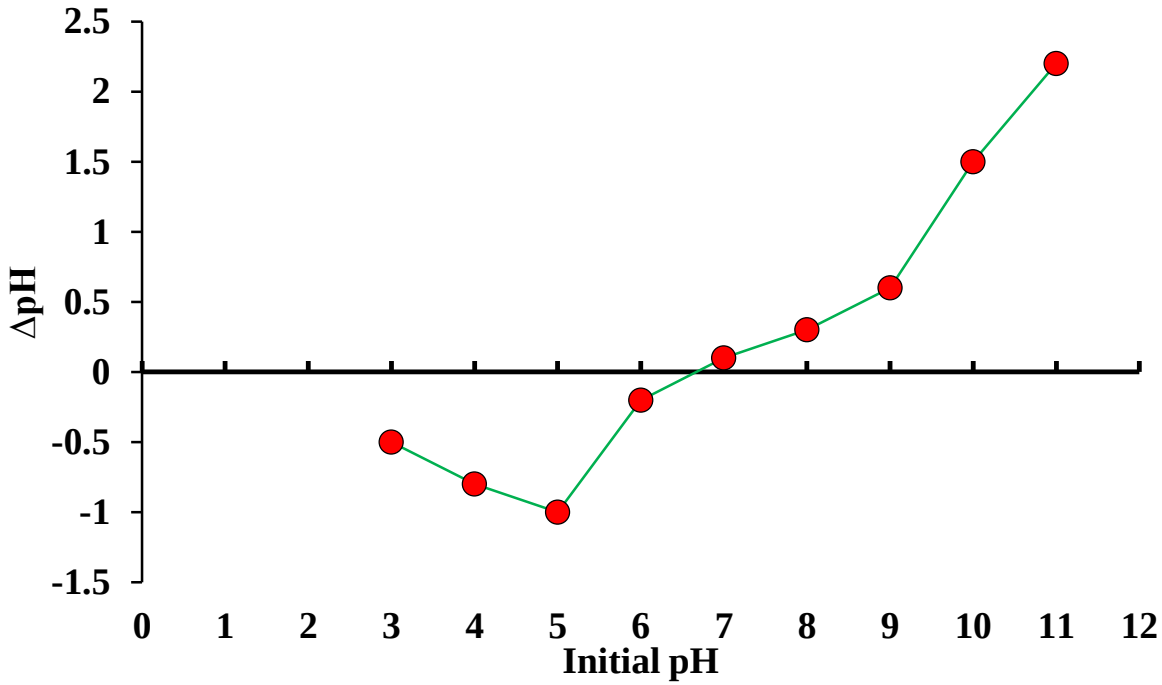

Figure (3-15): Determination of pH point zero charge

3.6 Determine the yield, moisture content and volatile production of Activated carbon: (Khangwichian et al 2022)

The yield of fig leaves was determined, where the weight of the sample before carbonization W_i =2.8869 g and after carbonization W_{ac} = 1.808 g, where the yield % was 64.3%. it was found through the following relationship

$$\text{Yield (wt\%)} = \frac{Wac}{wi} \times 100\% \quad (3\text{-}3)$$

As for the moisture content, it was obtained after drying the sample for three hours at a temperature 150 °C, and the weight of the sample was W_2 = 1.697 g, where the moisture content was 6.139%. it was found through the following relationship

$$\text{Moisture (wt\%)} = \frac{W1-W2}{W1} \times 100\% \quad (3\text{-}4)$$

As for the volatile matter they were calculated by putting the sample in the furnace temperature for half an hour at 950 °C, then the sample was weighed W_3 = 1.013 g, and the volatile matter % is 40.3%, which found through the following relationship

$$\text{Volatile matter (wt\%)} = \frac{W2-W3}{W2} \times 100\% \quad (3\text{-}5)$$

Table (3-4): Determine the yield, moisture content and volatile production of FLAC

Property	Value
Yield %	64.3
Moisture content %	6.139
Volatile matter%	40.3

3.7 Adsorption isotherms

The Langmuir and Freundlich models equation method was used to determine the value of the adsorption equilibrium constant Figure (3-16). The Freundlich model has the lowest R^2 of the two models (0.913), but the Langmuir model has a high R^2 of 0.9841. Adsorption kinetics models like the Langmuir isotherm model are frequently used to explain intricate adsorption dynamics. The maximal adsorption capacity in the current investigation was 41.67 mg. g^{-1}, and the Langmuir affinity constant (KL) was 0.37 L. mg^{-1}. This model accurately depicts the methylene blue adsorption by FLAC. In addition to the adsorbent's pores, the adsorption mechanism also depends on hydrogen bonds and Van der Waals interactions. The FLAC hydroxyl group, which binds the nitrogen element of methylene blue, contains hydrogen, which is what distinguishes the hydrogen bond in this adsorption method. Dipole ion interactions and electrostatic interactions are features of the Van der Waals force. An appropriate model to explain the chemical adsorption mechanism is the Langmuir isotherm one. The observable adsorption process, specifically the monolayer (Wang and Guo 2020), indicates this. This monolayer surface demonstrates that an active site, which can only be occupied by one molecule at a time, is responsible for carrying out the adsorption (Hasan et al. 2020).

Other earlier investigations also supported the Langmuir isotherm model for the methylene blue adsorption procedure utilizing activated carbon from leaf waste plants (Guo et al. 2020; Jawad et al. 2017).

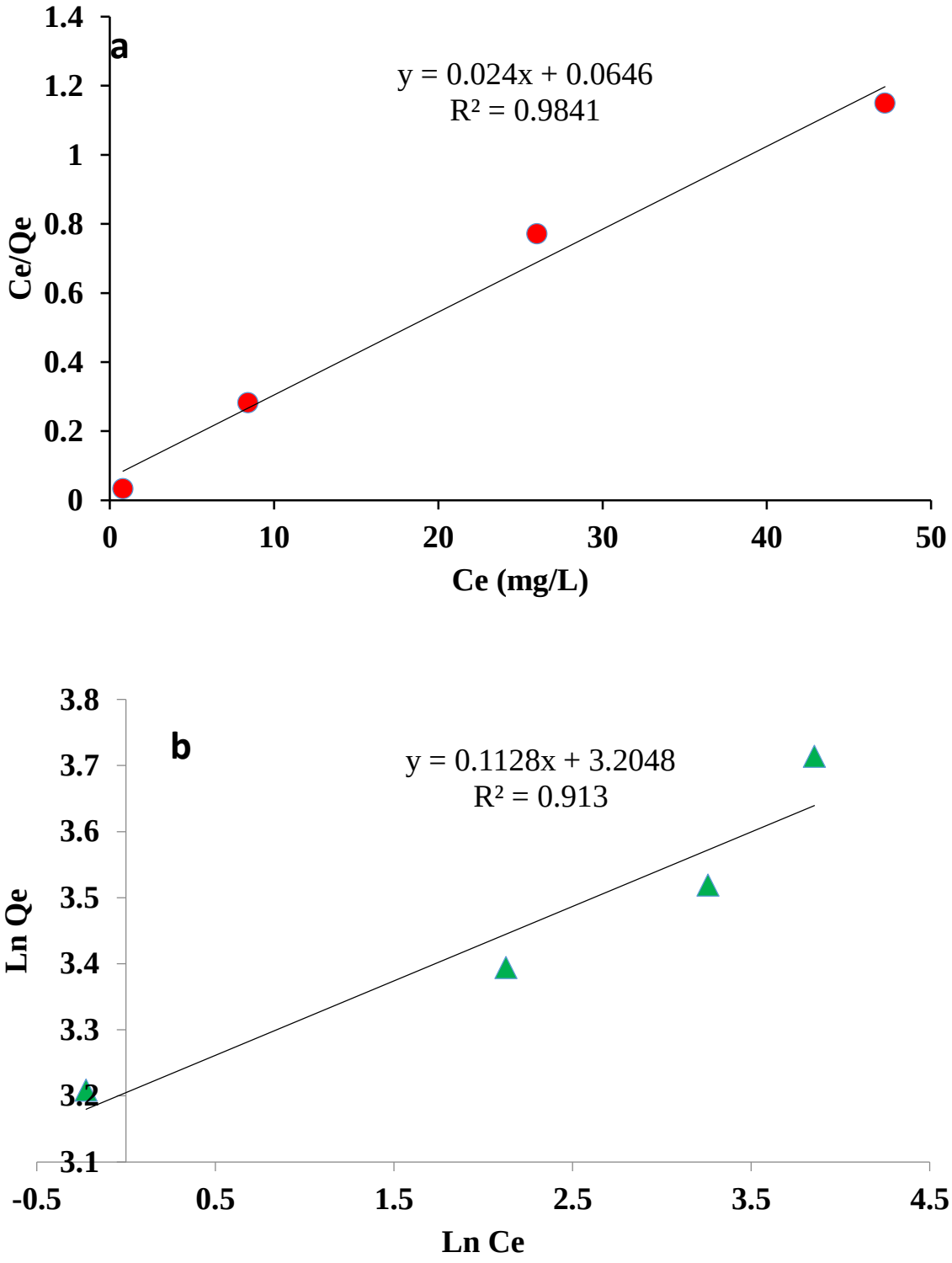

Figure (3-16). Isotherm plots (a) Langmuir (b) Freundlich for adsorption of MB on FLAC.

Table: (3-5) Isotherm parameters for Langmuir and Freundlich models.

Langmuir isotherm		
Qm (mg/g)	**KL (L/mg)**	**R^2**
41.67	0.37	0.9841

Freundlich isotherm		
KF (mg/g)(L/mg)$^{1/n}$)	**1/n**	**R^2**
24.65	0.1128	0.9130

3.8 Thermodynamic study

At 293, 303, 313, and 323 K, the impact of temperature on the adsorption of MB on FLAC adsorbent was examined. As the temperature rose from 293 to 323 K, it was found that the adsorption capacity increased from 29.2 to 30.9 mg. g^{-1}. These results suggested that the MB dye may be pushed from the solution phase to the solid surface due to the increased feasibility of adsorption at higher temperatures caused by the rise in kinetic energy of dye molecules (Dural et al. 2011). In the study on the adsorption of MB onto FLAC, a related finding was also made. Using Eq. (3-6) and Eq. (3-7), the thermodynamic parameters change in enthalpy (ΔH°), entropy (ΔS°), and Gibbs free energy (ΔG°) were calculated for the adsorption of MB on FLAC.

$$\ln\left(\frac{C_s}{C_e}\right) = \frac{\Delta S^\circ}{R} - \frac{\Delta H^\circ}{RT} \qquad (3-6)$$

$$\Delta G^\circ = \Delta H^\circ - T\Delta S^\circ \qquad (3-7)$$

where Ce is the dye's equilibrium concentration in solution (mg. L^{-1}) and Cs is its equilibrium concentration in the solid phase (mg. L^{-1}). Temperature is T, and gas constant R is 8.314 J/mol/K. Changes in enthalpy (kJ/mol), entropy (J/mol/K), and Gibb's free energy (kJ/mol) are denoted by the symbols ΔH°, ΔS°, and ΔG°, respectively. The slope ($\Delta H^\circ/R$) and intercept ($\Delta S^\circ/R$) of the plots of ln (Cs/Ce) vs. 1/T were used to get the values of ΔH° and ΔS°.

The coefficient of distribution is calculated using equation (3-8) which is named Kd.

$$K_d = \frac{C_s}{C_e} \qquad (3-8)$$

Table: (3-6) displays the thermodynamic parameter values. Negative values of ΔG° demonstrated the viability and spontaneity of the adsorption process. As the temperature rose, the values of ΔG° fell, indicating that the adsorption was more spontaneous at high temperatures. The increase in randomness at the adsorbent-solution interface during the adsorption was described by a positive value of ΔS°. The overall endothermic nature of the MB adsorption on FLAC is confirmed by a positive value for ΔH°.

Table: (3-6)

Thermodynamic parameters values for the adsorption of methylene blue onto FLAC at different temperatures.

	Thermodynamic parameters			
Temperature (K)	**Kd**	**ΔG° (kJ/mol)**	**ΔH° (kJ/mol)**	**ΔS° (J/mol.K)**
293	13.93	-6.47	49.3	190.33
303	28.41	-8.37		
313	54.56	-10.27		
323	89.9	-12.18		

3.9 Kinetic study

The kinetic data were investigated using the pseudo-first-order and pseudo-second-order linear models shown in equations (3-9) and (3-10), respectively (Mousavi et al. 2022).

$$\log(Q_e - Q_t) = \log Q_e - \frac{K_{ads1}}{2.303}\, t \qquad (3-9)$$

$$\frac{t}{Q_t} = \frac{1}{K_{ads2} \times Q_e^2} + \frac{1}{Q_e} t \qquad (3-10)$$

Where Q_e and Q_t are the adsorption capacities (measured in mg. g^{-1} of MB adsorbed on the material) at equilibrium and any time t (min), respectively. The rate constants for the pseudo-first-order (min^{-1}) and pseudo-second-order (g/mg.min) adsorption processes are K_{ad1} and K_{ad2}, respectively**.** The pseudo-first-order and pseudo-second-order models, respectively, for the kinetic processes of adsorption are shown in Figure (3-17) a, b**.** Each model's parameter values are displayed. When compared to the correlation coefficients obtained for the pseudo-first-order model, the data are demonstrated to suit the pseudo-second-order model well (R^2=0.9972) (Figure (3-17b). Chemisorption is therefore shown to occur because the process is dependent on the adsorbent and the concentration of the adsorbate.

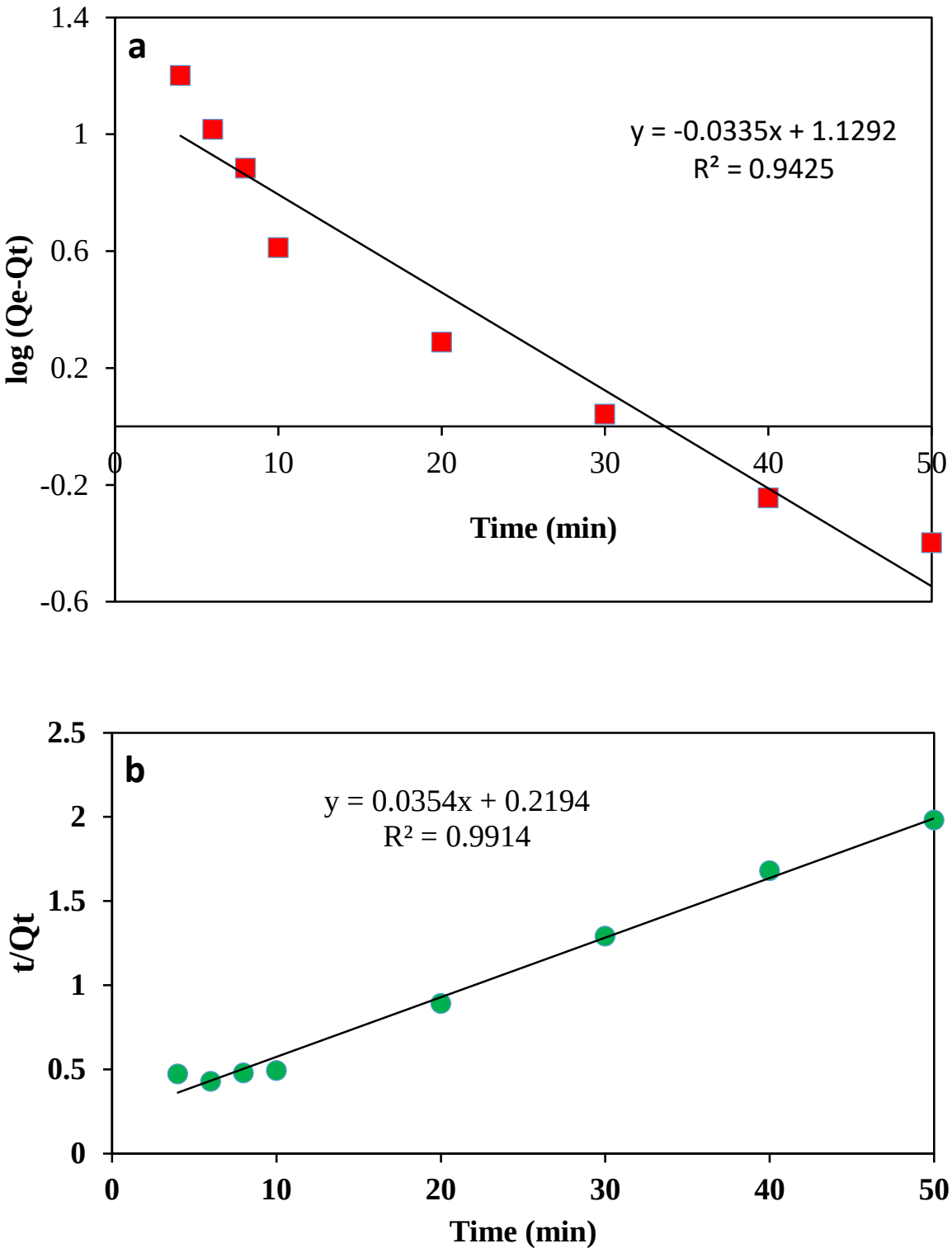

Figure (3-17). The kinetics study on the adsorption processes. Plots of (a) log (Q_e - Q_t) against time for pseudo-first order model, (b) t/ Q_t against time for pseudo-second order model.

Table: (3-7)

kinetic parameters of adsorption of MB on FLAC.

Pseudo-first order		Pseudo-second order	
K_{ads1} (min^{-1})	R^2	K_{ads2}	R^2
0.0771	0.9425	0.0057	0.9914

3.10 Mechanism of adsorption

Methylene blue adsorption mechanism

Fig leaves are agricultural waste and contain higher quantities of compounds that are rich in organic composition. However, after activation and carbonization the fig leaves, FLAC is the promising adsorbent to adsorb methylene blue dye from its aqueous solution. In MB adsorption, various active functional groups on the surface show the main role in adsorption of dye. Studies revealed two key elements that have an impact on the adsorption process. The methylene blue dye's structure is the first, and the presence of functional groups on the outside of the leaves is the second. The FTIR detection shows that different functional groups, including C=O, C-H, C-O, and O-H, were reachable from the adsorbents. These functional groups may be the reason why positively charged MB molecules are taken in. The positive charge molecules of MB and the negative charge exterior of the leaves may interact via electrostatic interaction, -interaction, H-bonding, π-π-interaction and n-π-interaction (Tran, You, and Chao 2017).

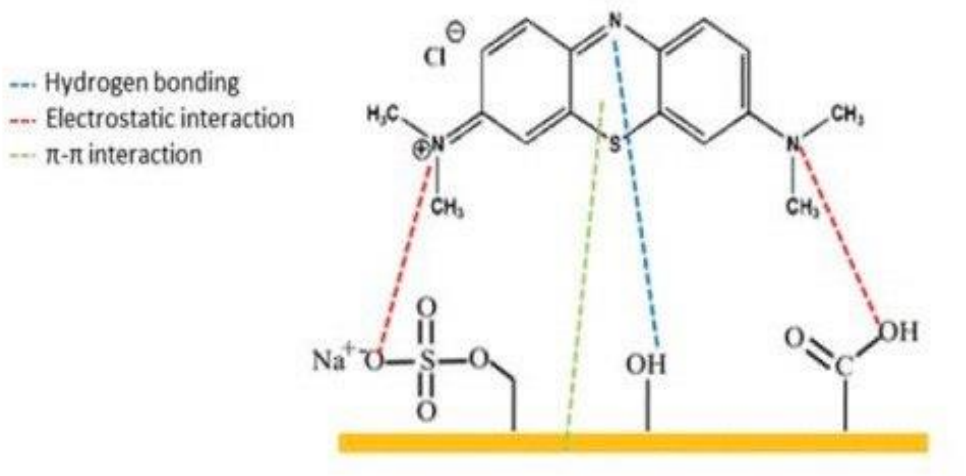

Figure (3-18): Mechanism of Methylene blue adsorption

3.11 Selectivity dye adsorption

In the field of selective dye adsorption and separation, earlier studies have shown that leaf waste activated carbon displayed excellent affinity for organic dyes. The heterocyclic aromatic organic compound known as the cationic MB dye is frequently utilized as a target molecule for wastewater treatment and water purification. The Figure (3-19) describe the chemical composition of the methylene blue organic dye in the study of selective dye adsorption. After 30 minutes of using 0.06 g FLAC as the MB adsorbent, the color of the 25 mL 40 mg. L^{-1} MB solution is almost vanished to the human sight. The cationic MB is electrostatically bound to the anionic hydroxyl groups on the FLAC surface. To demonstrate the selective dye adsorption property, Figure (3-19), UV-vis spectroscopy was used to record the solution's absorbance spectra. The MB peak is hardly discernible after adsorption

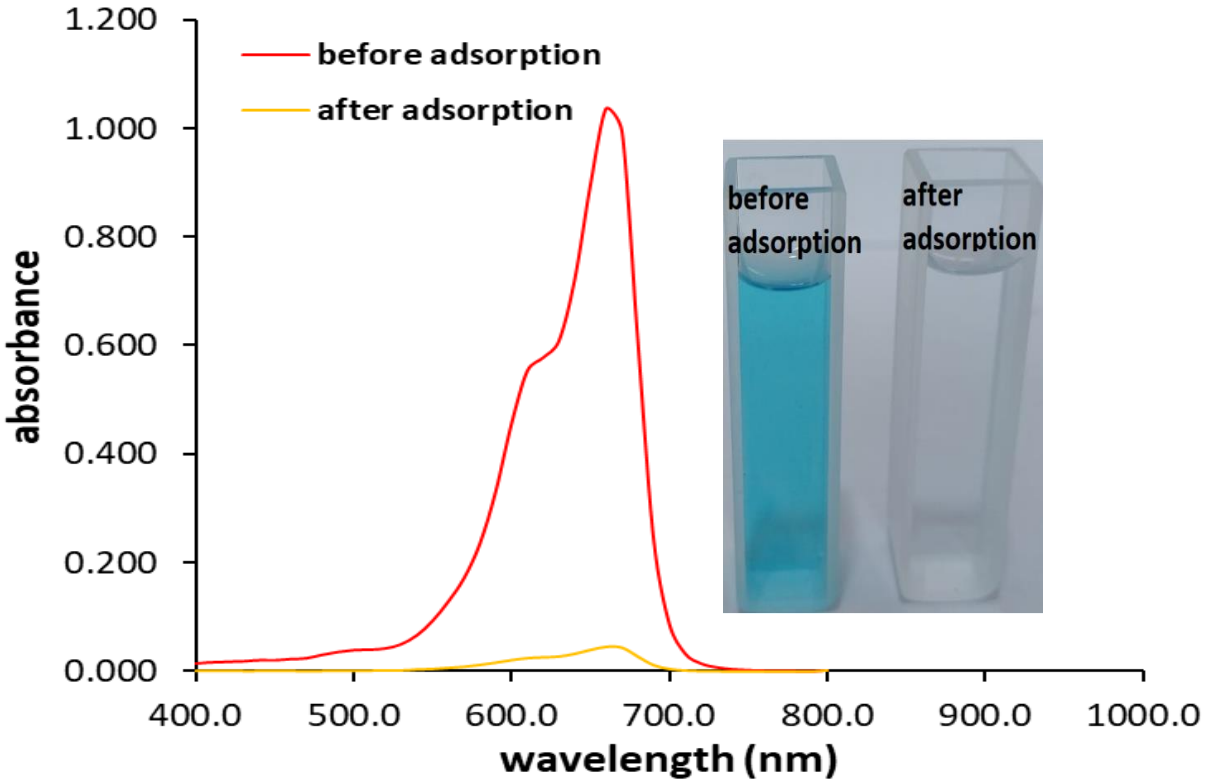

Figure (3-19). Adsorption profile for MB at equilibrium state. The insert is the photograph of MB dye solution before and after adsorption by FLAC. (40 mg. L^{-1} MB dye, 0.06 g adsorbent dose, and 30 min shaking time).

3.12 Conclusion

Fig leaves have been used as an activated carbon, they were applied in treatment of dyes for the first time. However, the viability of using fig leaves as a novel, inexpensive precursor in the production of activated carbon is examined in this present work. The outcomes show that FLAC is a powerful adsorbent for the adsorption of the methylene blue dye. This study shown that H_3PO_4 treatment could improve fig leaf activated carbon's ability to adsorb MB and from its aqueous solutions compared to other activating agents such as NaOH and H_2SO_4.

SEM scans showed that after adsorption, MB molecules had filled the active sites of FLAC. The surface of FLAC has numerous significant functional groups, including hydroxyl O-H, alkane C-H, and C=O, according to FTIR spectra. The FLAC possesses non-crystalline characteristics, according to the XRD instrument. When the initial MB dye concentration, contact time, temperature, and FLAC dose rose, so did the dye uptake clearly and explicity. The FLAC 's adsorption capacity was found to be 24.75 mg. g^{-1} for 0.08 g and 41 mg. g^{-1} for 0.02 g.

The results of the adsorption experiments showed that the pseudo-second-order model best described the kinetic uptake characteristics. The overall endothermic nature of the MB adsorption on FLAC is confirmed by a positive value for ΔH°. The negative values of ΔG° indicate that the adsorption was more spontaneous at low temperatures. The Langmuir model, on the other hand, does a good job of describing the adsorption isotherms. It was discovered that the maximum adsorption capacity was 41.7 mg. g^{-1} and the Langmuir affinity constant was 0.37 L. mg^{-1}. The FLAC as low-cost adsorbents for methylene blue dye has shown good cationic dye adsorption performance.

3.13 Recommendation

1. The fig leaves' waste have demonstrated their ability in methylene blue dye removal in several trials. However, it is essential to upgrade these systems to pilot plants.

2. Many towns have large farms and other green fields, so it is possible to collect leaf trash in one place. Furthermore, waste from various plant parts, such as stems, roots, and fallen fruit, can be collected in the same transportation facility, potentially lowering overall collection costs.

3. Once MB dye has been adsorbed on adsorbents, the massive amounts of activated carbon used must be recycled. In addition, after the dye has been taken out of the adsorbent, it is suggested to look into recycling and reuse options.

4. It is highly recommended to use technology during study sessions to save time and effort. Therefore, the features of bio-waste products can be used to define the fundamental information for computer programs to adapt models, notably with response surface approaches, that might predict the results.

5. The adsorbent surface is used to remove other contaminants such as heavy metals, pollutants and other dyes.

6. Improving the properties of fig leaves by using activating methods and other activating agents to increase the surface area and expand the pores

References

References:

- Abbas, A. F., & Ahmed, M. J. (2016). Mesoporous activated carbon from date stones (Phoenix dactylifera L.) by one-step microwave assisted K2CO3 pyrolysis. *Journal of Water Process Engineering*, *9*, 201-207.
- Abdulhameed, A. S., Hum, N. N. M. F., Rangabhashiyam, S., Jawad, A. H., Wilson, L. D., Yaseen, Z. M., et al. (2021). Statistical modeling and mechanistic pathway for methylene blue dye removal by high surface area and mesoporous grass-based activated carbon using K2CO3 activator. *Journal of Environmental Chemical Engineering*, *9*(4), 105530.
- AboBakr, A., Said, L. A., Madian, A. H., Elwakil, A. S., & Radwan, A. G. (2017). Experimental comparison of integer/fractional-order electrical models of plant. *AEU-International Journal of Electronics and Communications*, *80*, 1-9.
- Abualnaja, K. M., Alprol, A. E., Abu-Saied, M. A., Ashour, M., & Mansour, A. T. (2021). Removing of anionic dye from aqueous solutions by adsorption using of multiwalled carbon nanotubes and poly (Acrylonitrile-styrene) impregnated with activated carbon. *Sustainability*, *13*(13), 7077.
- Abuzerr, S., Darwish, M., & Mahvi, A. H. (2018). Simultaneous removal of cationic methylene blue and anionic reactive red 198 dyes using magnetic activated carbon nanoparticles: equilibrium, and kinetics analysis. *Water Science and Technology*, *2017*(2), 534–545.
- Ahmed, M. J., & Theydan, S. K. (2014). Optimization of microwave preparation conditions for activated carbon from Albizia lebbeck seed pods for methylene blue dye adsorption. *Journal of Analytical and Applied Pyrolysis*, *105*, 199-208.

References

- Ahn, C. K., Park, D., Woo, S. H., & Park, J. M. (2009). Removal of cationic heavy metal from aqueous solution by activated carbon impregnated with anionic surfactants. *Journal of hazardous materials*, *164*(2-3), 1130-1136.
- Ai, L., & Jiang, J. (2012). Removal of methylene blue from aqueous solution with self-assembled cylindrical graphene–carbon nanotube hybrid. *Chemical Engineering Journal*, *192*, 156-163.
- Alam, M. Z., Bari, M. N., & Kawsari, S. (2022). Statistical optimization of Methylene Blue dye removal from a synthetic textile wastewater using indigenous adsorbents. *Environmental and Sustainability Indicators*, *14*, 100176.
- Al-Degs, Y. S., El-Barghouthi, M. I., Issa, A. A., Khraisheh, M. A., & Walker, G. M. (2006). Sorption of Zn (II), Pb (II), and Co (II) using natural sorbents: equilibrium and kinetic studies. *Water research*, *40*(14), 2645-2658.
- Al-Ghouti, M. A., & Al-Absi, R. S. (2020). Mechanistic understanding of the adsorption and thermodynamic aspects of cationic methylene blue dye onto cellulosic olive stones biomass from wastewater. *Scientific Reports*, *10*(1), 1–18.
- Al-Ghouti, M. A., & Da'ana, D. A. (2020). Guidelines for the use and interpretation of adsorption isotherm models: A review. *Journal of hazardous materials*, *393*, 122383.
- Allwar, A. (2012). Characteristics of micro-and mesoporous structure and surface chemistry of activated carbons produced by oil palm shell. In *International Conference on Chemical, Ecology and Environmental Sciences Proceedings* (pp. 138-141).
- Al-Qodah, Z., & Shawabkah, R. (2009). Production and characterization of granular activated carbon from activated sludge. *Brazilian Journal of Chemical Engineering*, *26*, 127-136.

References

- Alslaibi, T. M., Abustan, I., Ahmad, M. A., & Foul, A. A. (2013). A review: production of activated carbon from agricultural byproducts via conventional and microwave heating. *Journal of Chemical Technology & Biotechnology*, *88*(7), 1183-1190.
- Anisuzzaman, S. M., Joseph, C. G., Krishnaiah, D., Bono, A., Suali, E., Abang, S., & Fai, L. M. (2016). Removal of chlorinated phenol from aqueous media by guava seed (Psidium guajava) tailored activated carbon. *Water resources and industry*, *16*, 29-36.
- Arami-Niya, A., Daud, W. M. A. W., & Mjalli, F. S. (2010). Using granular activated carbon prepared from oil palm shell by ZnCl2 and physical activation for methane adsorption. *Journal of Analytical and Applied Pyrolysis*, *89*(2), 197-203.
- Arslan-Alaton, I., Tureli, G., & Olmez-Hanci, T. (2009). Treatment of azo dye production wastewaters using Photo-Fenton-like advanced oxidation processes: Optimization by response surface methodology. *Journal of photochemistry and Photobiology A: Chemistry*, *202*(2-3), 142-153.
- Arslanoğlu, H. (2019). Direct and facile synthesis of highly porous low cost carbon from potassium-rich wine stone and their application for high-performance removal. *Journal of hazardous materials*, *374*, 238-247.
- Asfaram, A., Ghaedi, M., Azqhandi, M. A., Goudarzi, A., & Dastkhoon, M. J. R. A. (2016). Statistical experimental design, least squares-support vector machine (LS-SVM) and artificial neural network (ANN) methods for modeling the facilitated adsorption of methylene blue dye. *RSC advances*, *6*(46), 40502-40516.
- Ayinla, R. T., Dennis, J. O., Zaid, H. M., Sanusi, Y. K., Usman, F., & Adebayo, L. L. (2019). A review of technical advances of recent palm bio-

waste conversion to activated carbon for energy storage. *Journal of cleaner production*, *229*, 1427-1442.

- Azzopardi, E. A., Owens, S. E., Murison, M., Rees, D., Sawhney, M. A., Francis, L. W., ... & Whitaker, I. S. (2017). Chromophores in operative surgery: current practice and rationalized development. *Journal of Controlled Release*, *249*, 123-130.
- Badawy, A. A., Ibrahim, S. M., & Essawy, H. A. (2020). Enhancing the textile dye removal from aqueous solution using cobalt ferrite nanoparticles prepared in presence of fulvic acid. *Journal of Inorganic and Organometallic Polymers and Materials*, *30*, 1798-1813.
- Baker, M. J., Trevisan, J., Bassan, P., Bhargava, R., Butler, H. J., Dorling, K. M., ... & Martin, F. L. (2014). Using Fourier transform IR spectroscopy to analyze biological materials. *Nature protocols*, *9*(8), 1771-1791.
- Balahmar, N., Al-Jumialy, A. S., & Mokaya, R. (2017). Biomass to porous carbon in one step: directly activated biomass for high performance CO 2 storage. *Journal of Materials Chemistry A*, *5*(24), 12330-12339.
- Banerjee, S., & Chattopadhyaya, M. C. (2017). Adsorption characteristics for the removal of a toxic dye, tartrazine from aqueous solutions by a low cost agricultural by-product. *Arabian Journal of Chemistry*, *10*, S1629-S1638.
- Bao, N., Li, Y., Wei, Z., Yin, G., & Niu, J. (2011). Adsorption of dyes on hierarchical mesoporous TiO2 fibers and its enhanced photocatalytic properties. *The Journal of Physical Chemistry C*, *115*(13), 5708-5719.
- Batzias, F. A., & Sidiras, D. K. (2007). Dye adsorption by prehydrolysed beech sawdust in batch and fixed-bed systems. *Bioresource Technology*, *98*(6), 1208-1217.
- BENAISSA, A. (2012). Etude de la faisabilité d'élimination de certains colorants textiles par certains matériaux déchets d'origine naturelle.

References

- Bencheikh, I., Azoulay, K., Mabrouki, J., El Hajjaji, S., Dahchour, A., Moufti, A., & Dhiba, D. (2020). The adsorptive removal of MB using chemically treated artichoke leaves: parametric, kinetic, isotherm and thermodynamic study. *Scientific African*, *9*, e00509.
- Bharathi, K. S., & Ramesh, S. T. (2013). Removal of dyes using agricultural waste as low-cost adsorbents: a review. *Applied Water Science*, *3*(4), 773–790.
- Blaga, A. C., Tanasă, A. M., Cimpoesu, R., Tataru-Farmus, R.-E., & Suteu, D. (2022). Biosorbents based on biopolymers from natural sources and food waste to retain the methylene blue dye from the aqueous medium. *Polymers*, *14*(13), 2728.
- Budinova, T., Petrov, N., Parra, J., & Baloutzov, V. (2008). Use of an activated carbon from antibiotic waste for the removal of Hg (II) from aqueous solution. *Journal of environmental management*, *88*(1), 165-172.
- Bui, T. X., & Choi, H. (2010). Comment on "Adsorption and desorption of oxytetracycline and carbamazepine by multiwalled carbon nanotubes". *Environmental science & technology*, *44*(12), 4828-4828.
- Bulgariu, L., Escudero, L. B., Bello, O. S., Iqbal, M., Nisar, J., Adegoke, K. A., ... & Anastopoulos, I. (2019). The utilization of leaf-based adsorbents for dyes removal: A review. *Journal of Molecular Liquids*, *276*, 728-747.
- Cai, Z., Sun, Y., Liu, W., Pan, F., Sun, P., & Fu, J. (2017). An overview of nanomaterials applied for removing dyes from wastewater. *Environmental Science and Pollution Research*, *24*, 15882-15904.
- Canales-Flores, R. A., & Prieto-García, F. (2020). Taguchi optimization for production of activated carbon from phosphoric acid impregnated agricultural waste by microwave heating for the removal of methylene blue. *Diamond and Related Materials*, *109*, 108027.

References

- Carrott, P. J. M., Mourao, P. A. M., Ribeiro Carrott, M. M. L., & Gonçalves, E. M. (2005). Separating surface and solvent effects and the notion of critical adsorption energy in the adsorption of phenolic compounds by activated carbons. *Langmuir*, *21*(25), 11863-11869.
- Chan, L. S., Cheung, W. H., Allen, S. J., & McKay, G. (2012). Error analysis of adsorption isotherm models for acid dyes onto bamboo derived activated carbon. *Chinese Journal of Chemical Engineering*, *20*(3), 535-542.
- Chen, B., Hui, C. W., & McKay, G. (2001). Film-pore diffusion modeling and contact time optimization for the adsorption of dyestuffs on pith. *Chemical Engineering Journal*, *84*(2), 77-94.
- Chen, T., Da, T., & Ma, Y. (2021). Reasonable calculation of the thermodynamic parameters from adsorption equilibrium constant. *Journal of Molecular Liquids*, *322*, 114980.
- Chen, Y. D., Huang, M. J., Huang, B., & Chen, X. R. (2012). Mesoporous activated carbon from inherently potassium-rich pokeweed by in situ self-activation and its use for phenol removal. *Journal of Analytical and Applied Pyrolysis*, *98*, 159-165.
- Chen, Y., Zhang, Z., Chen, D., Chen, Y., Gu, Q., & Liu, H. (2019). Removal of coke powders in coking diesel distillate using recyclable chitosan-grafted Fe3O4 magnetic nanoparticles. *Fuel*, *238*, 345-353.
- Choudhary, A. (2017, November). Removal of oil from seawater using charcoal and rice hull. In *IOP Conference Series: Materials Science and Engineering* (Vol. 263, No. 3, p. 032007). IOP Publishing.
- Coughlin, R. W., & Ezra, F. S. (1968). Role of surface acidity in the adsorption of organic pollutants on the surface of carbon. *Environmental Science & Technology*, *2*(4), 291-297.

References

- Crini, G., & Lichtfouse, E. (2019). Advantages and disadvantages of techniques used for wastewater treatment. *Environmental Chemistry Letters*, *17*, 145-155.
- Dai, J., Tian, S., Jiang, Y., Chang, Z., Xie, A., Zhang, R., & Yan, Y. (2018). Facile synthesis of porous carbon sheets from potassium acetate via in-situ template and self-activation for highly efficient chloramphenicol removal. *Journal of Alloys and Compounds*, *732*, 222-232.
- Danish, M., Ahmad, T., Hashim, R., Said, N., Akhtar, M. N., Mohamad-Saleh, J., & Sulaiman, O. (2018). Comparison of surface properties of wood biomass activated carbons and their application against rhodamine B and methylene blue dye. *Surfaces and Interfaces*, *11*, 1-13.
- Dash, B. (2010). *Competitive Adsorption of dyes (congo red, methylene blue, malachite green) on Activated Carbon* (Doctoral dissertation).
- de Luna, M. D. G., Flores, E. D., Genuino, D. A. D., Futalan, C. M., & Wan, M. W. (2013). Adsorption of Eriochrome Black T (EBT) dye using activated carbon prepared from waste rice hulls—Optimization, isotherm and kinetic studies. *Journal of the Taiwan institute of chemical engineers*, *44*(4), 646-653.
- De Rossi, A., Rigon, M. R., Zaparoli, M., Braido, R. D., Colla, L. M., Dotto, G. L., & Piccin, J. S. (2018). Chromium (VI) biosorption by Saccharomyces cerevisiae subjected to chemical and thermal treatments. *Environmental Science and Pollution Research*, *25*, 19179-19186.
- Demirbas, A. (2009). Agricultural based activated carbons for the removal of dyes from aqueous solutions: a review. *Journal of hazardous materials*, *167*(1-3), 1-9.
- Dural, M. U., Cavas, L., Papageorgiou, S. K., & Katsaros, F. K. (2011). Methylene blue adsorption on activated carbon prepared from Posidonia

oceanica (L.) dead leaves: Kinetics and equilibrium studies. *Chemical Engineering Journal*, *168*(1), 77–85.

- Elmouwahidi, A., Bailón-García, E., Pérez-Cadenas, A. F., Maldonado-Hódar, F. J., & Carrasco-Marín, F. (2017). Activated carbons from KOH and H3PO4-activation of olive residues and its application as supercapacitor electrodes. *Electrochimica Acta*, *229*, 219-228.
- Eskizeybek, V., Sarı, F., Gülce, H., Gülce, A., & Avcı, A. (2012). Preparation of the new polyaniline/ZnO nanocomposite and its photocatalytic activity for degradation of methylene blue and malachite green dyes under UV and natural sun lights irradiations. *Applied Catalysis B: Environmental*, *119*, 197-206.
- Foo, K. Y., & Hameed, B. H. (2010). An overview of dye removal via activated carbon adsorption process. *Desalination and Water Treatment*, *19*(1-3), 255-274.
- Forgacs, E., Cserháti, T., & Oros, G. (2004). Removal of synthetic dyes from wastewaters: a review. *Environment international*, *30*(7), 953-971.
- Fu, Y., Shen, Y., Zhang, Z., Ge, X., & Chen, M. (2019). Activated bio-chars derived from rice husk via one-and two-step KOH-catalyzed pyrolysis for phenol adsorption. *Science of the Total Environment*, *646*, 1567-1577.
- Gao, Y., Yue, Q., Gao, B., & Li, A. (2020). Insight into activated carbon from different kinds of chemical activating agents: A review. *Science of the Total Environment*, *746*, 141094.
- Geckeler, K. E., & Volchek, K. (1996). Removal of hazardous substances from water using ultrafiltration in conjunction with soluble polymers. *Environmental science & technology*, *30*(3), 725-734.
- González-García, P. (2018). Activated carbon from lignocellulosics precursors: A review of the synthesis methods, characterization techniques

and applications. *Renewable and Sustainable Energy Reviews*, *82*, 1393-1414.

- Guo, D., Li, Y., Cui, B., Hu, M., Luo, S., Ji, B., & Liu, Y. (2020). Natural adsorption of methylene blue by waste fallen leaves of Magnoliaceae and its repeated thermal regeneration for reuse. *Journal of cleaner production*, *267*, 121903.
- Halysh, V., Sevastyanova, O., Pikus, S., Dobele, G., Pasalskiy, B., Gun'ko, V. M., & Kartel, M. (2020). Sugarcane bagasse and straw as low-cost lignocellulosic sorbents for the removal of dyes and metal ions from water. *Cellulose*, *27*(14), 8181–8197.
- Hameed, B. H., Din, A. M., & Ahmad, A. L. (2007). Adsorption of methylene blue onto bamboo-based activated carbon: kinetics and equilibrium studies. *Journal of hazardous materials*, *141*(3), 819-825.
- Hasan, R., Ying, W. J., Cheng, C. C., Jaafar, N. F., Jusoh, R., Jalil, A. A., & Setiabudi, H. D. (2020). Methylene Blue Adsorption onto Cockle Shells-Treated Banana Pith: Optimization, Isotherm, Kinetic, and Thermodynamic Studies. *Indonesian Journal of Chemistry*, *20*(2), 368–378.
- Hidayu, A. R., & Muda, N. J. P. E. (2016). Preparation and characterization of impregnated activated carbon from palm kernel shell and coconut shell for CO2 capture. *Procedia Engineering*, *148*, 106-113.
- Ho, Y. S., & McKay, G. (1999). Pseudo-second order model for sorption processes. *Process biochemistry*, *34*(5), 451-465.
- Hu, X.-S., Liang, R., & Sun, G. (2018). Super-adsorbent hydrogel for removal of methylene blue dye from aqueous solution. *Journal of Materials Chemistry A*, *6*(36), 17612–17624.
- Hui, T. S., & Zaini, M. A. A. (2015). Potassium hydroxide activation of activated carbon: a commentary. *Carbon letters*, *16*(4), 275-280.

References

- Husien, S., El-taweel, R. M., Salim, A. I., Fahim, I. S., Said, L. A., & Radwan, A. G. (2022). Review of activated carbon adsorbent material for textile dyes removal: Preparation, and modelling. *Current Research in Green and Sustainable Chemistry*, 100325.
- Islam, M. A., Ahmed, M. J., Khanday, W. A., Asif, M., & Hameed, B. H. (2017). Mesoporous activated coconut shell-derived hydrochar prepared via hydrothermal carbonization-NaOH activation for methylene blue adsorption. *Journal of environmental management*, *203*, 237–244.
- Izan, N. R., Zainol, M. M., Nordin, A. H., Asmadi, M., Wong, S. L., Azhar, M. A. I., & Alias, N. H. (2020). Removal of Methylene Blue via Adsorption using Magnetic Char Derived from Food Waste. *Jawad, AH, Bardhan, M., Islam, MA, Islam, MA, Syed-Hassan, SSA, Surip, SN, et al*.
- Jawad, A. H., Mallah, S. H., & Mastuli, M. S. (2018). Adsorption behavior of methylene blue on acid-treated rubber (Hevea brasiliensis) leaf. *Desalin Water Treat*, *124*, 297-307.
- Jawad, A. H., Ramlah, A. R., Khudzir, I., & Sabar, S. (2017). High surface area mesoporous activated carbon developed from coconut leaf by chemical activation with H3PO4 for adsorption of methylene blue. *Desalination and Water Treatment*, *74*, 326–335.
- Jeirani, Z., Niu, C. H., & Soltan, J. (2017). Adsorption of emerging pollutants on activated carbon. *Reviews in Chemical Engineering*, *33*(5), 491-522.
- Jiang, W., Zhang, L., Guo, X., Yang, M., Lu, Y., Wang, Y., et al. (2021). Adsorption of cationic dye from water using an iron oxide/activated carbon magnetic composites prepared from sugarcane bagasse by microwave method. *Environmental technology*, *42*(3), 337–350.

References

- Jolly, G., Dupont, L., Aplincourt, M., & Lambert, J. (2006). Improved Cu and Zn sorption on oxidized wheat lignocellulose. *Environmental Chemistry Letters*, *4*, 219-223.
- Kadhom, M., Albayati, N., Alalwan, H., & Al-Furaiji, M. (2020). Removal of dyes by agricultural waste. *Sustainable Chemistry and Pharmacy*, *16*, 100259.
- Karadirek, Ş., & Okkay, H. (2018). Statistical modeling of activated carbon production from spent mushroom compost. *Journal of industrial and engineering chemistry*, *63*, 340-347.
- Karagöz, S., Tay, T., Ucar, S., & Erdem, M. (2008). Activated carbons from waste biomass by sulfuric acid activation and their use on methylene blue adsorption. *Bioresource technology*, *99*(14), 6214-6222.
- Karcher, S., Kornmüller, A., & Jekel, M. (2002). Anion exchange resins for removal of reactive dyes from textile wastewaters. *Water research*, *36*(19), 4717-4724.
- Katuri, K. P., Mohan, S. V., Sridhar, S., Pati, B. R., & Sarma, P. N. (2009). Laccase-membrane reactors for decolorization of an acid azo dye in aqueous phase: process optimization. *Water research*, *43*(15), 3647-3658.
- Kemp, K., Griffiths, J., Campbell, S., & Lovell, K. (2013). An exploration of the follow-up up needs of patients with inflammatory bowel disease. *Journal of Crohn's and Colitis*, *7*(9), e386-e395.
- Khan, H., Yerramilli, A. S., D'Oliveira, A., Alford, T. L., Boffito, D. C., & Patience, G. S. (2020). Experimental methods in chemical engineering: X-ray diffraction spectroscopy—XRD. *The Canadian journal of chemical engineering*, *98*(6), 1255-1266.
- Khangwichian, W., Pattamasewe, S., Leesing, R., Knijnenburg, J. T. N., & Ngernyen, Y. (2022). Adsorption of cationic dye on activated carbon from hydrolyzed Dipterocarpus alatus leaves: Waste from biodiesel production.

Engineering and Applied Science Research, *49*(4), 531–544.

- Kleszyk, P., Ratajczak, P., Skowron, P., Jagiello, J., Abbas, Q., Frąckowiak, E., & Béguin, F. (2015). Carbons with narrow pore size distribution prepared by simultaneous carbonization and self-activation of tobacco stems and their application to supercapacitors. *Carbon*, *81*, 148-157.
- Koop, A., Voss, I., Thesing, A., Kohl, H., Reichelt, R., & Steinbüchel, A. (2007). Identification and localization of cyanophycin in bacteria cells via imaging of the nitrogen distribution using energy-filtering transmission electron microscopy. *Biomacromolecules*, *8*(9), 2675-2683.
- Kuang, Y., Zhang, X., & Zhou, S. (2020). Adsorption of methylene blue in water onto activated carbon by surfactant modification. *Water*, *12*(2), 587.
- Kumar, A., & Jena, H. M. (2016). Preparation and characterization of high surface area activated carbon from Fox nut (Euryale ferox) shell by chemical activation with H3PO4. *Results in Physics*, *6*, 651-658.
- Kushwaha, A. K., Gupta, N., & Chattopadhyaya, M. C. (2014). Removal of cationic methylene blue and malachite green dyes from aqueous solution by waste materials of Daucus carota. *Journal of Saudi Chemical Society*, *18*(3), 200–207.
- Labena, A., Abdelhamid, A. E., Husien, S., Youssef, T., Azab, E., Gobouri, A. A., & Safwat, G. (2021). Grafting of acrylic membrane prepared from fibers waste for dyes removal: methylene blue and Congo red. *Separations*, *8*(4), 42.
- LAURENT, A. D., WATHELET, V., BOUHY, M., JACQUEMIN, D., & PERPÈTE, E. (2010). Simulation de la perception des couleurs de colorants organiques.

References

- Li, S., Han, K., Li, J., Li, M., & Lu, C. (2017). Preparation and characterization of super activated carbon produced from gulfweed by KOH activation. *Microporous and Mesoporous Materials*, *243*, 291-300.
- Lu, B., Hu, L., Yin, H., Mao, X., Xiao, W., & Wang, D. (2016). Preparation and application of capacitive carbon from bamboo shells by one step molten carbonates carbonization. *International Journal of Hydrogen Energy*, *41*(41), 18713-18720.
- Ma, C. M., Hong, G. B., & Wang, Y. K. (2020). Performance evaluation and optimization of dyes removal using rice bran-based magnetic composite adsorbent. *Materials*, *13*(12), 2764.
- Magdy, A., Fouad, Y. O., Abdel-Aziz, M. H., & Konsowa, A. H. (2017). Synthesis and characterization of Fe3O4/kaolin magnetic nanocomposite and its application in wastewater treatment. *Journal of Industrial and Engineering Chemistry*, *56*, 299-311.
- Mahamad, M. N., Zaini, M. A. A., & Zakaria, Z. A. (2015). Preparation and characterization of activated carbon from pineapple waste biomass for dye removal. *International Biodeterioration & Biodegradation*, *102*, 274–280.
- Malhas, A. N., Abuknesha, R. A., & Price, R. G. (2002). Removal of detergents from protein extracts using activated charcoal prior to immunological analysis. *Journal of immunological methods*, *264*(1-2), 37-43.
- Markandeya, Singh, A., Shukla, S. P., Mohan, D., Singh, N. B., Bhargava, D. S., ... & Kisku, G. C. (2015). Adsorptive capacity of sawdust for the adsorption of MB dye and designing of two-stage batch adsorber. *Cogent Environmental Science*, *1*(1), 1075856.
- Martín-González, M. A., Susial, P., Pérez-Peña, J., & Doña-Rodríguez, J. M. (2013). Preparation of activated carbons from banana leaves by chemical

activation with phosphoric acid. Adsorption of methylene blue. *Revista mexicana de ingeniería química*, *12*(3), 595–608.

- Martins, A. C., Pezoti, O., Cazetta, A. L., Bedin, K. C., Yamazaki, D. A., Bandoch, G. F., ... & Almeida, V. C. (2015). Removal of tetracycline by NaOH-activated carbon produced from macadamia nut shells: kinetic and equilibrium studies. *Chemical Engineering Journal*, *260*, 291-299.
- McKay, G., Porter, J. F., & Prasad, G. R. (1999). The removal of dye colours from aqueous solutions by adsorption on low-cost materials. *Water, Air, and Soil Pollution*, *114*, 423-438.
- Mekuria, D., Diro, A., Melak, F., & Asere, T. G. (2022). Adsorptive Removal of Methylene Blue Dye Using Biowaste Materials: Barley Bran and Enset Midrib Leaf. *Journal of Chemistry*, *2022*.
- Moerz, S. T., & Huber, P. (2014). Protein adsorption into mesopores: a combination of electrostatic interaction, counterion release, and van der Waals forces. *Langmuir*, *30*(10), 2729-2737.
- Mohammed, T. M., Labena, A., Maziad, N. A., & Husien, S. (2020). Radiation Copolymerization of PVA/Malic acid/HEMA/Macro-algal (Sargassum sp.) Biomass for Removal of Hexavalent Chromium. *Egyptian Journal of Chemistry*, *63*(6), 2019-2035.
- Morin-Crini, N., Loiacono, S., Placet, V., Torri, G., Bradu, C., Kostić, M., ... & Crini, G. (2019). Hemp-based adsorbents for sequestration of metals: a review. *Environmental Chemistry Letters*, *17*, 393-408.
- Mourao, P. A. M., Carrott, P. J. M., & Carrott, M. R. (2006). Application of different equations to adsorption isotherms of phenolic compounds on activated carbons prepared from cork. *Carbon*, *44*(12), 2422-2429.
- Mousavi, S. A., Mahmoudi, A., Amiri, S., Darvishi, P., & Noori, E. (2022). Methylene blue removal using grape leaves waste: optimization and

modeling. *Applied Water Science*, *12*(5), 1–11.

- Mukherjee, K., Kedia, A., Rao, K. J., Dhir, S., & Paria, S. (2015). Adsorption enhancement of methylene blue dye at kaolinite clay–water interface influenced by electrolyte solutions. *RSC Advances*, *5*(39), 30654-30659.
- Mukherjee, S., Mukhopadhyay, S., Hashim, M. A., & Sen Gupta, B. (2015). Contemporary environmental issues of landfill leachate: assessment and remedies. *Critical reviews in environmental science and technology*, *45*(5), 472-590.
- Murthy, T. P. K., Gowrishankar, B. S., Krishna, R. H., Chandraprabha, M. N., & Mathew, B. B. (2020). Magnetic modification of coffee husk hydrochar for adsorptive removal of methylene blue: isotherms, kinetics and thermodynamic studies. *Environmental Chemistry and Ecotoxicology*, *2*, 205–212.
- Mustikaningrum, M., Cahyono, R. B., & Yuliansyah, A. T. (2022). Adsorption of Methylene Blue on Nano-Crystal Cellulose of Oil Palm Trunk: Kinetic and Thermodynamic Studies. *Indonesian Journal of Chemistry*, *22*(4), 953-964.
- Nayak, A., Bhushan, B., Gupta, V., & Sharma, P. (2017). Chemically activated carbon from lignocellulosic wastes for heavy metal wastewater remediation: Effect of activation conditions. *Journal of colloid and interface science*, *493*, 228-240.
- Nizam, N. U. M., Hanafiah, M. M., Mahmoudi, E., Halim, A. A., & Mohammad, A. W. (2021). The removal of anionic and cationic dyes from an aqueous solution using biomass-based activated carbon. *Scientific Reports*, *11*(1), 8623.
- Nordin, A. H., Wong, S., Ngadi, N., Zainol, M. M., Abd Latif, N. A. F., & Nabgan, W. (2021). Surface functionalization of cellulose with

polyethyleneimine and magnetic nanoparticles for efficient removal of anionic dye in wastewater. *Journal of Environmental Chemical Engineering*, *9*(1), 104639.

- Oginni, O., Singh, K., Oporto, G., Dawson-Andoh, B., McDonald, L., & Sabolsky, E. (2019). Influence of one-step and two-step KOH activation on activated carbon characteristics. *Bioresource technology reports*, *7*, 100266.
- Olivares-Marín, M., Fernández-González, C., Macías-García, A., & Gómez-Serrano, V. (2012). Preparation of activated carbon from cherry stones by physical activation in air. Influence of the chemical carbonisation with H2SO4. *Journal of analytical and applied pyrolysis*, *94*, 131-137.
- Ören, A. H., & Kaya, A. (2006). Factors affecting adsorption characteristics of Zn2+ on two natural zeolites. *Journal of hazardous materials*, *131*(1-3), 59-65.
- Patidar, R., Khanna, S., & Moholkar, V. S. (2012). Physical features of ultrasound assisted enzymatic degradation of recalcitrant organic pollutants. *Ultrasonics sonochemistry*, *19*(1), 104-118.
- Pernyeszi, T., Farkas, R., & Kovács, J. (2019). Methylene blue adsorption study on microcline particles in the function of particle size range and temperature. *Minerals*, *9*(9), 555.
- Piaskowski, K., Świderska-Dąbrowska, R., & Zarzycki, P. K. (2018). Dye removal from water and wastewater using various physical, chemical, and biological processes. *Journal of AOAC International*, *101*(5), 1371-1384.

- Prauchner, M. J., Sapag, K., & Rodríguez-Reinoso, F. (2016). Tailoring biomass-based activated carbon for CH4 storage by combining chemical activation with H3PO4 or ZnCl2 and physical activation with CO2. *Carbon*, *110*, 138-147.

References

- Qi, Y., Zhu, J., Fu, Q., Hu, H., & Huang, Q. (2017). Sorption of Cu by humic acid from the decomposition of rice straw in the absence and presence of clay minerals. *Journal of Environmental Management*, *200*, 304-311.
- Rápó, E., & Tonk, S. (2021). Factors affecting synthetic dye adsorption; desorption studies: a review of results from the last five years (2017–2021). *Molecules*, *26*(17), 5419.
- Rápó, E., Szép, R., Keresztesi, Á., Suciu, M., & Tonk, S. (2018). Adsorptive removal of cationic and anionic dyes from aqueous solutions by using eggshell household waste as biosorbent. *Acta Chimica Slovenica*, *65*(3), 709-717.
- Rashid, R., Shafiq, I., Akhter, P., Iqbal, M. J., & Hussain, M. (2021). A state-of-the-art review on wastewater treatment techniques: the effectiveness of adsorption method. *Environmental Science and Pollution Research*, *28*, 9050-9066.
- Razi, M. A. M., Hishammudin, M. N. A. M., & Hamdan, R. (2017). Factor affecting textile dye removal using adsorbent from activated carbon: A review. In *MATEC Web of Conferences* (Vol. 103, p. 06015). EDP Sciences.
- Reddy, K. S. K., Al Shoaibi, A., & Srinivasakannan, C. (2012). A comparison of microstructure and adsorption characteristics of activated carbons by CO2 and H3PO4 activation from date palm pits. *New Carbon Materials*, *27*(5), 344-351.
- Rohman, A. (2019). The employment of Fourier transform infrared spectroscopy coupled with chemometrics techniques for traceability and authentication of meat and meat products. *Journal of advanced veterinary and animal research*, *6*(1), 9.
- Rohman, A., & Salamah, N. (2018). The employment of spectroscopic techniques coupled with chemometrics for authentication analysis of halal

pharmaceuticals. *Journal of Applied Pharmaceutical Science*, *8*(10), 063-068.

- Saratale, R. G., Sun, Q., Munagapati, V. S., Saratale, G. D., Park, J., & Kim, D. S. (2021). The use of eggshell membrane for the treatment of dye-containing wastewater: Batch, kinetics and reusability studies. *Chemosphere*, *281*, 130777.
- Şentürk, İ., & Alzein, M. (2020). Adsorption of acid violet 17 onto acid-activated pistachio shell: isotherm, kinetic and thermodynamic studies. *Acta Chimica Slovenica*, *67*(1), 55-69.
- Severcan, F., Akkas, S. B., Turker, S., & Yucel, R. (2012). Methodological approaches from experimental to computational analysis in vibrational spectroscopy and microspectroscopy. *Severcan F, Haris PI. Vibrational Spectroscopy in Diagnosis and Screening. 1st ed. Amsterdam: IOS Press BV*, 12-52.
- Sevilla, M., & Mokaya, R. (2014). Energy storage applications of activated carbons: supercapacitors and hydrogen storage. *Energy & Environmental Science*, *7*(4), 1250-1280.
- Shakoor, S., & Nasar, A. (2017). Adsorptive treatment of hazardous methylene blue dye from artificially contaminated water using cucumis sativus peel waste as a low-cost adsorbent. *Groundwater for Sustainable Development*, *5*, 152–159.
- Shannon, M. A., Bohn, P. W., Elimelech, M., Georgiadis, J. G., Marinas, B. J., & Mayes, A. M. (2008). Science and technology for water purification in the coming decades. *Nature*, *452*(7185), 301-310.
- Sharma, G., Naushad, M., Kumar, A., Rana, S., Sharma, S., Bhatnagar, A., ... & Khan, M. R. (2017). Efficient removal of coomassie brilliant blue R-250

dye using starch/poly (alginic acid-cl-acrylamide) nanohydrogel. *Process Safety and Environmental Protection*, *109*, 301-310.

- Sharma, G., Sharma, S., Kumar, A., Lai, C. W., Naushad, M., Iqbal, J., & Stadler, F. J. (2022). Activated carbon as superadsorbent and sustainable material for diverse applications. *Adsorption Science & Technology*, *2022*.
- Shehzad, A., Bashir, M. J., Sethupathi, S., & Lim, J. W. (2015). An overview of heavily polluted landfill leachate treatment using food waste as an alternative and renewable source of activated carbon. *Process safety and environmental protection*, *98*, 309-318.
- Shelke, B. N., Jopale, M. K., & Kategaonkar, A. H. (2022). Exploration of biomass waste as low cost adsorbents for removal of methylene blue dye: A review. *Journal of the Indian Chemical Society*, 100530.
- Sims, R. A., Harmer, S. L., & Quinton, J. S. (2019). The role of physisorption and chemisorption in the oscillatory adsorption of organosilanes on aluminium oxide. *Polymers*, *11*(3), 410.
- Singh, J., Basu, S., & Bhunia, H. (2019). CO2 capture by modified porous carbon adsorbents: Effect of various activating agents. *Journal of the Taiwan Institute of Chemical Engineers*, *102*, 438-447.
- Singh, K., & Arora, S. (2011). Removal of synthetic textile dyes from wastewaters: a critical review on present treatment technologies. *Critical reviews in environmental science and technology*, *41*(9), 807-878.
- Skodras, G., Diamantopoulou, I., Zabaniotou, A., Stavropoulos, G., & Sakellaropoulos, G. P. (2007). Enhanced mercury adsorption in activated carbons from biomass materials and waste tires. *Fuel processing technology*, *88*(8), 749-758.
- Sonune, A., & Ghate, R. (2004). Developments in wastewater treatment methods. *Desalination*, *167*, 55-63.

References

- Stasinakis, A. S., Thomaidis, N. S., Arvaniti, O. S., Asimakopoulos, A. G., Samaras, V. G., Ajibola, A., ... & Lekkas, T. D. (2013). Contribution of primary and secondary treatment on the removal of benzothiazoles, benzotriazoles, endocrine disruptors, pharmaceuticals and perfluorinated compounds in a sewage treatment plant. *Science of the Total Environment*, *463*, 1067-1075.
- Subramanian, A., & Rodriguez-Saona, L. (2009). Fourier transform infrared (FTIR) spectroscopy. *Infrared spectroscopy for food quality analysis and control*, 145-178.
- Tan, K. L., & Hameed, B. H. (2017). Insight into the adsorption kinetics models for the removal of contaminants from aqueous solutions. *Journal of the Taiwan Institute of Chemical Engineers*, *74*, 25-48.
- Tara, N., Siddiqui, S. I., Rathi, G., Chaudhry, S. A., & Asiri, A. M. (2020). Nano-engineered adsorbent for the removal of dyes from water: A review. *Current Analytical Chemistry*, *16*(1), 14-40.
- Temesgen, F., Gabbiye, N., & Sahu, O. (2018). Biosorption of reactive red dye (RRD) on activated surface of banana and orange peels: economical alternative for textile effluent. *Surfaces and interfaces*, *12*, 151-159.
- Terangpi, P., & Chakraborty, S. (2017). Adsorption kinetics and equilibrium studies for removal of acid azo dyes by aniline formaldehyde condensate. *Applied Water Science*, *7*, 3661-3671.
- Torretta, V., Ferronato, N., Katsoyiannis, I. A., Tolkou, A. K., & Airoldi, M. (2016). Novel and conventional technologies for landfill leachates treatment: A review. *Sustainability*, *9*(1), 9.
- Tounsadi, H., Khalidi, A., Farnane, M., Abdennouri, M., & Barka, N. (2016). Experimental design for the optimization of preparation conditions of highly

efficient activated carbon from Glebionis coronaria L. and heavy metals removal ability. *Process Safety and Environmental Protection*, *102*, 710-723.

- Tran, H. N., You, S. J., & Chao, H. P. (2016). Effect of pyrolysis temperatures and times on the adsorption of cadmium onto orange peel derived biochar. *Waste Management & Research*, *34*(2), 129-138.
- Tran, H. N., You, S. J., & Chao, H. P. (2017). Fast and efficient adsorption of methylene green 5 on activated carbon prepared from new chemical activation method. *Journal of Environmental Management*, *188*, 322-336.
- Tran, H. N., You, S.-J., Nguyen, T. V., & Chao, H.-P. (2017). Insight into the adsorption mechanism of cationic dye onto biosorbents derived from agricultural wastes. *Chemical Engineering Communications*, *204*(9), 1020–1036.
- Tran, H. V., Hoang, L. T., & Huynh, C. D. (2020). An investigation on kinetic and thermodynamic parameters of methylene blue adsorption onto graphene-based nanocomposite. *Chemical Physics*, *535*, 110793.
- Uddin, M. K. (2017). A review on the adsorption of heavy metals by clay minerals, with special focus on the past decade. *Chemical Engineering Journal*, *308*, 438-462.
- Uddin, M. K., & Baig, U. (2019). Synthesis of Co3O4 nanoparticles and their performance towards methyl orange dye removal: Characterisation, adsorption and response surface methodology. *Journal of Cleaner Production*, *211*, 1141-1153.
- Wang, C., Wang, F., Xu, M., Zhu, C., Fang, W., & Wei, Y. (2015). Electrocatalytic degradation of methylene blue on Co doped Ti/TiO2 nanotube/PbO2 anodes prepared by pulse electrodeposition. *Journal of Electroanalytical Chemistry*, *759*, 158-166.
- Wang, J., & Guo, X. (2020). Adsorption kinetic models: Physical meanings,

applications, and solving methods. *Journal of Hazardous materials*, *390*, 122156.

- Wang, J., Liu, H., Yang, S., Zhang, J., Zhang, C., & Wu, H. (2014). Physicochemical characteristics and sorption capacities of heavy metal ions of activated carbons derived by activation with different alkyl phosphate triesters. *Applied surface science*, *316*, 443-450.
- Weber, W. J., & Smith, E. H. (1987). Simulation and design models for adsorption processes. *Environmental science & technology*, *21*(11), 1040-1050.
- Xu, Z., Yuan, Z., Zhang, D., Chen, W., Huang, Y., Zhang, T., ... & Sun, Z. (2018). Highly mesoporous activated carbon synthesized by pyrolysis of waste polyester textiles and MgCl2: physiochemical characteristics and pore-forming mechanism. *Journal of Cleaner Production*, *192*, 453-461.
- Yagub, M. T., Sen, T. K., Afroze, S., & Ang, H. M. (2014). Dye and its removal from aqueous solution by adsorption: a review. *Advances in colloid and interface science*, *209*, 172-184.
- Yakout, S. M., & El-Deen, G. S. (2016). Characterization of activated carbon prepared by phosphoric acid activation of olive stones. *Arabian journal of chemistry*, *9*, S1155-S1162.
- Ye, S., Yan, M., Tan, X., Liang, J., Zeng, G., Wu, H., ... & Wang, H. (2019). Facile assembled biochar-based nanocomposite with improved graphitization for efficient photocatalytic activity driven by visible light. *Applied Catalysis B: Environmental*, *250*, 78-88.
- Yeow, P. K., Wong, S. W., & Hadibarata, T. (2021). Removal of azo and anthraquinone dye by plant biomass as adsorbent–a review. *Biointerface Res Appl Chem*, *11*(1), 8218-8232.

References

- Yin, H., Lu, B., Xu, Y., Tang, D., Mao, X., Xiao, W., ... & Alshawabkeh, A. N. (2014). Harvesting capacitive carbon by carbonization of waste biomass in molten salts. *Environmental science & technology*, *48*(14), 8101-8108.
- Yousefi, M., Arami, S. M., Takallo, H., Hosseini, M., Radfard, M., Soleimani, H., & Mohammadi, A. A. (2019). Modification of pumice with HCl and NaOH enhancing its fluoride adsorption capacity: kinetic and isotherm studies. *Human and Ecological Risk Assessment: An International Journal*, *25*(6), 1508-1520.
- Zhang, Y., Song, X., Xu, Y., Shen, H., Kong, X., & Xu, H. (2019). Utilization of wheat bran for producing activated carbon with high specific surface area via NaOH activation using industrial furnace. *Journal of cleaner production*, *210*, 366-375.
- Zhang, Z., Lei, Y., Li, D., Zhao, J., Wang, Y., Zhou, G., ... & He, Q. (2020). Sudden heating of H3PO4-loaded coconut shell in CO2 flow to produce super activated carbon and its application for benzene adsorption. *Renewable Energy*, *153*, 1091-1099.
- Zou, H., Ma, W., & Wang, Y. (2015). A novel process of dye wastewater treatment by linking advanced chemical oxidation with biological oxidation. *Archives of Environmental Protection*.
- Zubair, M., Daud, M., McKay, G., Shehzad, F., & Al-Harthi, M. A. (2017). Recent progress in layered double hydroxides (LDH)-containing hybrids as adsorbents for water remediation. *Applied Clay Science*, *143*, 279-292.
- Zuo, L., Ai, J., Fu, H., Chen, W., Zheng, S., Xu, Z., & Zhu, D. (2016). Enhanced removal of sulfonamide antibiotics by KOH-activated anthracite coal: batch and fixed-bed studies. *Environmental Pollution*, *211*, 425-434.

الخلاصة

تم استخدام أوراق التين، وهو منتج صديق للبيئة من منتجات نباتات الفاكهة لأول مرة لعلاج صبغة المثيلين الزرقاء. تم تحضير الكربون المنشط لأوراق التين (FLAC)بنجاح واستخدامه لامتزاز صبغة المثيلين الزرقاء (MB).

تمت دراسة خصائص الفيزيائية والكيميائية للمادة الممتزة باستخدام عدة تقنيات: مطيافية الاشعة تحت الحمراء، تحليل حيود الاشعة السينية، والمجهر الالكتروني الماسح والمساحة السطحية

[FT-IR, XRD, SEM, BET]

في هذه الدراسة، تمت فحص التراكيز الأولية للأصباغ، ووقت التلامس، وكميه FLAC ,ودرجات الحرارة، والاس الهيدروجيني للمحاليل، وحجم المحاليل، عوامل التنشيط، وفرن الكربنة ومقارنةFLAC مع أوراق لنباتات أخرى. علاوة على ذلك، تم فحص التركيز الاولي لصبغه المثيلين الزرقاء بتركيزات مختلفة من $20,40, 80,120,200\ mg.\ L^{-1}$

تم فحص محلول الاس الهيدروجيني عند هذه القيم pH11,pH8,pH7,pH3 . علاوة على ذلك, تم النظر في درجات حرارة الامتزاز البالغة ٢٠ و ٣٠ و ٤٠ و ٥٠ درجة مئوية للتحقيق في كيفية عمل FLAC على إزالة صبغةMB

تم تحديد قدرة امتزاز FLAC لتكون ٢٤,٧٥mg/g عند 0.08(g) و٤١ mg/g عند ٠,٠٢(g)

اتبعت عملية الامتزاز نحو نموذج لانكماير متساوي الحرارة(0.9841) $R^2=$ حيث أدى الامتزاز الى تكوين طبقة أحادية تغطي سطح المادة الممتزة. بالإضافة الى ذلك، تم اكتشاف السعة القصوى للامتزاز (Qmax) كانت ٤١,٧mg\g وثابت لانكماير كان 0.37 L/mg

أظهرت الدراسة الحركية لتجارب الامتزاز ان نموذج الدرجة الثانية الكاذبة هو افضل وصف لخصائص الامتزاز الحركي.

اظهر،FLAC باعتباره مادة ماصة منخفضة التكلفة لصبغة المثيلين الزرقاء، اداء جيدا لامتزاز الصبغة الكاتيونية.

جمهورية العراق

وزارة التعليم العالي والبحث العلمي

جامعة بابل/ كلية العلوم للبنات

قسم الكيمياء

ازالة صبغة الميثيلين الزرقاء من المحاليل المائية باستخدام مخلفات أوراق التين

رسالة قدمتها

الى مجلس كلية العلوم للبنات-جامعه بابل

كجزء من متطلبات نيل درجة الماجستير في العلوم / الكيمياء

من قبل

صفاء طالب كاظم عبد

بكالوريوس في الكيمياء

جامعة بابل/كلية العلوم للبنات (٢٠٢٠-٢٠١٩) م

بإشراف

أ.م. د فؤاد فاضل القيم

2023م

١٤٤٤ه